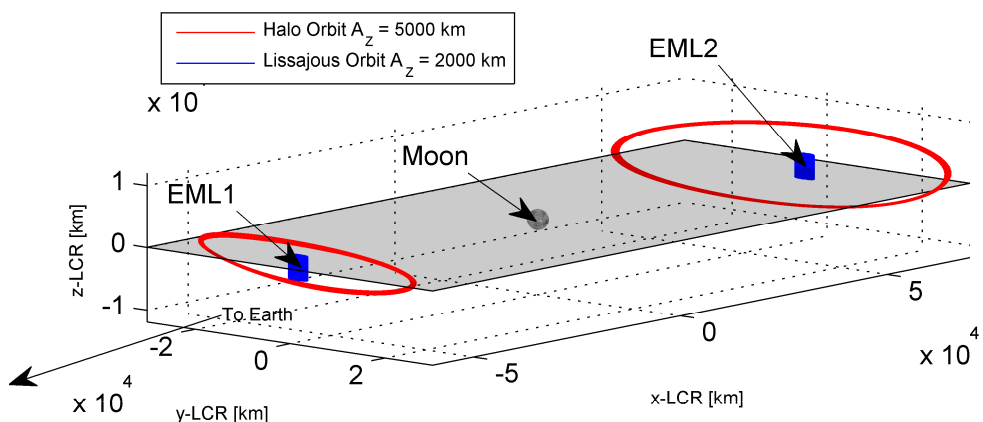


Investigation on Low Cost Transfer Options to the Earth-Moon Libration Point Region

Studienarbeit: IRS - 08 - S47

cand. aer. Andreas Stock



Prof. Dr. rer. nat. E. Messerschmid
Dipl.-Ing. F. Renk

31. Januar 2009

Institut für Raumfahrtssysteme / Universität Stuttgart
ESOC Darmstadt / ESA

Stuttgart, (WS 2008/09)

Danksagung

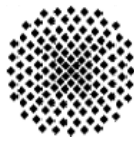
Ich möchte mich bei meinem Betreuer Herrn Dipl. Ing. Florian Renk für die so wichtige Unterstützung während meiner Studienarbeit bedanken. Ohne Seine Hilfe wäre diese Arbeit nicht möglich gewesen.

Des Weiteren möchte ich mich bei Herrn Prof. Dr. rer. nat. E. Messerschmid dafür bedanken, die Möglichkeit erhalten zu haben auf einem so spannenden und faszinierenden Gebiet arbeiten zu dürfen.

Ich möchte mich außerdem bei Herrn Dr. J. Schoenmaekers und Herrn Dipl. Math. M. Hechler bedanken, dass ich seitens der ESA unterstützt wurde und die Gelegenheit bekommen habe am ESOC einen Teil meiner Studienarbeit zu bewerkstelligen.

Stuttgart, der 31.01.2009

Andreas Stock

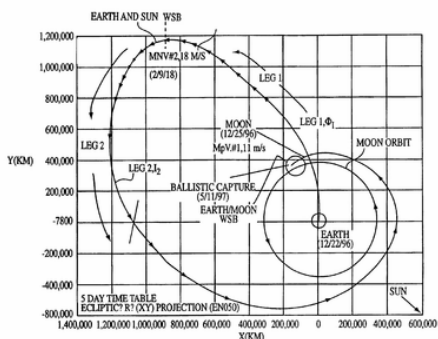


Diploma Thesis

Investigations on Low Cost Transfer Options to the Earth-Moon Libration Point Region

The Astronautics and Space Station department deals with the conceptual design of crewed space missions. This involves System- and Mission Analysis as well as Simulation of planned Systems. While the initial focus of this work was on the design of Space Stations in Low Earth Orbit (LEO) it has now shifted to manned mission leaving LEO going to the Moon and beyond.

Intensive investigations are currently undertaken to assess the utilization of the Earth-Moon Libration Points as a staging location for future exploration missions. The Libration Points have the advantage of a constant geometry with respect to the lunar surface, avoiding costly plane change manoeuvres in case of contingencies. Additionally they provide a low-energy access to the Sun-Earth Libration point region.



For piloted missions long travel times are undesirable in order to minimize the risk for the Crew and the effort for the Environmental Control and Life Support System. This makes the utilization of Low Cost Transfer Trajectories in manned missions difficult, since in general these low cost trajectories exploit long term effects to gain the intended savings in the transfer ΔV . Unmanned supply flights can however greatly benefit from the lower ΔV requirements, allowing for larger payload masses.

Within the scope of this thesis a literature review shall be done, focusing on transfers utilizing moon resonances and the Weak Stability Boundary (WSB) transfer. For the latter one the possibility of lunar fly-bys exists. Requirements on the Mission Analysis software shall be derived from the literature review and the existing software package shall be adapted and extended to allow for optimization of the afore mentioned trajectories.

In a third step the newly implemented software shall be used to assess the ΔV requirements for the transfer to the Earth-Moon Libration points for different Earth departure scenarios and rendezvous point on the libration point orbit.

Solid FORTRAN programming skills and a good understanding of orbital mechanics are a prerequisite for this work.

Prof. Dr. rer. nat. E. Messerschmid

Tutor: Prof. Dr. rer. nat. E. Messerschmid

Co-Tutor: Dipl.-Ing. F. Renk, Room 2.225, renk@irs.uni-stuttgart.de

Deutsche Kurzfassung

Im Rahmen dieser Arbeit werden die Möglichkeiten niederenergetischer Transfers zwischen dem niedrigen Erdorbit (LEO) und den mondnahen Librationspunkten EML1 und EML2 des Erde-Mond-Systems untersucht. Die niederenergetischen Transfers bieten auf Grund ihrer langen Transferzeiten lediglich für unbemannte Versorgungs- und Wissenschaftsmissionen einen potentiellen Nutzen. Im Rahmen von permanenten bemannten Missionen zum Mond und darüber hinaus muss jedoch über die Möglichkeit der Versorgung nachgedacht werden. Die Librationspunkte und deren Nutzung wurde erstmalig von R. Farquhar [1] in den frühen siebziger Jahren des 20. Jahrhunderts erwähnt und spielen nach wie vor eine elementare Rolle in zukünftigen Explorationsszenarien, wie die IAA Next Step Cosmic Study 2004 [2] oder der Space-Station-Design-Workshop 2008 von Messerschmid et. al [3] zeigt. Diese Arbeit ergänzt die Untersuchung der schnellen Transfers von F. Renk [4] und basiert auf seinen Vorarbeiten. Folgende Transfers werden für die jeweiligen Librationspunkte untersucht:

1. EML1: Transfers, die sich des lunaren Resonanz-Effektes bedienen, erwähnt von Schoenmaekers [5, 6].
2. EML2: Der WSB-Transfer, bekannt gemacht und erstmalig erwähnt durch Belbruno [7].

Hierbei wurden anhand zweier Beispielorbits - einem in der Amplitude 2000 km großen Lissajous Orbit und einem 5000 km großen Halo Orbit - vergleichbare Ergebnisse zu den bereits vorhandenen Transferoptionen aus [4] berechnet.

Für den WSB-Transfer existiert bereits eine Menge Literatur bezüglich Methodik und Optimierung, weswegen bei der Untersuchung auch auf diese zurückgegriffen wurde und der Fokus vor allem auf die Berechnung der Transfers und nicht auf die Entwicklung der Methode gelegt wurde.

Der WSB-Transfer bedient sich der Anziehungskraft der Sonne, um die orbitale Energie der Transferbahn zu erhöhen, so dass ein Transfer zum EML2 ohne zusätzlichen Apogäumsmanöver erreicht werden kann und das Perigäum auf die Höhe des EML2 angehoben wird, wenn bestimmte Voraussetzungen erfüllt sind. Das für den Hohmann Transfer notwendige Apogäums- Δv fällt hierbei vollständig weg. Nur noch ein Einschussmanöver in den Librationspunktorbit von überwiegend ≤ 1 m/s wird bei dieser Methode benötigt. Der Transfer wurde zunächst nur auf die natürlichen Transfers hin systematisch über eine Einjahresperiode in täglichen Intervallen untersucht, ohne dabei die Parameter des Abflugorbits an der Erde zu berücksichtigen. Lediglich die Höhe des Orbits wird mit 400 km auf einen typischen LEO festgesetzt. Eine Variation der Inkination des Abflugorbits von 0° bis 50° wurde bei dieser Untersuchung festgestellt. Das Δv_{Total} des sogenannten freien Transfers wurde hierbei - basierend auf einer Rückwärts-Integrations-Methode - mit $\sim 3,145$ km/s für den Lissajous und $\sim 3,14$ km/s für den Halo Orbit errechnet.

In einem weiteren Schritt wurde eine Optimierung von Transfers für fixe Inkinationen des Abflugorbits auf Basis der bereits errechneten freien Transfers implementiert. Diese bedient sich eines korrigierenden Manövers im Apogäum der Transferbahn, um die Inkinationsunterschiede des mit $51,6^\circ$ inklinierten Abflugorbits auszugleichen. Dabei wurde eine Abhängigkeit zwischen der relativen Inkination - dem Inkinationsunterschied der freien oszillierenden Inkinationen und der fixen

Inklination - und dem zusätzlichen Δv des Korrekturmanövers festgestellt. Je höher die relative Inklination, um so höher das Δv des zusätzlichen Manövers. Das Δv_{Total} für diesen optimierten Transfers lag damit auch nur um das des Korrekturmanövers höher. Im Falle des Halo Orbits lag dieses - das Korrekturmanöver - maximal bei 70 m/s und im Falle des Lissajous Orbits bei 66 m/s. Das Δv_{Total} wurde hierbei mit durchschnittlich $\sim 3,175$ km/s für den Lissajous und $\sim 3,18$ km/s für den Halo Orbit errechnet. Damit konnte selbst für spezifische Inklinationen nur eine moderate Erhöhung des Δv_{Total} festgestellt werden.

Für den Resonanz-Transfer konnte nicht auf ein so breites Erbe an Informationen zurück gegriffen werden, wie im Falle des WSB-Transfers. Deswegen lag vor allem im ersten Teil der Untersuchung der Schwerpunkt auf der Analyse der Eigenschaften und der Erarbeitung einer Methodik zur Berechnung von diesen Transfers. Im zweiten Teil der Untersuchung wurden konkrete Berechnungen für Transfers ebenfalls über eine 365-Tage Periode in eintages Intervallen durchgeführt.

Der Resonanz-Transfer bedient sich hierbei der gravitationellen Anziehung des Mondes für hochelliptische Erdorbits mit Apogäen zwischen $2,5 \cdot 10^5$ und $3,5 \cdot 10^5$ km. Dabei gilt es die Orbitperiode auf ein ganzzahliges Vielfaches der lunaren Umlauperiode von 27,3 Tagen abzustimmen. Im Falle einer Resonanz treffen Mond und Raumschiff im Apogäum des Erdorbits immer wieder aufeinander. Die Steuerung dieser Resonanz-Sequenz geschieht mittels Korrekturmanövern im Perigäum vor einem Zusammentreffen des Mondes und des Apogäums des Erdorbits.

Die Optimierung im Falle der Resonanz-Transfers gestaltet sich angesichts einer multiplen Zielsetzung als äusserst schwierig und ist eine Abwägung bezüglich der Effektivität einer einzelnen Resonanz-Sequenz gegenüber dem Δv , welches zur Korrektur benötigt wird. Dabei haben sich zwei Methoden herauskristallisiert, welche im Folgenden zur konkreten Berechnung eines kompletten Transfers vom LEO zu einem speziellen Punkt auf einem der beiden Librationspunktörbits um den EML1 dienten.

Die berechneten Δv 's für die Korrekturmanöver schwanken je nach Anzahl der Resonanzen zwischen minimal 45 m/s für den Halo Orbit und maximal 130 m/s für den Lissajous Orbit. Hinzu kommen Einschuss-Manöver vom LEO, welche in der gleichen Größenordnung wie die Δv_{Total} 's des WSB-Transfers liegen.

Nicht zuletzt die nicht vollständig eliminierbaren Korrekturmanöver des Resonanz-Transfers führen zu einer geringeren Effektivität dieser Transfers gegenüber des WSB-Transfers was zur Folge hat, dass der EML2 als ein präferabeleres Ziel zur potentiellen Nutzung im Rahmen von zukünftigen bemannten Explorationen erscheint. Der WSB-Transfer zum EML2 bietet die einmalige Möglichkeit nur mittels eines einzigen hochimpulsiven Manövers an der Erde, welches von hocheffizienten kryogenen Systemen bewerkstelligt werden kann, einen direkten Einschuss in einen Librationspunktorbit am Mond zu ermöglichen, welcher für viele wissenschaftliche Nutzungen - lunare Erkundung, Teleskope, Relaisstationen, Raumstationen - ausgezeichnete Voraussetzungen bietet. Zudem ist der EML2 auch mit dem von F. Renk in [4] beschriebenen schnellen lunaren Fly-By Transfers günstig erreichbar. Für operationelle Aspekte ergänzen sich daher der langsame WSB Transfer und die schnellen lunaren Fly-By Transfers besonders gut. Unbemannte Nachschub- und Versorgungsmissionen oder auch Module für Raumstationen könnten über den WSB Transfer günstig zum EML2 transportiert werden, während bemannte Raumfahrzeuge den schnellen Fly-By Transfer nutzen können.

Contents

Task Description	i
Deutsche Kurzfassung	ii
Table of Contents	iv
Abbreviations	vi
1 Introduction	1
1.1 Future Space Exploration - The role of Libration Points	1
1.2 Fundamentals in Orbital Mechanics	2
1.2.1 Orbital Elements and Coordinate Frames	3
1.2.2 The n-Body-Problem and the numerical Approach	4
1.2.3 Circular Restricted Three-Body Problem and Libration Points	5
1.2.4 Libration Point Orbits	7
1.2.5 Invariant Manifolds - Tubes in Space	9
1.3 Weak Stability Boundary Region Transfer	10
1.4 Transfers utilizing Lunar Resonances	12
1.4.1 Moon orbit properties	12
1.4.2 Effect of Moon perturbation on high elliptic orbits: Hopping	13
1.4.3 Lunar Resonances	14
1.5 Outline & Structure	15
2 WSB Transfer to EML2	16
2.1 Weak Stability Boundary Region Transfers to EML2	16
2.2 Free transfers from LEO to EML2 Orbit	20
2.2.1 The Bisection Method	20
2.2.2 Results	21
2.2.3 Conclusions on Free Transfer Scans	28
2.3 Optimized transfers from LEO with fixed inclination	29
2.3.1 Formulation of the Optimization Problem	29
2.3.2 Influence of Earth departure Inclination	31
2.3.3 Results	32
2.3.4 Conclusions on Optimized Transfer	37
3 Lunar Resonance Transfer to EML1	38
3.1 Natural Behavior of Lunar Resonances	38
3.2 Approaching EML1 Orbits - Traveling along the Invariant Manifold	40
3.3 LEO to EML1 Transfer Trajectory Design - It's all about phasing	42
3.3.1 Entire Transfer - Strategy and Optimization Issues	43
3.3.2 Computing Transfers - Results	51

3.3.3	Conclusions on the Resonance Transfers without departure orbit consideration	56
3.4	Optimized transfers from LEO with fixed inclination	57
4	Summary and Conclusions	59
4.1	Summary	59
4.2	Conclusions	60
4.3	Outlook	61
Bibliography		62
5	Appendix	64
5.1	Appendix: Introduction	64
5.1.1	Libration Point Orbits	64
5.2	Tools	67
5.2.1	Optimized transfers from LEO with fixed inclination	68
5.3	Results	70
5.3.1	Optimized transfers from LEO with fixed inclination	70

Abbreviations

CDF	Concurrent Design Facility
ECI	Earth-centered-inertial
EML	Earth-Moon Libration Point
ESA	European Space Agency
ESOC	European Space Operations Center
IAA	International Academy of Astronautics
JWST	James Webb Space Telescope
LCR	Lunar-centered-rotating
LEO	Low Earth Orbit
LLO	Low Lunar Orbit
MJD2000	Modified Julian Day 2000: 1. January 2000 noon \Rightarrow 2451545.0 Julian date (JD)
NASA	National Aeronautics and Space Administration
ODE	Ordinary Differential Equation
S/C	Space-Craft
SEL	Sun-Earth Libration Point
SOHO	Solar and Heliospheric Observatory
SSDW	Space Station Design Workshop
WSB Transfer ..	Weak Stability Boundary Region Transfer

1 Introduction

1.1 Future Space Exploration - The role of Libration Points

Future manned space exploration is focused on the ultimate goal of landing humans on Mars. Whereas Mars is the goal some mile stones have to be taken before going there. One of the major steps is going back to the Moon. In this scope it is possible using the Earth-Moon libration points EML1 and EML2, which are located at a distance of about 60.000 km from the Moon, as staging location for missions both to the Moon (LLO or Lunar Surface), to NEO's as precursor mission to Mars and the Sun-Earth Libration Points SEL1 and SEL2 as described by the IAA Next Step Cosmic Study in 2004 [2]. Today the Wilkinson Microwave Anisotropy Probe (WMAP) observatory mapping the cosmic microwave background radiation over the full sky already is placed in SEL2 [8]. The Solar and Heliospheric Observatory (SOHO) probe from NASA and ESA is placed in SEL1 and still working after more than ten years mission duration. In future three observatories are planed to be installed at SEL2 (Herschel, Planck and JWST, XEUS, Lisa Pathfinder and many more). Servicing missions can be performed as transfer opportunity between EML2 and both SEL1 and 2 points for nearly zero Δv exist as described by Renk & Hechler [4] or Canalias & Masdemot [9].

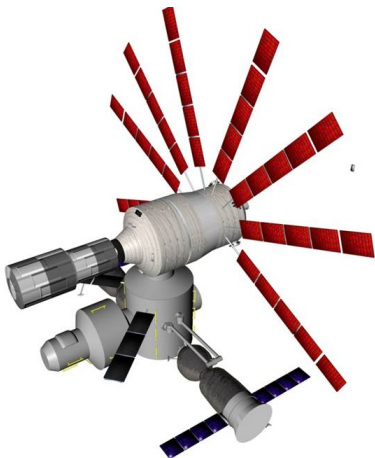
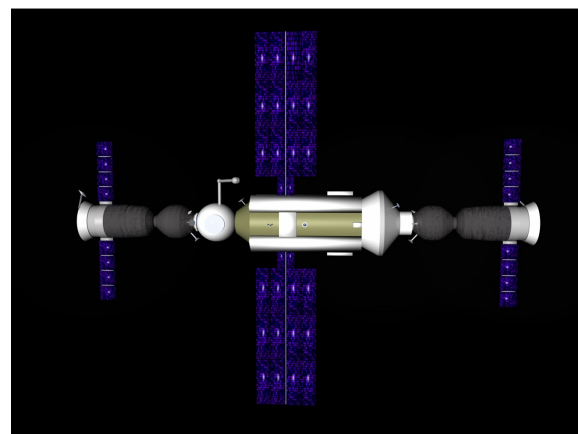


Figure 1.1: Team RED: EML2 Lunar Access and **Figure 1.2:** Team BLUE: EML2 Station - SSDW Rescue Station - SSDW 2008



Utilization of the collinear libration points in Earth-Moon system was described by Farquhar [1] in the early seventy's already. As a hub for future manned space exploration activities these points could be ideal to place a station in an orbit around them. In 2008 Space-Station-Design-Workshop (SSDW) - a special Workshop for design and mission analysis of a Space-Station organized by the department of Astronautics at Universitaet Stuttgart by Messerschmid et al. since 1996 [3] - two competing teams (RED and BLUE) investigated a mission scenario for the use of the Earth-Moon Libration Points as staging location for future Moon and Near-Earth-Object (NEO) exploration.

The result for both teams was a permanent station in EML2. Team RED called its station LARS - Lunar Access and Rescue Station - shown in Figure 1.1. Team BLUE had a 3 modules configuration (TERRA, SELENE and the Main-Station) as shown in Figure 1.2. ESA's CDF Moon Exploration Architecture Study from December 2007 has been investigating the possibility of using EML1 as staging location for manned lunar missions [10]. The result of the SSDW in 2008 showed that it can be possible to place a permanent station in EML2 with a minimum number of 3 Launches by an ARIANE V ECB or a Russian PROTON launcher. EML2 was chosen due to the cheaper lunar fly-by trajectories described by Renk [4]. Additionally a crewed mission to lunar surface and rescue mission from lunar surface could be supported. Due to the almost fixed geometry of the libration points with respect to the lunar surface they can be used to achieve permanent access to lunar surface locations without any launch window consideration which still today is the most safety critical issue for manned mission to lunar surface from LLO. In this scope Europe could play an important partner for future Moon exploration scenarios within an international cooperation. But also maintenance for SEL observatories and platforms could be performed from these stations. Even the possibility of a mission to a NEO was purposed by one of the SSDW'08 teams. This shows the possibilities and chances of an permanent outpost at one of the EML points.

As these points can play a major role in future space activities an investigation of low-cost transfers to the libration point orbits seems logical. As a major drawback of these transfer using lunar and solar perturbation to save Δv the long transfer duration has to be pointed out. Whereas manned space flight requires short transfer times, low-cost transfers with their long transfer times (≥ 3 month) give a cheap alternative for cargo missions utilizing and re-supplying of permanent human outposts beyond LEO.

The following work adds to the fast transfer investigation in [4] and is bases upon the already done work of F. Renk. In the scope of this work an investigation on two transfer options will be done:

- Weak Stability Boundary Region Transfer
- Transfers utilizing Lunar Resonances

First, an introduction into orbital mechanics from the fundamentals to the special problems is provided. Later in Chapters 2 and 3 the methodology of the work and the results for both transfers will be presented.

1.2 Fundamentals in Orbital Mechanics

The two-body problem describes the motion of two masses moving around their barycenter interacting only with each other. The fundamental physical behavior of the two bodies was formulated by Johannes Kepler (1571-1630) known as the three Kepler Law's. Therefore the two-body problem also is known as Kepler's Problem.

In 1665 Isaac Newton (1642-1727) formulated his famous inverse square law as an analytical description of the behavior of celestial bodies:

$$F = \frac{Gm_1m_2}{r^2} \quad (1.1)$$

where G is a universal constant called the gravitational constant and perhaps the most difficult physical constant to measure as gravity is much weaker than other fundamental forces [11]. It was measured 1798 - 71 years after after Newton's death - by Henry Cavendish. Even today the value of G

is only known to an accuracy of an order of $\pm 10^{-4}$. The value of G is $(6.67428 \pm 0.00067) \cdot 10^{-11} \frac{m^3}{kg s^2}$. The value of $\mu = GM_E$, on the other hand, where M_E is the mass of the Earth is known to a much higher accuracy. The value of μ is 398600.4418 ± 0.0008 $\frac{km^3}{s^2}$. m_1 and m_2 are the masses of the two considered bodies and $r = |r_1 - r_2|$ is the distance between them.

For the two body-problem Equation 1.1 is for each body:

$$\begin{aligned} m_1 \cdot \ddot{r}_1 &= -\frac{Gm_1m_2}{r^2} \cdot \hat{r} \\ m_2 \cdot \ddot{r}_2 &= -\frac{Gm_1m_2}{r^2} \cdot \hat{r}. \end{aligned} \quad (1.2)$$

where

$$\hat{r} = \frac{|r_1 - r_2|}{r} \quad (1.3)$$

is the unity vector pointing from body 2 to 1. Dividing the factors m_1 and m_2 and subtraction the resulting equations one gets the differential equation:

$$\ddot{r} = -\frac{Gm_1m_2}{r^2} \cdot \hat{r} \quad (1.4)$$

which is the analytical description of the two-body problem.

1.2.1 Orbital Elements and Coordinate Frames

As a matter of fact we need to describe an orbit with certain quantities which are known as orbital elements. These Elements and the global framework in which they are defined will be described during this section. Equation 1.4 can be completely solved analytically and the resulting orbits can be described by six orbital elements, also known as the Keplerian Elements:

- Semimajor axis (a): describes the size of the ellipse
- Eccentricity (e): describes the shape of an ellipse¹
- Inclination (i): the angle between the angular momentum vector and the unit vector in z direction ($0^\circ..180^\circ$)
- Right ascension of the ascending node (Ω ; RAAN): the angle from the vernal equinox to the ascending node. The ascending node is the point where the satellite passes through the equatorial plane moving from south to north. ($0^\circ..360^\circ$)
- Argument of perigee (ω): defines the orientation of the ellipse (in which direction it is flattened compared to a circle) in the orbital plane, as an angle measured from the ascending node to the semimajor axis. ($0^\circ..360^\circ$)
- True anomaly (Θ or ν): defines the position of the orbiting body along the ellipse at a specific time. ($0^\circ..360^\circ$)

Figure 1.3 shows the meaning of these elements. The elements are described in an earth-centered-inertial coordinate system (ECI) as shown in Figure 1.4 with the following axis:

- The x-axis is in vernal equinox direction.
- The z-axis is Earth's rotation axis perpendicular to equatorial plane.
- The y-axis is in the equatorial plane given by the right hands rule.

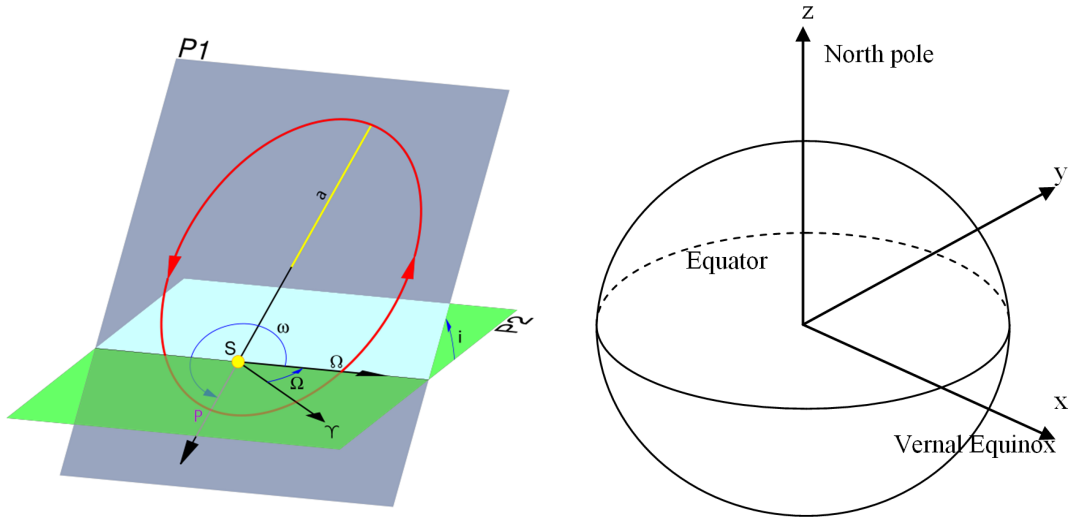


Figure 1.3: Keplerian orbital elements from wikipedia [12] **Figure 1.4:** earth-centered-inertial coordinate system

ECI coordinate frame will be used mainly during this work. To show a specific character of an orbit it sometimes might be necessary to change the center of the coordinate system. In this work the lunar-centered rotating coordinate frame (LCR) will serve for these reasons. The center is located at Moon center. The entire coordinate frame is rotating with the Moon around Earth. This might sometimes be confusing as straight lines becomes curves and vice versa. The LCR coordinate frame is defined by:

- The x-axis is pointing to the earth center building the connection between Moon and Earth center.
- The y-axis is in the equatorial plane of the moon perpendicular to the x-axis.
- The z-axis is given by the right hands rule.

1.2.2 The n-Body-Problem and the numerical Approach

The following part is based on Valado [13]:

As the two-body problem is only a special case of the general n-body problem which is the problem of finding, given the initial masses m_1, m_2, \dots, m_n of n point-masses, positions $x_j(0)$ and velocities $\dot{x}_j(0)$ of n particles with $x_j(0) \neq x_k(0)$ for all mutually distinct j and k, their subsequent motions - the solution of the second order system -

$$F_k = m_k \ddot{x}_k = G \sum_{j=1, j \neq k}^n \frac{m_j m_k (x_k - x_j)}{|x_k - x_j|^3}, \quad j = 1, \dots, n. \quad (1.5)$$

Equation 1.5 is simply Newton's second law of motion; the left-hand side is the mass times acceleration for the j^{th} particle, whereas the right-hand side is the sum of the forces on that particle. The forces are assumed here to be gravitational and given by

¹ $e = 0$: circle / $0 < e < 1$: ellipse / $e = 1$: parabola / $e > 1$: hyperbola

Newton's law of universal gravitation (Equation 1.1). Solving differential equations normally requires a fixed number of integration constants. When initial conditions alone don't provide a solution, integrals of the motion can reduce the order of the differential equation, also called degrees of freedom. The n -body problem contains $6n$ variables - three space and three velocity components - in a system of $3n$ second-order differential equation. Therefore we need $6n$ integrals of the motion for a complete solution: Conservation of linear momentum provides six, conservation of energy one, and conservation of linear angular momentum three, for a total of ten. This leaves a system of $6n - 10$ for $n \geq 3$. These equations for n -bodies, $n \geq 3$, defy all attempts at closed-form solutions. H. Brun showed that there were no other algebraic integrals in 1887. Poincaré later generalized Brun's work even though it did not bring out any further integrals.

Today the equation of motion can be integrated numerically by first-order ODE's methods of line like the Runge-Kutta scheme. As the basic idea behind the numerical integration is to add all forces of n bodies on a point in space and integrating them up in time, it is possible to recognize as many bodies as requested for the specific problem. Theoretically one could take all planets of our solar-system into account to calculate the forces on a certain point in space. But this would request a lot of computational effort which is not always necessary, as for example the influence of Jupiter on a S/C traveling on an orbit around earth is negligible - apart from that a double precision variable can only display 16 digits which is much too less for the difference between forces of Jupiter and Earth.

In this work the numerical integration only will take Sun, Earth and Moon into account for calculating the forces on the S/C at a certain point in space. For this work it is important to use these three bodies as we want to use the gravitational effects of them on a S/C to design special trajectories which would not be possible to generate without recognizing these bodies.

Implementation has been done with MATLAB (version 2007b) using MATLAB-executable-functions (mex-function) written in FORTRAN for the integration due to the speed-up for FORTRAN implemented software. Integration has been performed by a 7th order Runge-Kutta-Fehlberg-Scheme Formula 7(8) [14] - also known as RKF78 - which is a standard integration routine for astrodynamical computations. This version is based on ESOC's mission analysis software.

1.2.3 Circular Restricted Three-Body Problem and Libration Points

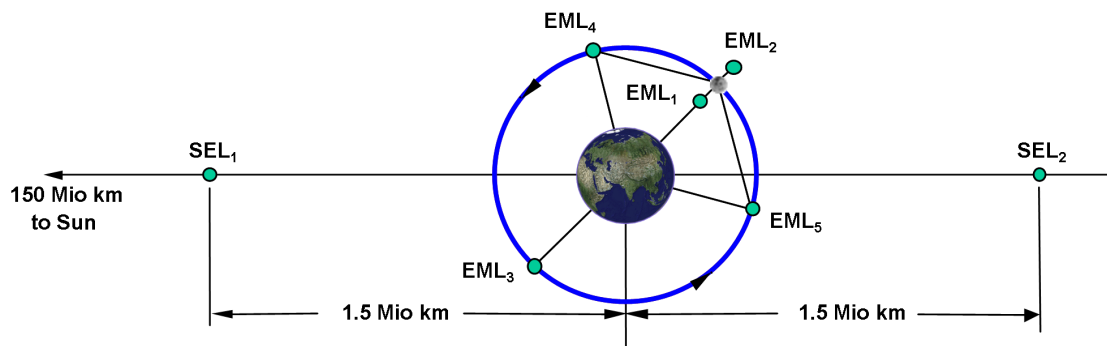


Figure 1.5: Libration Points in Sun-Earth-Moon-System by Farquhar [1]

As it was not possible to solve the general three body problem work has focused on simplifying the general problem. Sundman found a series solution in 1912. One special analytical solution has been known since the time of Euler and Lagrange² - the Restricted Three-Body Problem (RC3BP) - this problem has received significant attention. It makes two simplifying assumptions:

1. The primary and secondary bodies move in circular orbits about the center of mass, which lies between the two objects.
2. The mass of the third body (e.g. satellite) is negligible compared to the ones of the major bodies, i.e. it does not affect the motion of the other two bodies.

As the general three-body problem would require 18 scalar first-order differential equations to completely describe the resulting motion the restricted three-body problem could according to the mass distribution make some major simplifications. As the mass of the third body was negligible w.r.t. to the mass of the two primary bodies - and so on the influence of gravitational effects of the third body on the primaries - the solution of their motion is reduced to a two-body problem [15].

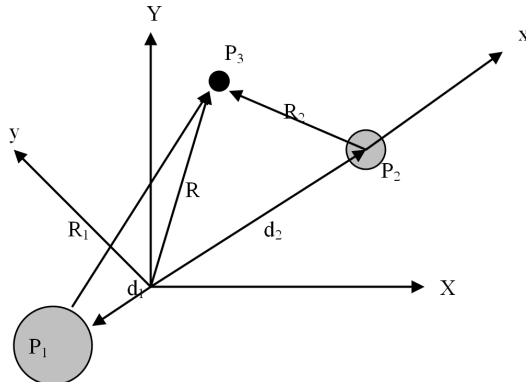


Figure 1.6: Geometry of the restricted three-body problem (RC3BP) from McInnes [15]

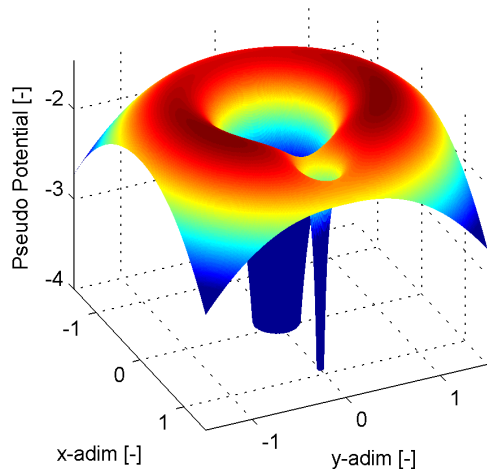


Figure 1.7: Pseudo potential map of Earth-Moon system in adimensional barycentric coordinates

The following part is taken from F. Renk [4]:

In a rotating coordinate frame shown in Figure 1.6, where the x-axis points from the primary body to the secondary, e.g. the Earth to the Moon, the z-axis points in the direction of the orbit normal and the y-axis supplements the system to be a right hand one, the well known linear approximation for the differential equation for the motion in the circular restricted three-body problem (RC3BP) can be written as

$$\begin{aligned} \ddot{x} - 2\dot{y} &= U_x, \\ \ddot{y} - 2\dot{x} &= U_y, \\ \ddot{z} &= U_z. \end{aligned} \tag{1.6}$$

²It was first formulated by Leonhard Euler in 1762 [15]

The distances and velocities are normalized by the current distance between the primaries and their angular velocity, respectively, and the pseudo-potential U is:

$$U = \frac{1-\mu}{r_1} + \frac{\mu}{r_2} + \frac{1}{2}(x^2 + y^2) \quad (1.7)$$

with $\mu = \frac{m_2}{m_1+m_2}$ and m_1, r_1 and m_2, r_2 being the masses and distances of the spacecraft (S/C) from primary and secondary, respectively.

A more detailed explanation of the mathematical solution of the restricted three-body problem can be found in [16] or [15].

From Equation 1.6 an equilibrium solution exists to the rotating frame shown in Figure 1.6 when the partial derivatives of the pseudo-potential in Equation 1.7 (U_x, U_y, U_z) are all zero, i.e., $\nabla U = 0$. In other words this means for Equation 1.5 ($n = 3$) the forces of the major bodies on the third body equals zero. This leads to 5 unique points named libration points, also known as the equilibrium or Lagrange Points. Three of them are called "collinear" points, since they lie along the line joining the primaries ³. The other two points, known as the "triangular" libration points since they form equilateral triangles with the primaries in the plane of primary motion ⁴ are located on the circular orbit of the second primary body. Figure 1.5 shows the location of the five Earth-Moon libration points and the two collinear near Earth located libration points of the Sun-Earth. While L_1, L_2 and L_3 are unstable L_4 and L_5 are stable points. In Figure 1.7 the pseudo-potential of the RC3BP shows the reason for this. The pseudo-potential has a saddle environment around L_1, L_2 and L_3 whereas L_4 and L_5 are located in a potential valley. The mathematical formulation of this will be given in Section 1.2.4.

1.2.4 Libration Point Orbits

The following part is taken from [4] by courtesy of F. Renk:

Even though this work does not mainly deal with the construction of libration point orbits a brief view to the fundamentals of the mathematics behind these orbits shall be given. The mathematical fundamentals of the construction of libration point orbit is based on the restricted circular three body problem (RC3BP) which is a simplification of the real planetary motion. It only takes the two primary bodies (Moon and Earth in this case) and the third body - the S/C - into account.

The general solution for the collinear points can be written as:

$$\begin{aligned} x &= A_1 e^{\lambda_{xy} t} + A_2 e^{-\lambda_{xy} t} + A_3 \cos(\omega_{xy} t) + A_4 \sin(\omega_{xy} t), \\ y &= c_1 A_1 e^{\lambda_{xy} t} - c_1 A_2 e^{-\lambda_{xy} t} + c_2 A_4 \cos(\omega_{xy} t) - c_2 A_3 \sin(\omega_{xy} t). \\ z &= A_z \cos(\omega_z t + \Phi_z) \end{aligned} \quad (1.8)$$

with the constants $c_1, c_2, \lambda_{xy}, \lambda_z, \omega_{xy}$ and ω_z solely depending on the mass parameter μ and the integration constants $A_1, A_2, A_x, A_y, A_z, \Phi_{xy}$ and Φ_z depending on the initial condition of the system. This solution gives a good idea of the motion on a libration orbit and also about a transfer strategy. The initial conditions \vec{x}_0 can be selected in such a way that only the oscillatory mode with the amplitudes A_3, A_4 and A_z are excited. The exponential terms are then not involved in the solution and we have two oscillations with

³Identified 1762 by Leonhard Euler [15]

⁴Identified 1772 by the Italian mathematician Joseph-Louis Lagrange [15]

slightly different frequencies, one in the xy-plane and one in the z-direction- For the in- and out-of-plane motion the amplitudes A_x , $A_y = c_2 A_x$ and A_z can be calculated. The resulting trajectory in the rotating frame is a Lissajous figure, hence, these orbits are called Lissajous orbits. The solution to the equations of motion as provided in Equation 1.8 is based in the linearized equations of motion of the RC3BP and is therefore only valid on the vicinity of the associated libration points. For large libration point orbit amplitudes the non-linear effects will have to be taken into account. Since a numerical propagation in a realistic system, e.g. taking the eccentricity and third body perturbations into account, will always deviate from this solution, a set of "osculating Lissajous elements" $[A_1, A_2, A_x, A_y, A_z, \Phi_{xy}, \Phi_z]$ can be defined similar to the "osculating Kepler elements". The following relationship allows for their calculation at a given epoch (setting $t=0$):

$$\begin{aligned} x &= A_1 e^{\lambda_{xy} t} + A_2 e^{-\lambda_{xy} t} + A_x \cos(\omega_{xy} t + \Phi_{xy}), \\ y &= c_1 A_1 e^{\lambda_{xy} t} - c_1 A_2 e^{-\lambda_{xy} t} - c_2 A_x \cos(\omega_{xy} t + \Phi_{xy}), \\ z &= A_z \cos(\omega_z t + \Phi_z), \\ \dot{x} &= A_1 \lambda_{xy} e^{\lambda_{xy} t} - A_2 \lambda_{xy} e^{-\lambda_{xy} t} - A_x \cos(\omega_{xy} t + \Phi_{xy}), \\ \dot{y} &= c_1 A_1 e^{\lambda_{xy} t} + c_1 A_2 e^{-\lambda_{xy} t} - c_2 A_x \cos(\omega_{xy} t + \Phi_{xy}), \\ \dot{z} &= A_z \omega_z \sin(\omega_z t + \Phi_z). \end{aligned} \quad (1.9)$$

Perturbations on the trajectory will always cause a small A_1 component to exist, making the collinear libration point orbits unstable.

The two exponential terms in Equation 1.9 represented by the so called stable and unstable amplitudes A_2 and A_1 , can be associated with the so called "stable" and "unstable" manifolds - shown in Figure 1.8 - which are "tubes" in space leading to or departing from the libration point orbit [4]. These terms can be excited for a S/C moving on a libration point orbit by firing either in the unstable direction:

$$\vec{u}_1 = \begin{pmatrix} \frac{-c_2}{d_2} \\ \frac{1}{d_1} \\ \frac{1}{d_1} \end{pmatrix}, \quad (1.10)$$

or the perpendicular stable direction:

$$\vec{s}_1 = \begin{pmatrix} \frac{1}{d_1} \\ \frac{c_2}{d_2} \\ \frac{1}{d_2} \end{pmatrix}, \quad (1.11)$$

based upon the constants c_1 , c_2 , solely depending on the mass parameter μ and the integration constants $A_1, A_2, A_x, A_y, A_z, \Phi_{xy}$ and Φ_z depending on the initial condition of the system.

As long as $A_1 = 0$ and A_2 gets terminated by the exponential part of the expression the left part of the equation with cosine and sinus will dominate the motion. The result of such a motion is a libration point orbit. Even though it not will be explained how to construct such an orbit in this work at least an easy explanation is to make sure by adding a certain Δv - which has to be seen as a numerical correction - either in the stable or unstable direction to keep both the A_1 and A_2 parts of the equation within certain boundaries. This can be done by different methods as described by Renk [4], Gomez [17], Hechler [18] or McInnes [15].

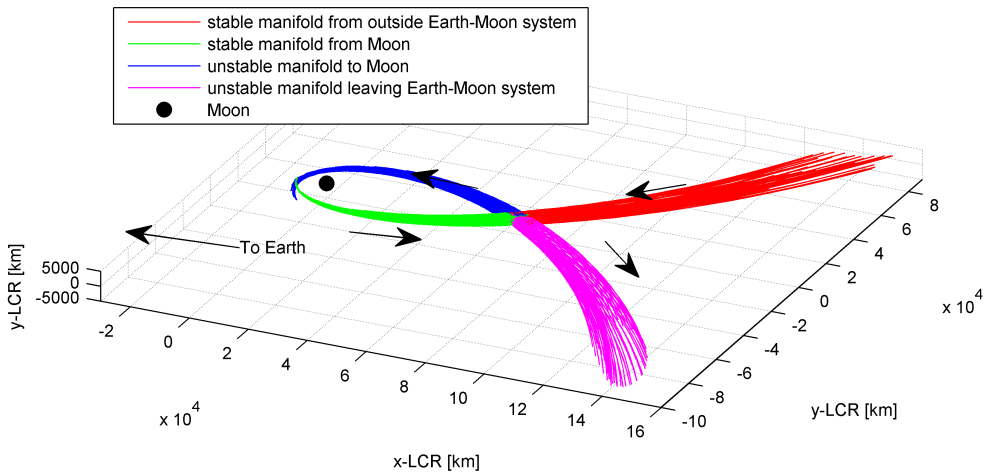


Figure 1.8: stable and unstable manifolds for EML2 Lissajous orbit (for further orbit information: see Appendix 5.1.1)

1.2.5 Invariant Manifolds - Tubes in Space

Imagine a S/C being on a Lissajous orbit around EML2: By firing into negative stable direction and integrating backwards in time leads to a trajectory leaving the Moon. Mathematically this means that the exponential terms of Equation 1.9 gets excited and forces the S/C to leave the libration point orbit. Doing this from different points of the trajectory will lead to a set of trajectories building "tube" - the so called stable manifold shown in Figure 1.8. Remember that this is a backwards integration in time. Forward in time this would mean that the surface of the tube is generated by all the trajectories that asymptotically wind onto the libration point orbit. The outcome of the integration depends of course from the direction in which the manoeuvre has been performed. It can happen, that the tube either comes from the Moon or goes away from it. As long as the trajectory leads to an libration point orbit it is coming from the stable manifold.

This leads to the following definition of the invariant manifolds:

1. The **Stable Manifold** is the surface of the tube generated by all the trajectories that asymptotically wind onto the libration point orbit. It can be generated by firing into stable direction and integrating backward in time.
2. The **Unstable Manifold** is the surface of the tube generated by all the trajectories that asymptotically wind off of the libration point orbit. It can be generated by firing into unstable direction and integrating forward in time.

The expression stable and unstable manifold comes from the "chaos theory". For further reading about the invariant manifold - the global approach to the stable- and unstable manifolds - the following articles by Gomez, Lo and Mardsen are recommended [19] and [20]⁵.

Summarizing the last points leads to: Every libration point orbit has both a stable and an unstable manifold. The stable manifold will always lead to the libration point orbit whereas the unstable

⁵Both articles are available at <http://www.gg.caltech.edu/mwl/publications/publications2.html>

manifold will lead away from the orbit.

In EML1 manifolds are coming either from the Moon or from the Earth but not from outside the Earth-Moon system. This is the major difference to the EML2 manifolds and makes it hardly possible to design a transfers to EML1 via the WSB region like transfer to EML2 - even though it might be possible. Figure 1.9 shows the manifolds of an orbit around EML1.

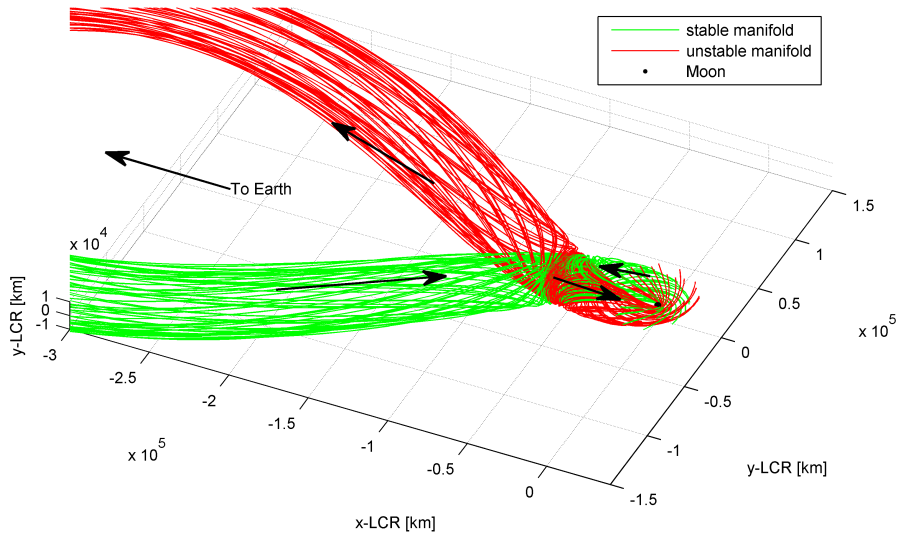


Figure 1.9: stable and unstable manifolds for EML1 Halo orbit (for further orbit information: see Appendix 5.1.1)

1.3 Weak Stability Boundary Region Transfer

In April 1991 the Japanese S/C "Hiten" (known before launch as Muses-A) became the first S/C to fly to the Moon on a low energy lunar transfer via the Weak Stability Boundary (WSB) region by only using 10 % of the required fuel to make it into lunar orbit [21].

Transfers using the WSB region⁶ near the SEL points - first described by E. Belbruno [7], [22] and [23] - uses the gravitational pull of the Sun excited by the Sun gravity gradient shown Figure 1.11 to raise the pericenter altitude of the transfer trajectory as shown in Figure 1.12. The gravitational gradient is defined by:

$$\text{SunGravityGradient} = \frac{\mu_{\text{Sun}}}{R^3} \cdot [3RR - u]r. \quad (1.12)$$

where R is the Earth to Sun radius vector, r is the Earth to satellite radius vector, μ_S is the Sun gravitational constant, u is the unit dyadic [24]. The different stages of the transfers commonly described are:

1. The S/C must travel to an apogee with an altitude of about 1.5 million km (SEL-Region) in order to achieve the desired effect of the gravitational pull of the Sun passing through the WSB region shown in Figure 1.13.

⁶shown in Figure 1.13

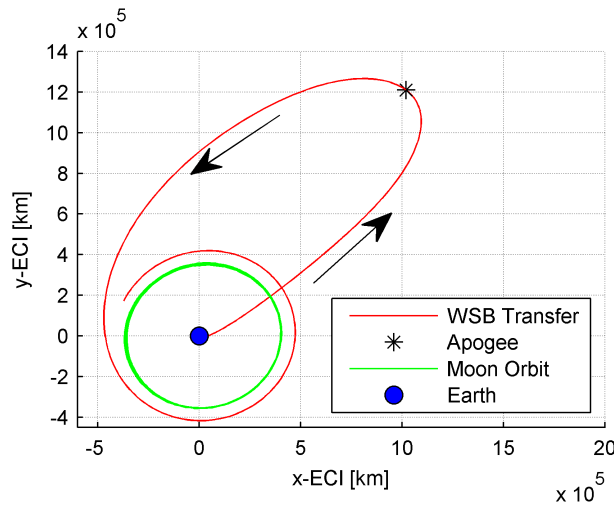


Figure 1.10: EML2 WSB transfer - bifurcation

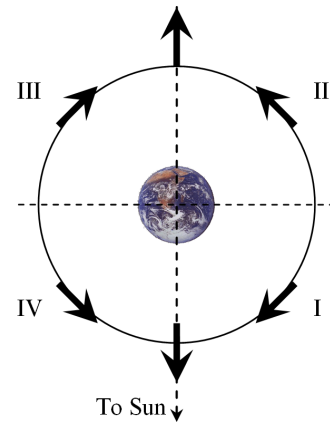


Figure 1.11: Sun gravity gradient

2. Going back from the apogee the gravitational pull of the Moon leads to a ballistic capture of the S/C.
3. To go into LLO an additional circularization manoeuvre has to be performed.

Such a high apogee will result in a very long transfer duration (≥ 90 days) due to the small speed in high eccentric orbit apogees which also is the major drawback of this transfer. A WSB transfers have been investigated by GMV and the software tool WESBOT [24] to design WSB transfers to lunar orbits has been developed and is available at ESOC.

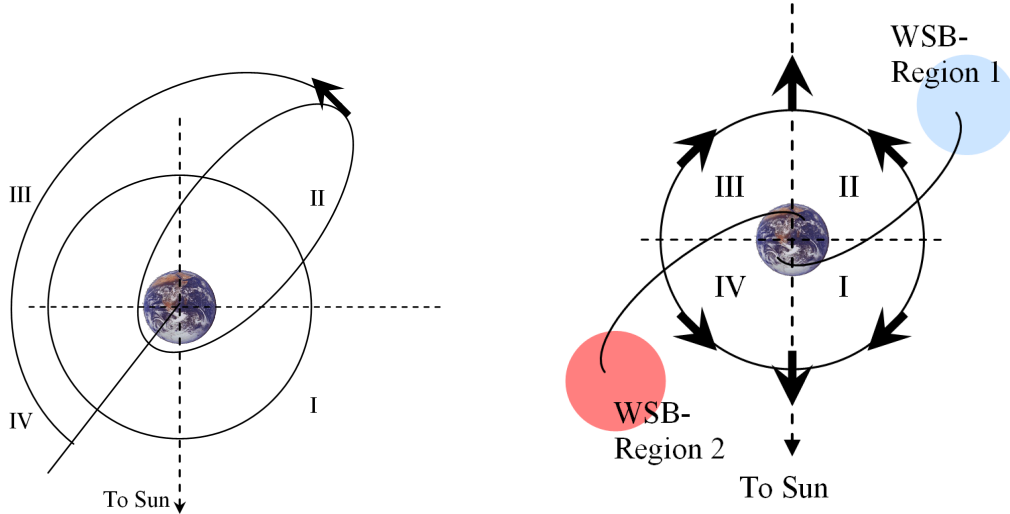


Figure 1.12: Perigee raising via Sun perturbation (for pro-grade transfers)

Figure 1.13: Sun-Earth-WSB regions w.r.t. the Sun position (pro-grade transfers)

WSB transfer only appears when the S/C is passing through the WSB regions. Passing the WSB region in different positions w.r.t. to the Sun position leads to very different gravity perturbations by the Sun. Of course the Sun gravity gradient is always perturbing the trajectory when going to a

distance of ~ 1.5 million km away from Earth but only in the right constellation this perturbation leads to a WSB transfer. Figure 1.13 gives a simplified setup of this constellation. Only transfers reaching their apogee in quadrant II and IV will get the right acceleration to perform a WSB transfer while transfers reaching their apogee in quadrant III and I will get the wrong acceleration and a WSB transfer will not result. At least not pro-grade transfers going into the shown direction. Retrograde transfers of course will be accelerated in the right way and a transfer can occur.

1.4 Transfers utilizing Lunar Resonances

Most former approaches to design a transfer from Earth to EML1 mainly do not take lunar resonances into account. Even though most of the described ones (e.g. by Farquhar [1] or Renk [4]) are using the gravitational attraction of the Moon to gain orbital energy the successive use of the gravitational pull of the Moon at every lunar encounter of the S/C is a different way to design transfers. The first mission using the gravitational pull of the Moon to raise the perigee was SMART 1 in 2003 [6]. In the following sections a brief introduction to the idea behind the lunar resonances will be given.

1.4.1 Moon orbit properties

To achieve a lunar resonance a good knowledge about the Moon orbit w.r.t. the Earth is necessary. Therefore a brief view to the Moon orbit properties will be given, mainly taken from CS mission analysis working paper by J. Schoenmaekers, ESOC, [5]:

The Moon is orbiting the Earth, inclined by 5.1 deg to the ecliptic with a perigee radius around 365 tkm, an apogee radius of 405 tkm and a revolution 27.3 days. The Earth-Moon distance over 20 years is shown in Figure 1.14. The perigee rotates forward with a period 8.9 years as shown in Figure 1.15. The ascending node of the Moon in the ecliptic rotates backwards with a period of 18.6 years. Because of the inclination of the ecliptic of 23.5 deg to the equator, this leads to a variation in the inclination of the Moon orbit w.r.t. the equator between 18.3 and 28.6 deg. From this also follows a variation of the right ascension of the ascending node w.r.t. the equator between -13 and +13 deg as shown in Figure 1.16.

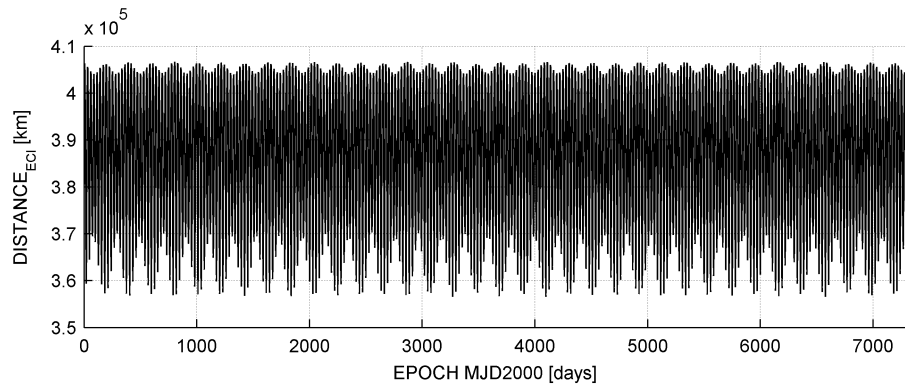


Figure 1.14: Earth-Moon distance

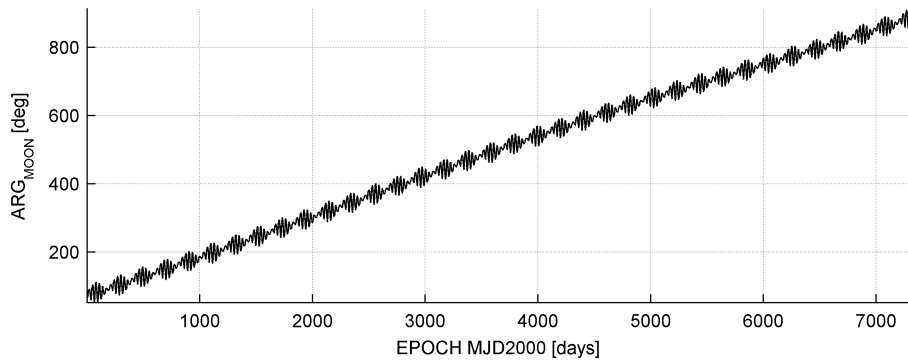


Figure 1.15: Moon orbit: Perigee right ascension Ω

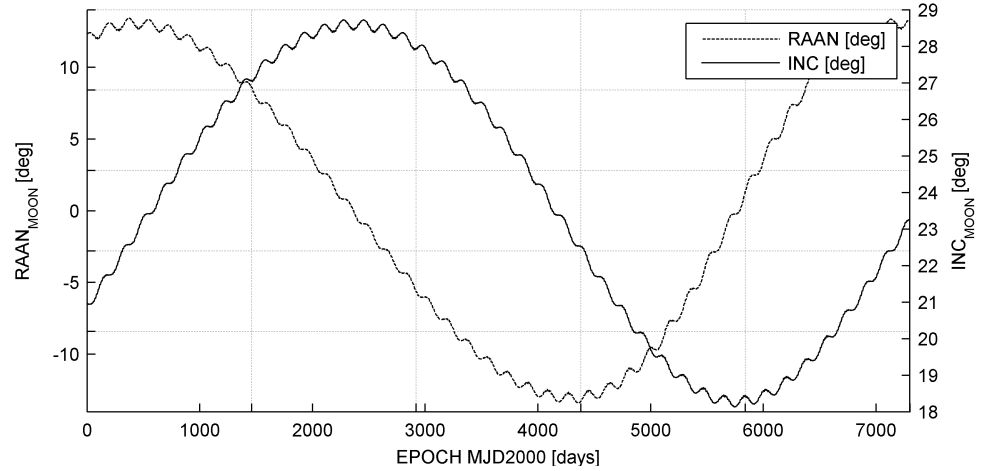


Figure 1.16: Moon orbit: Inclination and Ω

1.4.2 Effect of Moon perturbation on high elliptic orbits: Hopping

A transfer utilizing lunar resonances makes use of the gravitational pull of the Moon in order to raise the perigee of an S/C orbit lagging behind the Moon at a close encounter. The maximum perigee increase is obtained for a phase difference of about 15 deg. Figure 1.17 shows the principle behind a lunar encounter. In the apogee the S/C gets attracted by lunar gravitational pull and the perigee is raised by a lunar encounter. The gravitational attraction of Moon is the perturbing acceleration on a S/C orbiting around the Earth encountering Moon in its apogee as shown in Figure 1.18. The angle α is the phase offset of the S/C and the Moon. It has a main influence on the force components in an along track (T) and a cross track (S). Angle β has the main influence on the out of plane component (W). For high eccentric orbits with an apogee altitude of 150 tkm up to 350 tkm this acceleration will raise the perigee very effective and a so called hop appears. Phasing the lunar encounter makes it possible to raise the perigee again after an integer number of revolutions around Earth. This phenomena is called a lunar resonance.

These resonances can be reproduced in sequences and a certain Δv saving will appear at each lunar encounter.

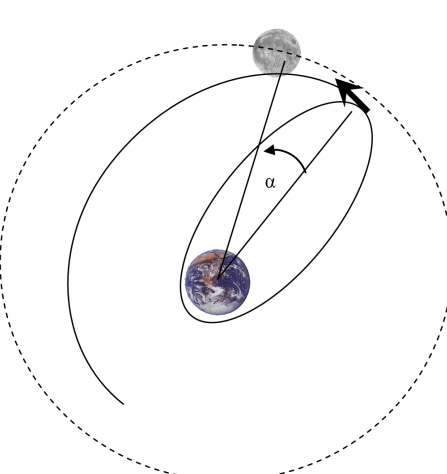


Figure 1.17: Basic idea of lunar resonance

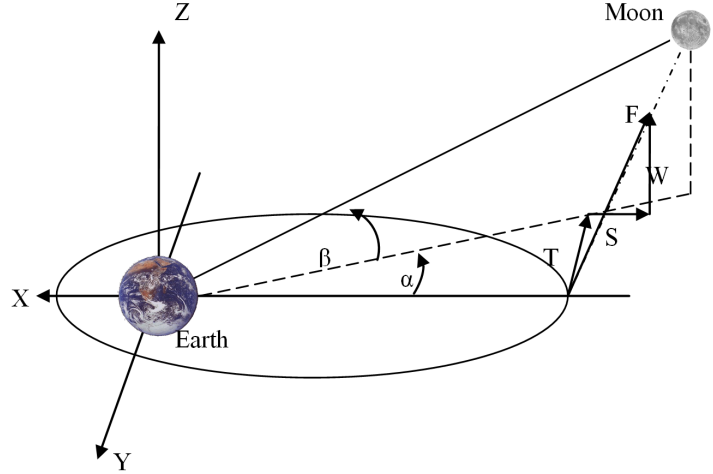


Figure 1.18: S/C acceleration by Moon resonance: Forces at lunar encounter (from [5])

1.4.3 Lunar Resonances

While Section 1.4.2 mainly dealt with the effect of lunar perturbations on orbits encountering the Moon in their apogee this section will deal with a more global aspect of this phenomenon. The idea behind a resonance sequence of orbits is to keep the orbital period on an integer part of an entire lunar revolution to get a lunar encounter after a certain number of revolutions again. Let m be the number of lunar revolution and n the number of orbital revolutions the following relation must be fulfilled to achieve a resonance:

$$n_{\text{Orbit}} \cdot P_{\text{Orbit}} = m_{\text{Moon}} \cdot P_{\text{Moon}}. \quad (1.13)$$

As the orbital period is defined by:

$$P_{\text{Orbit}} = \frac{2 \cdot \pi \cdot a^{3/2}}{\mu} = \frac{m_{\text{Moon}} \cdot P_{\text{Moon}}}{n_{\text{Orbit}}} \quad (1.14)$$

the semi major axis of the resonant orbit has to be:

$$a = \left(\frac{m_{\text{Moon}} \cdot P_{\text{Moon}}}{n_{\text{Orbit}} \cdot 2\pi} \sqrt{\mu} \right)^{2/3}. \quad (1.15)$$

If the perigee radius r_{Peri} is known the apogee radius r_{Apo} can be calculated by:

$$r_{\text{Apo}} = 2a - r_{\text{Peri}}. \quad (1.16)$$

Figure 1.19 shows a selection of possible sequences of lunar resonances calculated by this formulas. The major questions to be solved for a transfer from LEO to an EML1 orbit is to find the right resonance sequences and the number of sequences to be performed to raise the apogee and perigee on the required altitude to approach the specific libration point orbit. Table 1.1 shows the semi major axis resulting from the different resonance sequences. In deed, this information does not have such a big impact on the analysis as the major parameter for the efficiency of a resonance always will be the apogee altitude.

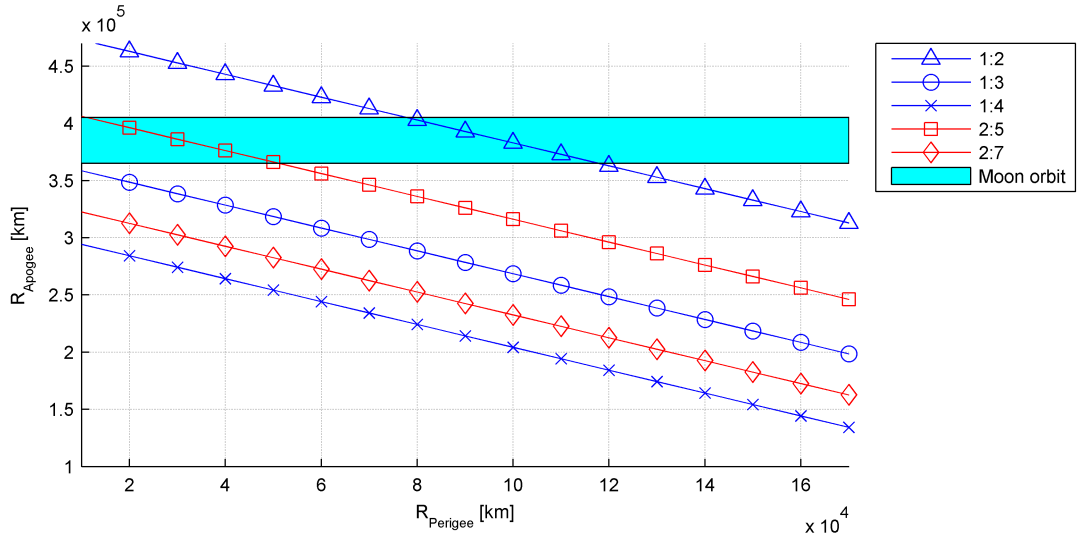


Figure 1.19: Possible Lunar Resonances for different perigee-apogee combinations

$m_{Moon} : n_{Orbit}$	Semi major Axis [km]
1:2	241450
2:5	208075
1:3	184261
1:4	152104

Table 1.1: Resonance sequences and the semi major axis of orbits fulfilling these sequences (by Equation 1.15)

1.5 Outline & Structure

In the following Chapters the WSB transfer will be described in detail, followed by the description of the applied methods to design the different transfers. First a simple single shoot method will be explained. After this an optimization approach towards more specific launch orbit requirements will be explained and a method to apply this approach will be presented. An analysis to the gained results will be made and the essential conclusion will be pointed out.

In Chapter 3 the natural features of the transfers utilizing lunar resonances will be described in detail, followed by an analysis about the possible optimization techniques toward autonomously transfer design. The applied method to generate transfers utilizing lunar resonances will be explained and an analysis towards the results of the computations will be given.

Finally a summary will provide an overview to the performed research of this work followed by a short analysis and the major conclusions drawn from the results. A trade off between the two transfers toward different issues will be given and a final rating of which transfers could be the favorable one in future space exploration activities.

An outlook to the possibilities the transfers offers will be made. Open questions that could not be solved within this work will be pointed out. Additionally data of used orbits, tools and results will be provided in the appendix.

2 WSB Transfer to EML2

The Weak Stability Boundary Region Transfer will be investigated to design an optimal low cost transfer to the trans lunar collinear libration point EML2 in the Earth Moon system. Investigating this transfer will be done in three steps:

- Bifurcations and natural behavior of transfers to EML2
- Free transfers from LEO to EML2
- Optimized transfers from LEO with fixed inclination

The first part of this chapter will give an explanation to the basic principles of the WSB transfers aided by some numerical experiment to make them more comprehensive. During this section all necessary information to understand the following application for WSB transfer design will be given. The first method used to compute WSB transfer by an easy backwards shooting method will be explained and the results of this method will be analyzed. An optimization approach to reach more launch orbit requirement will be the next step in the analysis of the WSB transfer. The relation between the first method and the optimized method will be analyzed.

2.1 Weak Stability Boundary Region Transfers to EML2

Generating a WSB transfer requires a lot information about the basic principles behind such a transfer. This knowledge will be provided throughout this section. For the later application of these transfers the given information in this section will be essentially. At first a description of the transfer and its different phases will be given and than how the transfer can be generated. A backwards shooting method will be used to create transfers for different arrival epochs on the given EML2 orbits. This is necessary as these fundamental techniques will be base of the later WSB transfer generators.

The natural appearing WSB transfer from LEO to the Moon passing the Sun-Earth Weak Stability Boundary region has a typical shape which is shown in Figure 1.10. These transfers occurs suddenly with small changes in the initial conditions at Earth departure which also leads to another well known name given to these transfers: Fuzzy Boundary Transfers. Now the typical path of a WSB transfer to an EML2 orbit will be described. Propagating a trajectory forward in time into the Sun-Earth WSB region - as shown in Figure 1.13 - from a given LEO with a Δv of 10 to 50 m/s smaller than the Δv_{Escape} a certain apogee will be reached at a distance of ~ 1.5 million km. In the WSB region the Sun pulls the S/C and the typical bow appears on the descending arc of the transfer which draws the S/C onto a trajectory leading to an orbit around EML2. This part of the transfer makes use of the stable manifold which should lead, by the definition given in Section 1.2.5, to an orbit around EML2. In this case we can not say that the S/C is directly traveling the entire stable manifold but it is using it.

Cruising close to the stable manifold followed by a manoeuvre into the negative stable direction at a

certain point leads to an earlier insertion into an orbit around the libration point instead of traveling the entire stable manifold until the orbit is reached.

The reason for shooting into the negative direction and not into positive one is the behavior of the transfers appearing from this. To use the stable manifold a Δv into the stable direction integrating backwards in time has to be performed as described in Section 1.2.5.

In the following the different phases of the WSB-Transfer will be summarized:

- Departure from LEO into transfer trajectory
- Reaching the apogee in the WSB region
- Cruising close to the stable manifold of the ELM2 orbit
- Insertion manoeuvre on the EML2 orbit at a certain point

The last phase is the most interesting part of the entire transfer because of the special behavior towards the transfer time. As long as the transfer comes from the same WSB region it travels along the same stable manifold. Only the insertion manoeuvre brings it on its arrival state of the EML2 orbit. The interesting thing of this manoeuvre is that, the longer a S/C travels along the stable manifold the less Δv_{EML2} will be required to insert it on an orbit. In fact the S/C has to travel longer or shorter on the libration point orbit always coming from the same insertion point but traveling to different points on the orbit. This can be formulated by the following relation

$$\Delta v_{EML2} \sim \Delta T_{Traveltime-along-stable-manifold} \quad (2.1)$$

Concerning orbit rendezvous issues this allows tuning to different arrival dates - and therewith phase angles Φ of the orbit insertion - even though the S/C comes from the same quadrant of the WSB region. As the WSB region fixes the transfer geometry to a fixed departure epoch this leads to launch windows.

Later in this work the launch windows will play important role and a proper analysis to this issue will be given. This section will go with the method how to create a WSB transfer and give a rough idea of the implementation.

As it is very unlikely to find this transfer in forward method from LEO due to the wide range of Δv_{LEO} that leads to the right manifold another method has to be used. With a forward method this could be compared to mount a fiber to a certain needle in a stack full of needles by shooting the fiber in to the stack from a fixed point. Obviously it's much easier to do it in a backwards procedure since we know which needle we want to mount the fiber on. So we shoot the fiber mounted to the needle to the fixed position from where the procedure should start. Analogue to this example the transfer between LEO and a certain point on a libration point orbit can be done in a backwards propagation methods from this point.

To hit the right apogee of the transfer trajectory passing the WSB region is the main issue of this method. Shooting from different arrival epochs backward in time should lead sooner or later to a trajectory passing the WSB region.

To get a better idea of the distribution of transfers for a certain arrival epoch numerical experiments has been performed. The first experiment starts from a Lissajous orbit shooting with a $\Delta v_{EML2} = 1$ m/s and integrating backwards on the stable manifold leaving the Earth-Moon system. Starting on thirty sequent days from different phase angles leads to Figure 2.1 when stopping at a distance of ~ 1.5 million km which should be in the right constellation the WSB region. Additionally, the scaled position of the Sun is shown in the apogees of the shown trajectories.

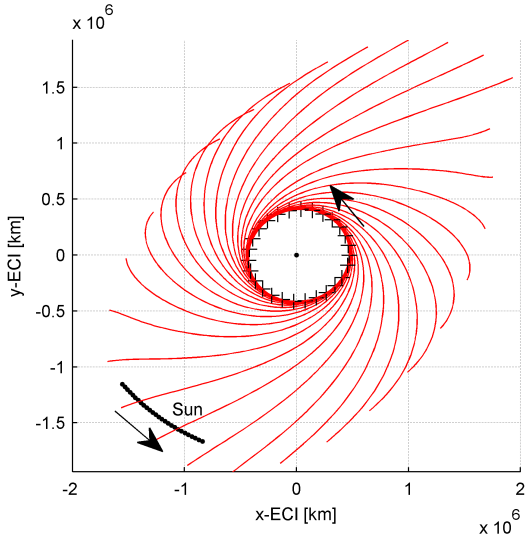


Figure 2.1: stable manifold for Lissajous orbit at EML2 in ECI frame

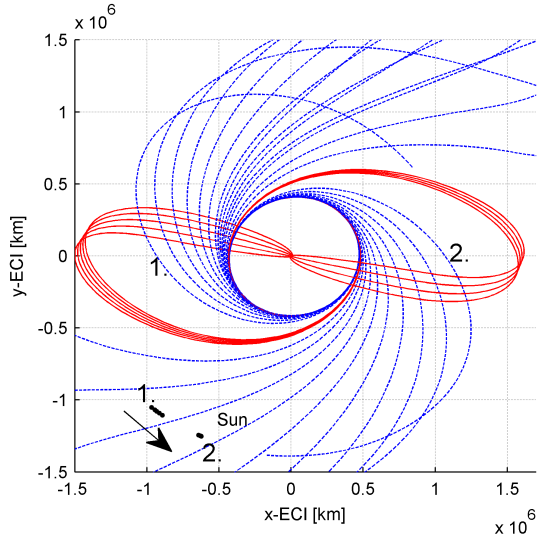


Figure 2.2: Transfers occurring when the stable manifold passes the WSB region

It can be found that exactly at the positions where the WSB regions should be suggested the trajectories are getting an apogee at about 1.5 million km distance to Earth. This gives a first guess of how to reach the WSB region in a backwards approach. But for now only half the way to earth has been done. The next step will be to integrate the trajectory for a longer time and to see where it ends up.

Figure 2.2 shows what happens when integrating the trajectories until they either reach Earth at a distance ≤ 10 tkm radius or when escaping Earth-Moon system. Again the position of the Sun is shown, but now only for the WSB transfers reaching Earth. It can be found that the WSB region gets passed twice during a 30 days period and that WSB transfers only occurs in in Figure 1.13 mentioned areas.

For a fixed Δv_{EML2} a transfer can occur if it start from the right epoch as shown in Figure 2.2. This makes it impossible to achieve a transfer with the same Δv_{EML2} on every epoch. Due to the mission analysis requirement to reach a libration point orbit at a certain epoch this fact is very unsatisfying as we are not able to reach an orbit at every epoch with the same Δv_{EML2} . Event though from a computational point of view this would be very good as is means low computational effort - integrating only once per epoch - it is clear that another method has to be chosen.

In the following a better method to find transfers for every arrival epoch without any constraints will be explained.

Relation 2.1 tells that different Δv_{EML2} will lead to different insertion epochs into the libration point orbit. As we can not predict the exact Δv_{EML2} that will be required we need to check this numerically by scanning through the Δv_{EML2} range. Shooting with the correct Δv_{EML2} would lead to a transfer directly to an orbit passing Earth at a certain distance defined by the user. The basic working principle of this method is shown in Figure 2.3. Figure 2.4 shows how many transfers are occurring over a Δv_{EML2} range of 1...10 m/s scanning with a step size of 0.1 m/s. Every line stands for a transfer. Some trajectories are escaping the Earth-Moon system and some are reaching the distance of 10 tkm radius above Earth which leads to an abort of the integration. For one epoch three windows where WSB transfers occurs can be identified as shown in Table 2.1. Scanning with

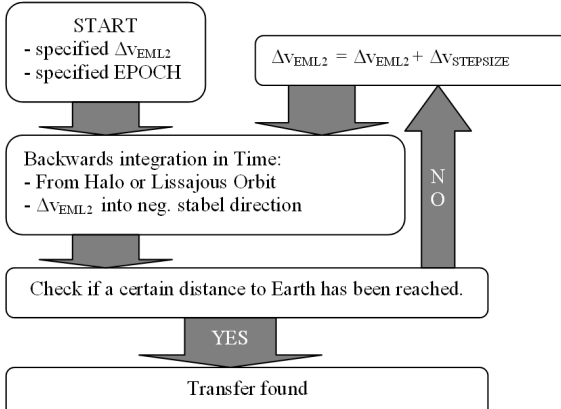


Figure 2.3: EML2 simple event integrator for abort at certain distance to Earth

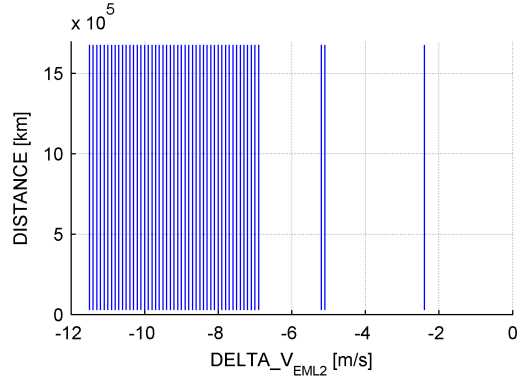


Figure 2.4: backwards integration from EML2 orbit for 0...-10 m/s into stable direction

	1.	2.	3.
Δv_{EML2} [m/s]	-2.5	-5.1	-6.8 to -10

Table 2.1: Transfer distribution for Δv_{EML2} range: 0...-10 m/s into stable direction at epoch 7400 MJD2000

discrete Δv_{EML2} steps leads to a big numerical problem. To find a transfer a lot of integrations have to be performed which will result in a huge computational effort. The second problem is the sampling of the result which can be found in Figure 2.1. Without knowing how big the stepsize needs to be to find all interesting transfers a lot of computational power can be wasted in scanning through a specific Δv_{EML2} range. In the shown experiment the range was limited to 1...10 m/s. Later scans will reduce this range to 0...1 m/s and the stepsize also will be reduced to 0.001 m/s. This has a tremendous impact on the computation time as for every epoch at least 1000 integrations have to be performed. Anyway, a method to find a transfer from EML2 to LEO has been found and can be used to analyze transfers in a general way.

2.2 Free transfers from LEO to EML2 Orbit

The gained knowledge about the method to find transfers without any further mid course manoeuvres will be used in the following section to find so called "Free Transfers" - because only an Earth departure manoeuvre is required - and to analyze them towards mission analysis requirements, such as:

- Δv
- Travel time
- Launcher requirements (Inclination, ω and Ω)

2.2.1 The Bisection Method

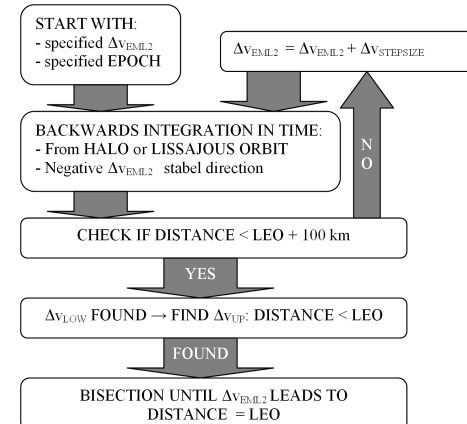
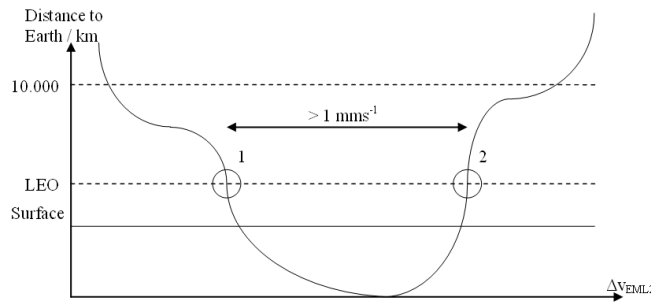


Figure 2.5: distance to Earth vs. Δv_{EML2}

Figure 2.6: free transfer can method

This section will deal with a more precise method finding transfers for a specified departure orbit from Earth w.r.t. mission analysis requirements. Basic scanning method presented in Section 2.1 only works on high altitudes for Earth orbits (higher than 10 tkm) to resolve satisfactory results. For smaller altitudes due to the need of smaller step sizes this scanning method did not work satisfactory any more. This has to do with the sampling problem. By scanning through the Δv_{EML2} range depending on the step size one could get a matching result from ± 1000 km which is not very satisfactory due to the more accurate needs of proper mission analysis. At least one could hit the favored result by chance. The goal is to get a 100 % matching orbit to the aimed 400 km altitude LEO. To realize this an adapting step size method had to be implemented in the already working scan program. Figure 2.5 shows how the perigee altitude develops over the Δv_{EML2} range for a transfer window. LEO is reached on two points of the Δv_{EML2} range. We will only focus on the

first point in the presented method to find the exact Δv_{EML2} as it is the cheaper one. The main idea was to use a bisection algorithm once the scan has reached an altitude lower than LEO + 100 km. With the bisection method a very accurate result can be achieved. Figure 2.7 shows which part of the Δv_{EML2} range gets scoped by the bisection method. Figure 2.6 shows the schematic of the entire method for the free transfer scan with a bisection method.

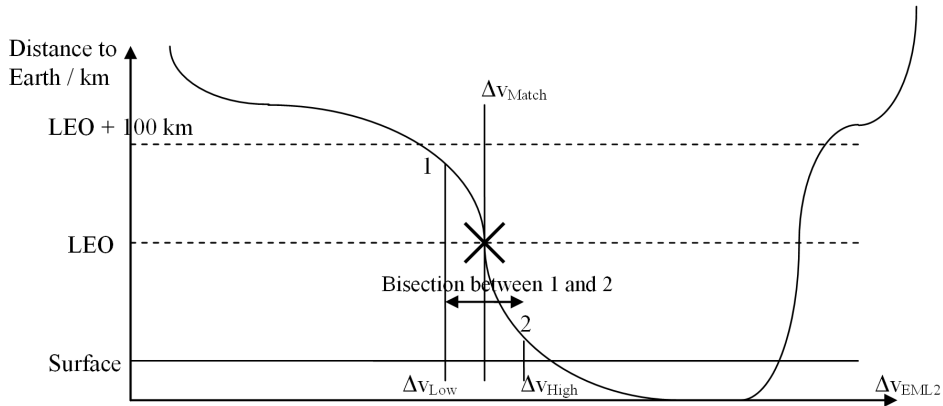


Figure 2.7: free transfer scan method: bisection

2.2.2 Results

This section will deal with the result gained from the computations. The first part will describe the concept and the scheme for the computations. Than a brief view to the results will be given followed by a detailed analysis of the data.

Concept and Scheme

A scan over a period of an entire year in one day steps on both example orbits described in Appendix 5.1.1 has been performed to show the schematics of the transfers. The scan starts at 7305 days in MJD2000 system - Modified Julian Day 2000: 1. January 2000 noon \Rightarrow 2451545.0 Julian date (JD) - and going until 7670 days.

Overview to the Results

Table 2.2 shows a summary to the found free transfers with some characteristic values.

	Lissajous Orbit	Halo Orbit
Maximum Δv_{Total} [km/s]	3.1756	3.1600
Minimum Δv_{Total} [km/s]	3.0761	3.1289
Variation [km/s]	0.0996	0.0311
Maximum Earth Departure Δv_{Earth} [km/s]	3.1755	3.154
Minimum Earth Departure Δv_{Earth} [km/s]	3.076	3.1198
Variation [km/s]	0.0215	0.0342
Maximum EML2 Orbit insertion Δv_{EML2} [km/s]	0.0014889	0.016341
Minimum EML2 Orbit insertion Δv_{EML2} [km/s]	1.7998e-6	2.4219e-9
$\Delta v_{EML2} \leq 1$ m/s [%]	99.1781	84.3836
Variation [km/s]	0.001488	0.016341
TTR _{max} [days]	119	120
TTR _{min} [days]	86	92
Variation [days]	33	28
Maximum Inclination [deg]	45.6	35.5
Minimum Inclination [deg]	11	2
Variation [days]	34.6	33.5

Table 2.2: Free transfer from LEO to EML2 Lissajous and Halo orbit via WSB region transfers: characteristic values

The following analysis shall investigate the gained results w.r.t. different points of interest:

- Difference between Halo and Lissajous orbits
- Launch windows
- Anomalies
- Departure orbit characteristics: Ω, ω, i
- Transfer time
- Δv

Halo vs. Lissajous orbit

First the difference between the Lissajous and the Halo orbit will be analyzed. The Halo orbit has a lower Δv_{Total} than the Lissajous orbit. With Δv_{Total} the entire magnitude of all manoeuvres - the burn getting from LEO into the WSB transfer trajectory and the insertion burn into the EML2 orbit - are summed up. This fact can be explained by the apogee of the Halo orbit which is much nearer (about 100 tkm nearer) than the one of the Lissajous orbit. This brings a lower Δv_{Escape} at Earth (LEO) departure from about 10 m/s which can be seen in the Figure 2.8. Additional numerical investigation on this phenomenon can be found in Figure 2.10 showing the transfer trajectories in LCR frame integrated to the first apogee. It can be seen that the stable manifold of the Halo orbit spreads much more than the one of the Lissajous. This means that the distances of the apogees can be located much nearer to Earth than the ones of the Lissajous orbit. The bigger the libration point orbits are the bigger the stable manifolds gets and therewith the reachable distances to the primary bodies are getting closer. Of course also much higher apogees can be reached now, but for an optimal

transfer only the lowest apogees are considered.

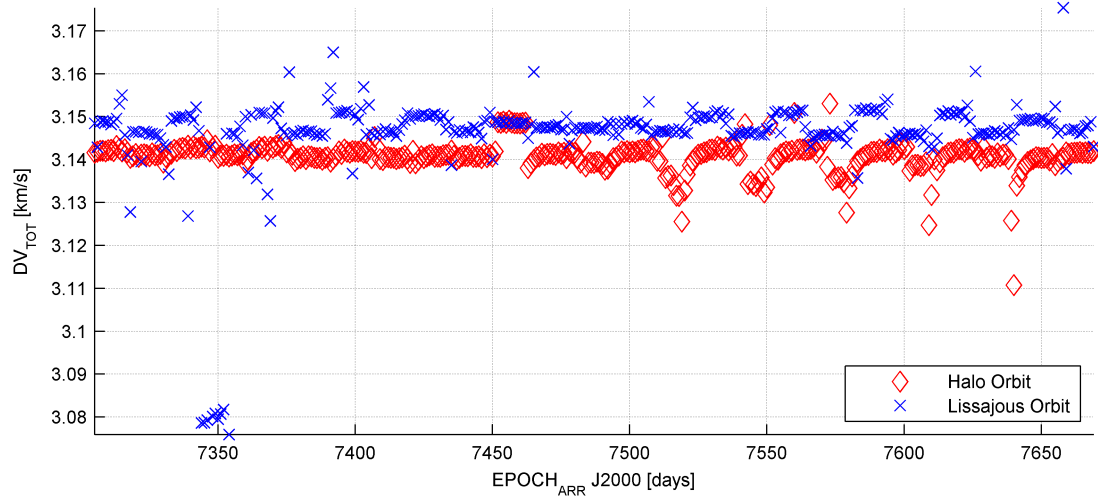


Figure 2.8: free transfer: Δv_{Total} Halo vs. Lissajous orbit

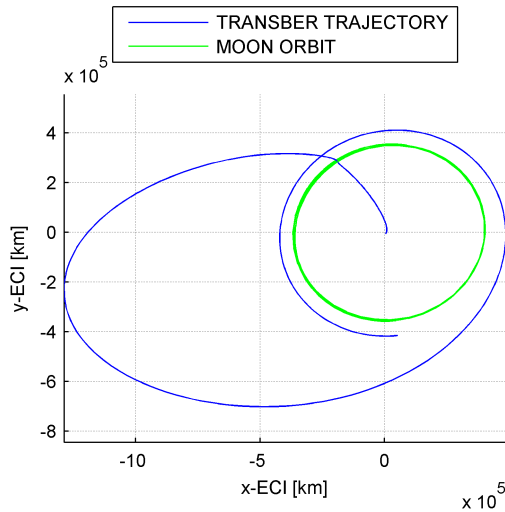


Figure 2.9: lunar fly-by WSB transfer

Lunar Fly-by Anomaly

After focusing on the Δv_{Total} another remarkable anomaly can be found in Figure 2.8. The Δv_{Total} of the Lissajous orbit transfer has strong descent in the period between 7340 and 7355. A couple of about 10 transfers seem to be cheaper than all the other ones. This can be explained by a lunar fly by which is shown in Figure 2.9. Utilizing this phenomenon additionally Δv savings of ~ 80 m/s

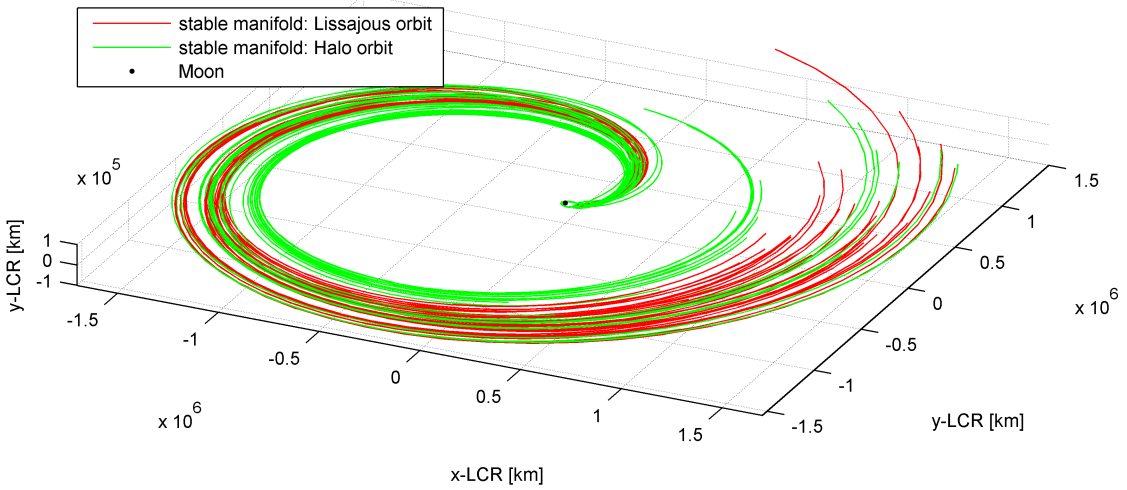


Figure 2.10: EML2 manifold in LCR frame integrated to the first apogee

and therewith much cheaper transfers could be achieved. A further analysis towards the solar and lunar constellation has to be performed due to this issue.

Launch Windows

A launch window allows transfers only for certain discrete epochs and raises a strong constraint towards mission analysis requirements. As the WSB transfer is strongly linked to certain solar constellation issues - the WSB regions as shown in Figure 1.13 - this have to be analyzed in more detail. Therefor the following part of the analysis will deal with launch windows for the WSB transfer.

Figure 2.11 shows the clustering of departure epochs in more detail. Departure epoch is always the same for the same WSB region. From the WSB region the stable manifold can lead into the specified orbit. This works for a period of about 14 to 21 days depending on the WSB region, on the Moon and the position of the Sun. Figure 2.12¹ shows the jump in the WSB regions between two clusters of launch windows. To give a better impression about the launch window length which poorly can be taken from Figure 2.11 due to the limited resolution (every cross stands for a transfer \Rightarrow one line of crosses stands for a launch window.) Figure 2.13 gives a better idea of the mean length of the launch windows. It can be seen that as long as the angle between the Sun-Earth and Earth-WSB-Apsidial is high ($\geq \approx 40^\circ$) the launch window can be extended up to 21 days. Even though the solar constellation is important for the transfer it has to be pointed out that the launch window in the end only depends on the Δv_{EML2} .

¹Launch Window I:(7406-7420), Launch Window II: (7421-7435); in [MJD2000]

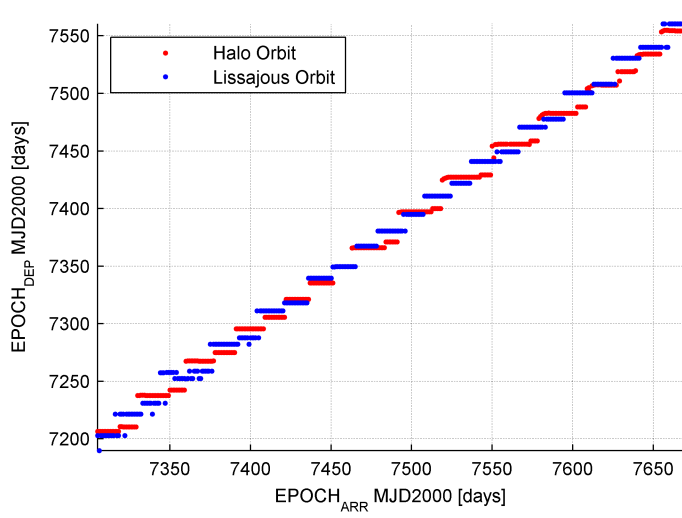


Figure 2.11: free transfer: Epoch_{Arr} vs. Epoch_{Dep}

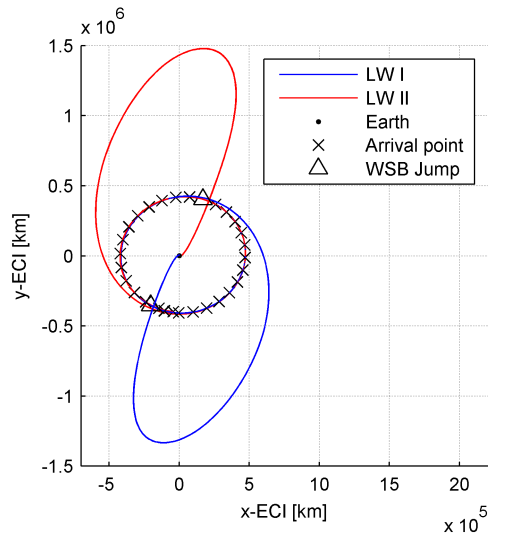


Figure 2.12: WSB region jump

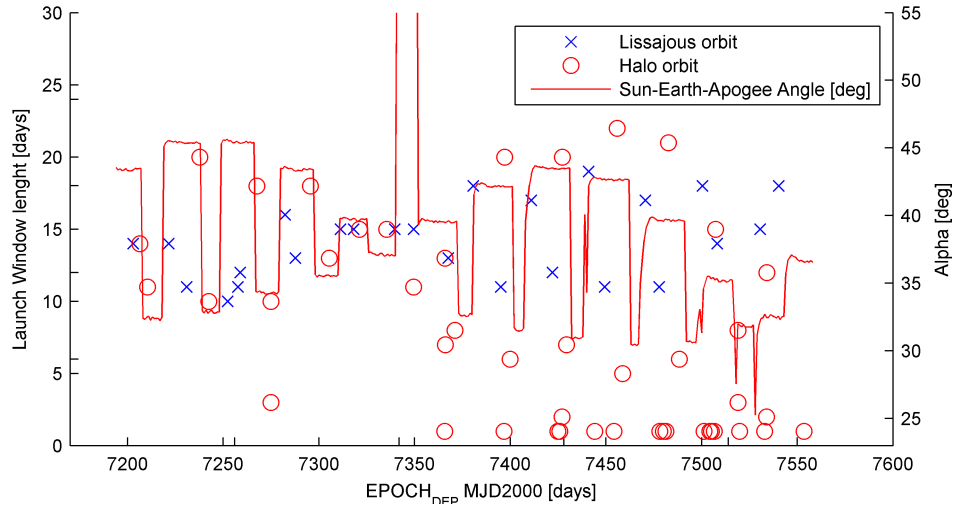


Figure 2.13: EML2 launch window length

Is it really a free Free Transfer?

The main reason why this transfer is called "Free Transfer" is that no high impulsive manoeuvre has to be performed but the departure manoeuvre from LEO into the transfer trajectory. As this is a very strong system requirement due to the fact that no high impulsive propulsion would be required a more detailed view on this issues has to be taken. The following section will give closer look on this.

An important outcome of the performed computations and the analysis is that the Δv_{EML2} - in a fair approximation - ≈ 0 m/s as shown in Figure 2.14. 85 % of the values in Figure 2.14 are ≤ 1 m/s depending on the arrival date in EML2 orbit. It is always possible to find a very cheap transfer for every launch window as a detailed view of them is shown in Figure 2.15.

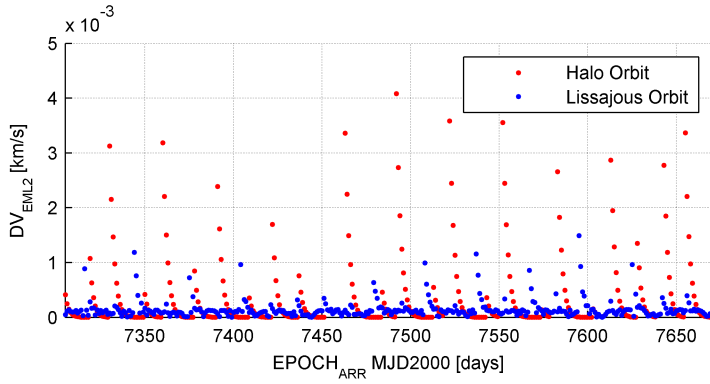


Figure 2.14: free transfer: Δv_{EML2} Halo vs. Lissajous orbit results

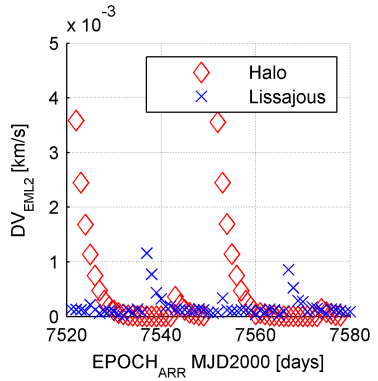


Figure 2.15: detailed view of Δv_{EML2}

Impact on Mission Design

The propulsion system and fuel always takes a big amount of the total S/C mass budget. Downsizing this mass would allow to transfer much more payload to EML2. No additional main engine has to be used for the insertion manoeuvre. This has a big impact on the mission design. The insertion manoeuvre can be performed by smaller AOCS like thrusters. The entire Δv_{Total} of the mission can be performed via high efficient cryogenic fuel thruster in LEO directly after launch. From $\Delta v_{EML2} \approx 0$ m/s follows:

$$\Delta v_{LEO} \approx \Delta v_{Total}. \quad (2.2)$$

This is the major advantage with the biggest impact on mission design of the shown transfer. With a need of $\Delta v_{LEO-Liss} \approx 3.145$ km/s and a $\Delta v_{LEO-Halo} \approx 3.14$ km/s a rough mass budget from ≈ 9 t for a ARIANE V ECB (heavy version) can be estimated [3]. This is of course a very rough estimation without any detailed launcher performance considerations. To perform these transfers a free ω is required which means restartable upper stage rocket engines which is very likely to be developed at least for ARIANE V in the future.

Launch Orbit Requirements

A major outcome of the scans are launch orbit requirements as the found transfers ended up on LEO's with very different characteristics. To match these characteristics is one of the big problems to be solved in future work because not every launch state can be easily reached by a launcher. Especially the launcher performance is a function of the initial state of the transfer. Therefor a detailed look on the gained launch orbit requirements will be given in the following section.

The inclinations for the free transfer in LEO follows a periodic scheme as shown in Figure 2.16 for both orbits which oscillates between 0° and 50° , so it is impossible to get a free transfer from 51.6° , which is the minimum inclination for the launch site Baikonur in Kazakhstan.

Right ascension Ω and the argument ω are sometimes switching 180° for the north- and southbound solution as shown in Figure 2.17. At least the switch does not follow any predictable scheme whereas the Ω is oscillating in a 100° range.

Figure 2.18 shows the transfer times. Here also the launch window dependence on the quadrant of the WSB region can be found. The shortest transfer is not the cheapest one w.r.t. Δv_{EML2} .

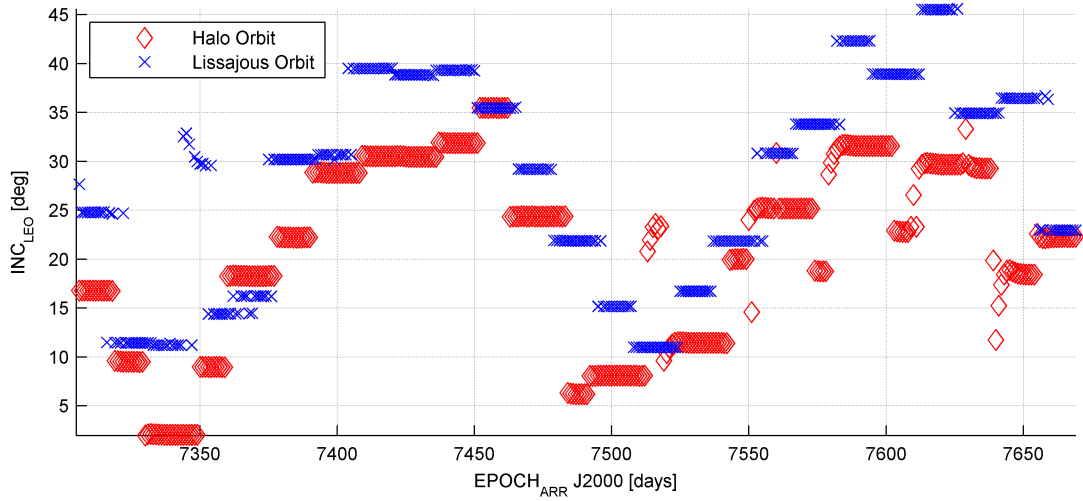


Figure 2.16: free transfer: inclination Halo vs. Lissajous orbit

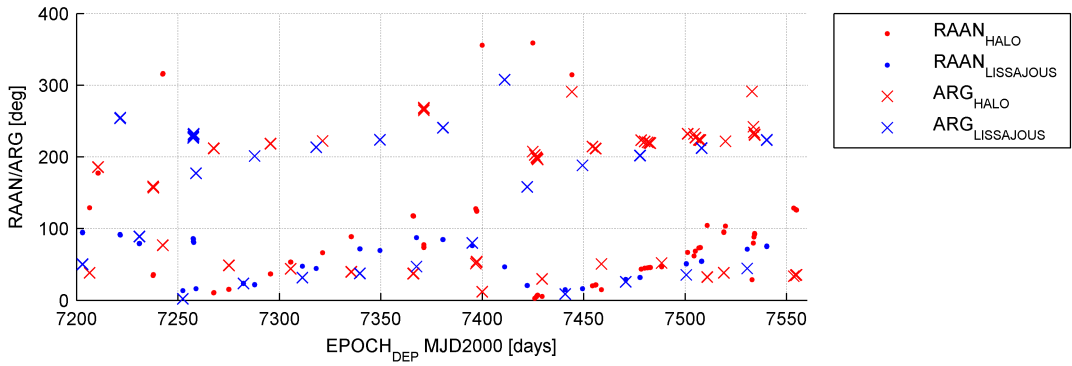


Figure 2.17: free transfer: Ω and ω Halo vs. Lissajous orbit

The longer the transfer time get the lower the Δv_{EML2} gets. This can be verified with Figure 2.15. The explanation to this effect is simple. To travel along the stable manifold the exponential terms of Equation 1.9 needs to be excited. Without any correctional manoeuvres this happens after a very long time and the S/C is leaving the EML2 orbit on the invariant manifold. By forcing the exponential terms being excited by a certain manoeuvre this can happen earlier. As every transfer of a launch window travels along the same manifold only differing in the time they have to excite the exponential terms it seems obvious, that transfers with shorter travel times needs more Δv_{EML2} to excite these terms.

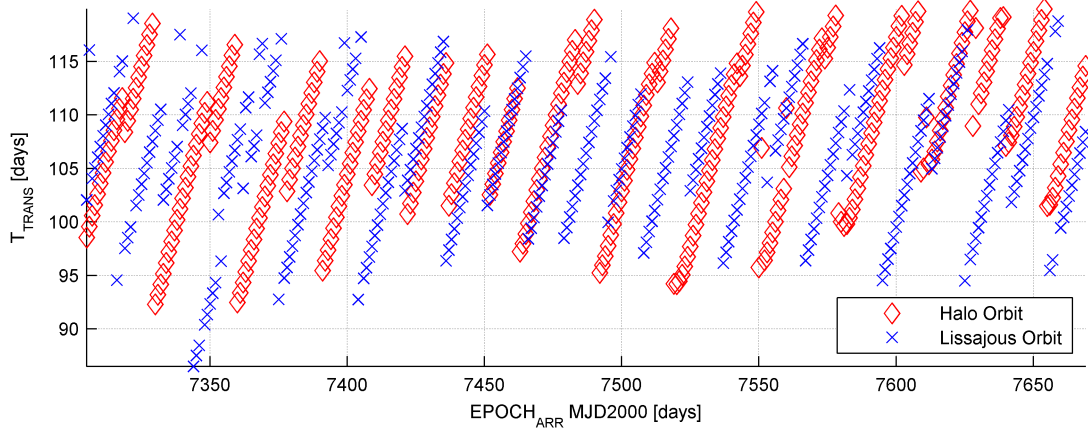


Figure 2.18: free transfer: transfer time Halo vs. Lissajous orbit

2.2.3 Conclusions on Free Transfer Scans

A method to find free transfers to both example EML2 orbits has been presented. The big advantage of this transfer can be seen in the fact that only one impulsive manoeuvre has to be performed in LEO which makes it possible to design a mission base only on high efficient cryogenic fuel. No storage problems have to be considered as the second impulsive manoeuvre for the EML2 orbit insertion only requires a small magnitude of thrust which can be performed by AOCS like systems, which always will be required even for cargo modules. The launch performance as a function of the inclination and the argument of perigee has to be taken into account. A more detailed analysis towards this fact has to done. Suggested launchers are:

- ARIAN V ECB
- SOYUZ
- PROTON

2.3 Optimized transfers from LEO with fixed inclination

A free transfer could be achieved only from inclinations lower than 50° and with an oscillation between 0° and 50° among the period of half a year. For further mission analysis requirements a forced transfer with a specific departure orbit inclination has to be investigated. An inclination of 51.6° has been chosen for this investigation as it represents the minimum launchable inclination of the launch site Baikonur. As Baikonur can play an important role in future space exploration scenarios this seems to be a good choice. The transfer mechanisms of the WSB transfer will be the same but an additional manoeuvre has been added to the problem in order to achieve always a transfer from a specific inclination in LEO. The optimization will also be done over a period of 365 days. The following section will deal with the formulation of the optimization problem and the gained results.

2.3.1 Formulation of the Optimization Problem

As already described a scan throughout the stable manifold by exciting the stable amplitude A_2 with a small Δv and integrating backwards will lead to an apogee in the WSB region. The position and the epoch of this apogee are used to calculate an initial guess for the transfer arc coming from Earth. The guess is based on Kepler's laws and gives an Earth departure location and velocity. The entire initial guess generator will be explained in the Appendix Section 5.2.1. As the arrival epoch is fixed the departure epoch can be calculated by the estimated transfer time by:

$$\begin{aligned} T_{Departure} &= T_{Arrival} - (T_{Arc1} + T_{Arc2}), \\ T_{Total} &= T_{Arc1} + T_{Arc2}, \end{aligned} \quad (2.3)$$

with ARC2 as the one from the libration point orbit and ARC1 the one from LEO. ARC2 will be integrated backwards in time from the libration point orbit whereas ARC1 will be integrated forward in time from LEO. Together with the time constraint in Equation 2.3 an implicit matching in time at the end of the integration will be achieved. Now after the matching in time is assured only the matching in space has to be defined as the constraint of the optimization. In order to achieve a certain flexibility in optimizing the two arcs and matching them in space T_{ARC1} and T_{ARC2} are linked with the parameter σ by:

$$\begin{aligned} T_{Arc2} &= \sigma T_{Total}, \\ T_{Arc1} &= (1 - \sigma) T_{Total} \end{aligned} \quad (2.4)$$

As only a matching in time and space is required but not in the velocity a Δv_{Match} in the matching point will always result from the optimization. The formulation of the entire optimization problem has the following parameters where Δ stands for the change of the initial guess and not the parameter itself.

Optimization parameters:

- velocity change in LEO: $\Delta|\Delta v|$
- EML2 orbit insertion manoeuvre: Δv_{EML2}
- Ω at Earth departure: $\Delta\Omega_{Departure}$
- Argument of Perigee ω at Earth departure: $\Delta\omega_{Departure}$
- transfer time: ΔT

- time fraction between Arc1 and Arc2: $\Delta\sigma$

Constraints:

- position at matching point: $r_{Arc1}(T_{Match}) = r_{Arc2}(T_{Match})$

Cost function:

- total transfer $\Delta v_{Total} = \Delta v_{EML2} + \Delta v_{Match} + \Delta v_{Departure}$

Initialization parameters:

- transfer time: T_{Trans}
- time fraction: σ
- Δv_{EML2}
- orbital parameters for LEO departure state

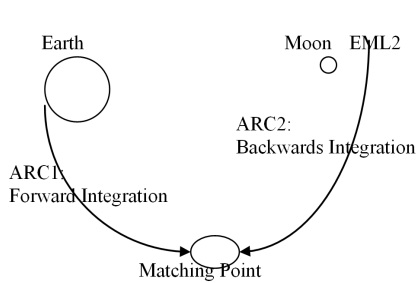


Figure 2.19: WSB transfer optimization

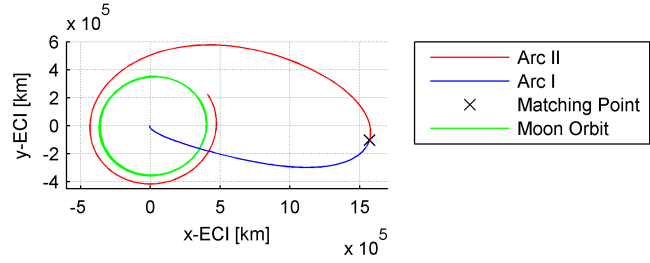


Figure 2.20: optimized WSB transfer

Figure 2.19 gives a brief view on the idea of the optimization whereas 2.20 shows the result of an optimized transfer. Summarized the optimization scheme operates the following way:

- Propagating a trajectory backwards in time from EML2 orbit into first apogee.
- Generating an initial guess for Earth departure state due to match a trajectory coming from Earth in the before computed apogee.
- Building a transfer with one arc coming from Earth and one from EML2 matching in the apogee.
- Optimizing both trajectories due to match them in time and space and to find the lowest Δv_{Total} .

Initialization of the Optimization

The main problem for any robust scan over a period of 365 days with the optimization method is the initialization of the problem which has to be done for every day again and again. The heritage of one day to another in the initialization parameters (σ , T_{Trans} , Δv_{EML2}) could be used for the same WSB region. The results were satisfying as long as the transfer passed through the same quadrant of the WSB region. But as jumps in the WSB region occurs at least every 14 to 21 days it is impossible to use these heritage results. After each jump the optimization has to be reinitialized. This is time

intensive and very ineffective due to the amount of days that has to be scanned (LISS and HALO; South- and North-Bound). By using results of the free transfer scans to initialize the fixed inclination optimization it was possible to reveal an initial guess which already was in the right WSB region. Jumps are automatically considered as they appear on the free transfers as well. This brought up a robust and stable method to scan throughout an entire cycle of 365 days for both north- and southbound solutions.

Summarized the forced transfer for fixed inclinations has the following attributes compared to the free transfer:

- Same WSB region following the same trajectory of the stable manifold
- Nearly same Δv_{EML2}
- Δv_{Total} only differs in Δv_{Match}

2.3.2 Influence of Earth departure Inclination

First a short look on the influence of the departure orbit inclination on the different Δv 's will be given. As inclination can be fixed to a certain value by the user a performance analysis on the entire inclination range was done with the following parameters:

- Arrival Epoch: 7400 MJD2000 [days]
- Inclination Range: 23° to 90°
- Lissajous Orbit

Figures 2.21 and 2.22 shows the results of the optimizations:

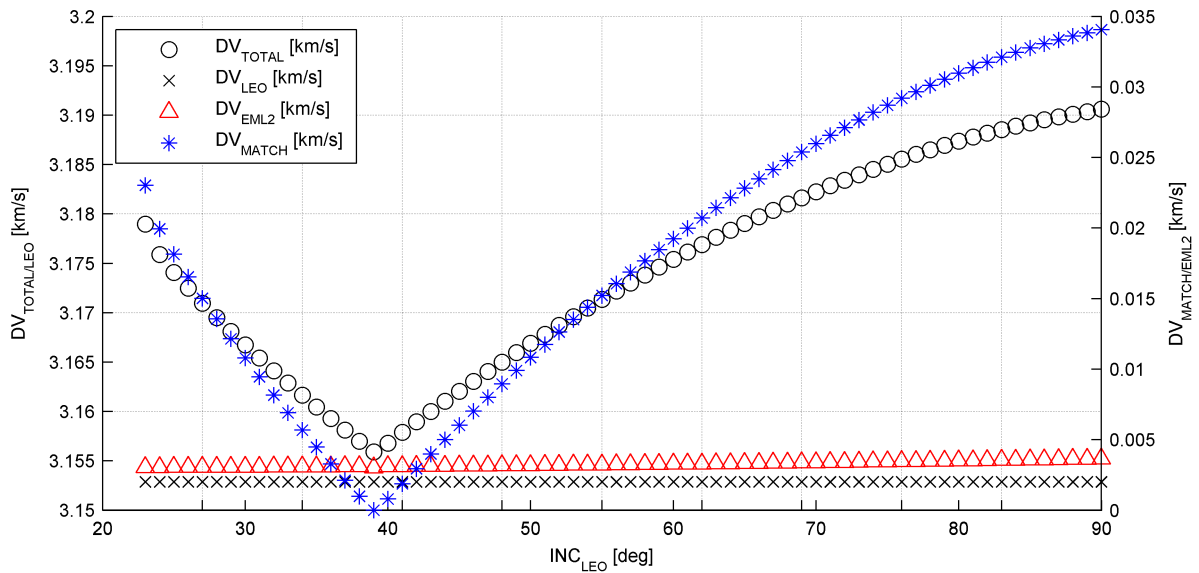


Figure 2.21: variable inclination scan: velocities

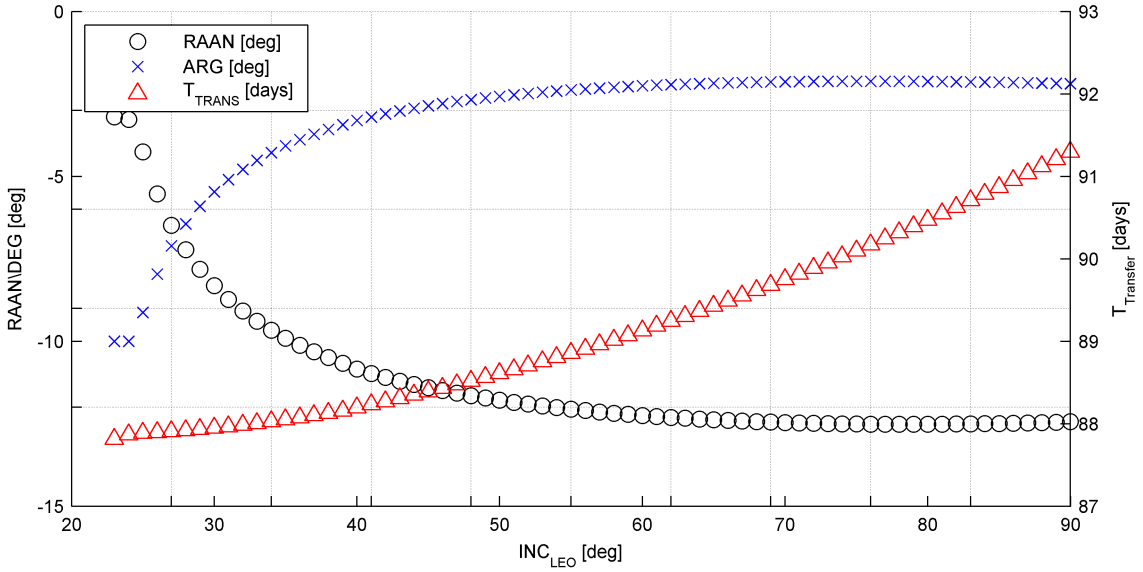


Figure 2.22: variable inclination scan: time and Keplerian elements

The highest impact on the transfer Δv comes from the matching point Δv_{Match} . The influence to the Δv_{EML2} is very low (0...3 m/s) and the influence on the Δv_{LEO} is nearly zero. The free transfer for this epoch also can be seen in the diagrams due to the lowest Δv_{Total} at about 40° inclination. In other epochs this will change to other inclinations. The transfer time is rising with higher inclination. This can be explained by the longer time the trajectory to the apogee that is requested in order to change the inclination to the requested plane for approaching the EML2 orbit.

2.3.3 Results

This section deals with the results of the computations performed with the explained optimization method. Then a analysis on optimized transfers with a fixed inclination of 51.6° for both example EML2 orbit will be done. The same time scheme like the one for the free transfer have been chosen for the optimized transfer scans aiming to achieve comparable results. This means that 365 sequent transfers in one day intervals have been generated.

Halo vs. Lissajous

This part of the analysis will deal with the results from 365 day scans and the differences found between the Halo and the Lissajous orbit.

A typical resulting trajectory of the optimization can be found in Figure 2.20. Whereas the free transfer has no Δv_{Match} the main difference in the Δv_{Total} - which can be found in Figure 2.23 - will occur from the matching Δv as shown in Figure 2.24. The results shows the the north- and southbound dependency of the transfer. As the optimization has to be initiated by an initial guess which either can create a north- or a southbound solution for the shown results always the cheaper one of both solution w.r.t. the Δv_{Total} has been chosen. In the Appendix Section 5.3.1 the analysis

for the north- and southbound solution can be found in more detail with all results.

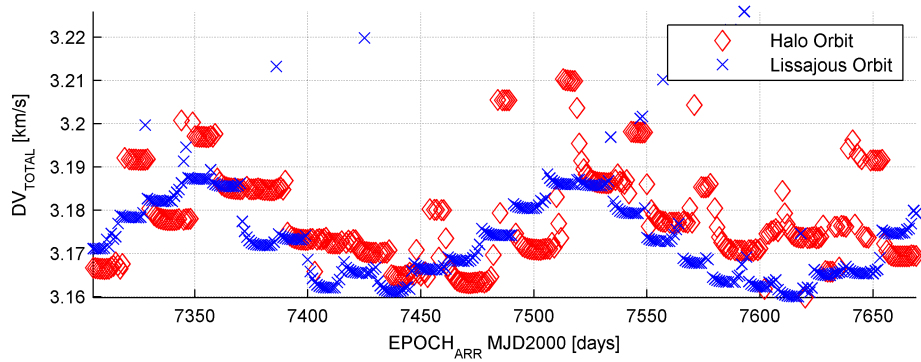


Figure 2.23: EML2 optimized transfer: Δv_{Total}

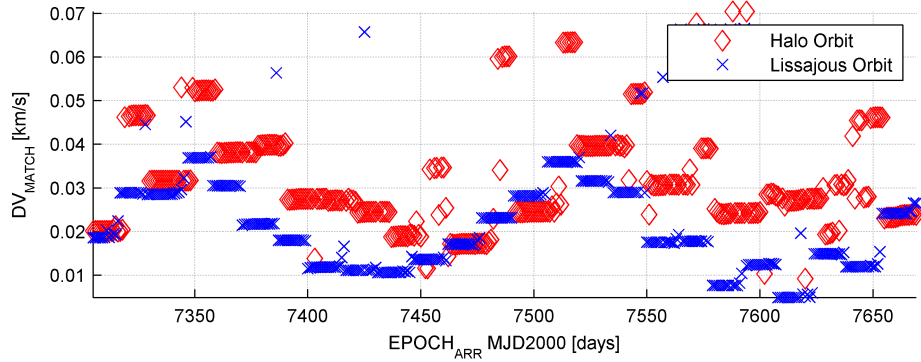


Figure 2.24: EML2 optimized transfer: Δv_{Match}

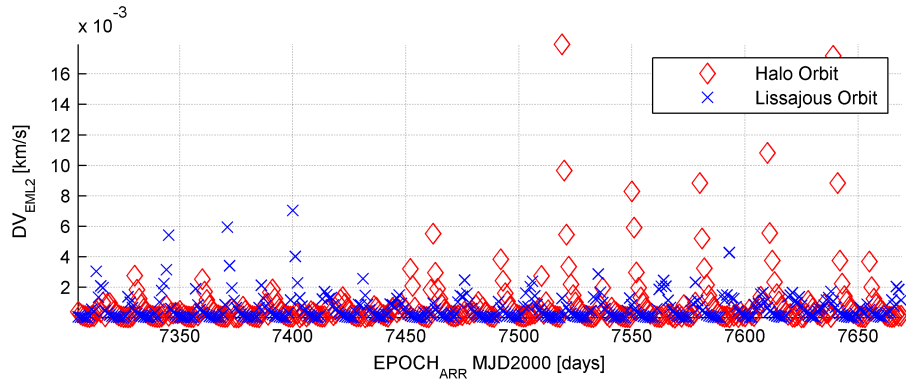


Figure 2.25: EML2 optimized transfer: Δv_{EML2}

Δv Issues

Looking on Δv_{EML2} in Figure 2.25 shows that also in the case of the optimized transfer the behavior is the same as for the free transfer. Figure 2.15 also showed this behavior. As the S/C always travels towards the libration point on the same trajectory on the stable manifold the insertion Δv_{EML2} has to be adapted to the arrival epoch constraint. In fact the S/C has to travel longer or shorter on the libration point orbit always coming from the same insertion point but traveling to different points on the orbit. The general evolution of the Δv_{Total} among a launch window shows exactly this dependency which also can be found in Figure 2.12. As long as the S/C uses the same WSB region to approach the libration point orbit it always travels on the same trajectory towards the libration point orbit. This explanation also gives a hint on the possible magnitude of the insertion Δv_{EML2} . Theoretically the transfer can be forced to a minimum Δv_{EML2} .

The oscillation of Δv_{Match} depends on the difference from the fixed departure inclination to the free transfer inclination - the so called relative inclination - as shown in Figure 2.26 for the Lissajous orbit. For the Halo orbit this relation is the same as shown in Figure 2.27 but w.r.t. Δv_{Total} which

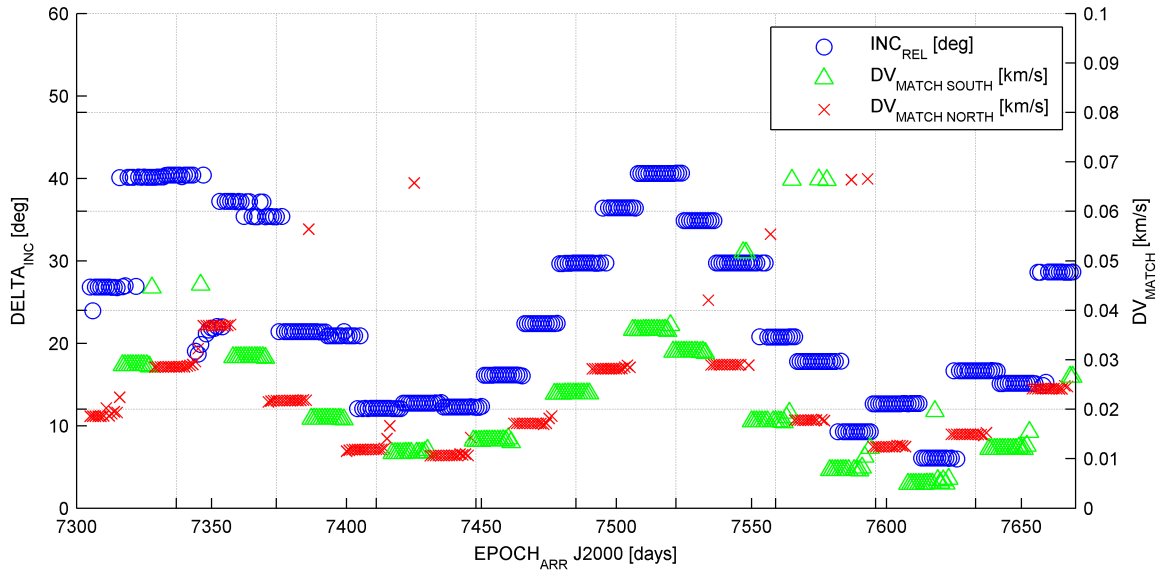


Figure 2.26: Lissajous orbit: relative inclination vs. Δv_{Match}

only differs from the free transfer because of the Δv_{Match} what can be seen in Figure 2.28.

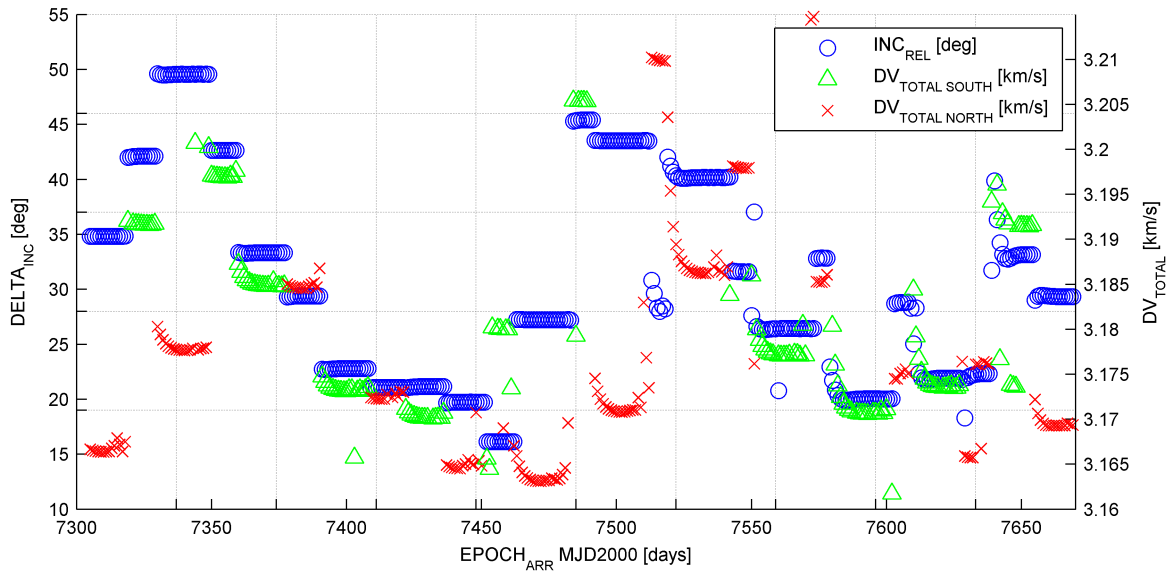


Figure 2.27: Halo orbit: relative inclination vs. Δv_{Total}

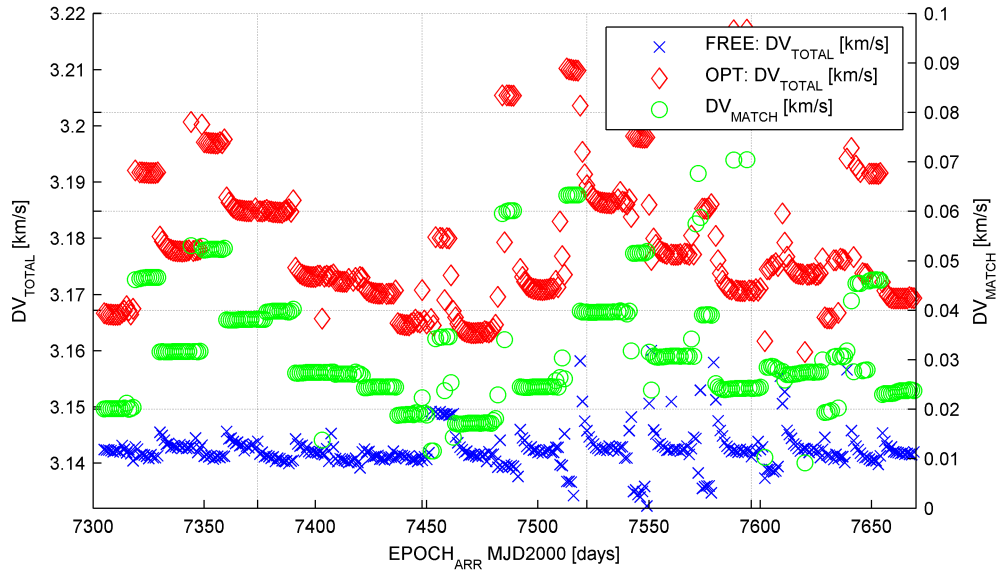


Figure 2.28: Halo: free Δv_{Total} vs. Δv_{Match}

Transfer time and transfer windows did not change for the optimized transfers as shown in Figure 2.29.

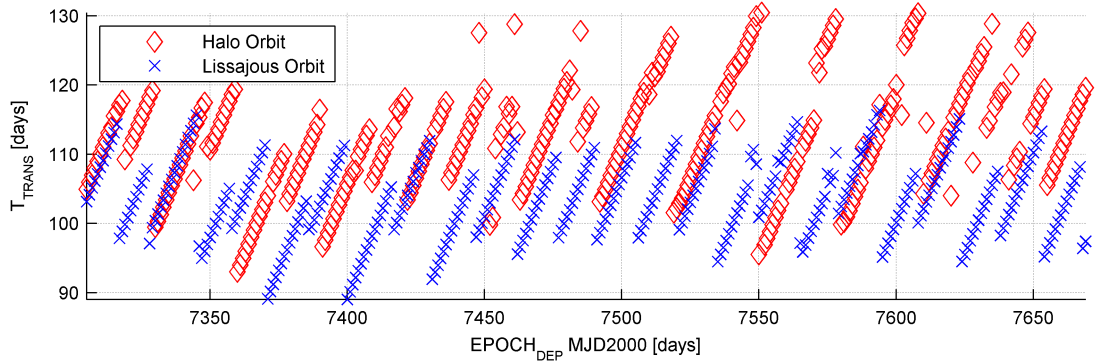


Figure 2.29: EML2 optimized transfer: transfer time for Lissajous and Halo orbit

Table 2.3 shows a summary of the found optimized transfers characteristic values.

	Lissajous Orbit	Halo Orbit
Maximum Δv_{Total} [km/s]	3.2259	3.2171
Minimum Δv_{Total} [km/s]	3.1600	3.1598
Variation [km/s]	0.0659	0.0573
Maximum Earth Departure Δv_{Earth} [km/s]	3.1557	3.1552
Minimum Earth Departure Δv_{Earth} [km/s]	3.1488	3.1445
Variation [km/s]	0.0069	0.0107
Maximum Δv_{Match} [km/s]	0.066558	0.070455
Minimum Δv_{Match} [km/s]	0.004901	0.009202
Variation [km/s]	0.061657	0.061253
Maximum EML2 Orbit insertion Δv_{EML2} [km/s]	0.0070386	0.017957
Minimum EML2 Orbit insertion Δv_{EML2} [km/s]	3.4775e-6	3.1914e-6
Variation [km/s]	0.0070	0.01795
$\Delta v_{EML2} \leq 1$ m/s [%]	78.6301	83.0946
TTR _{max} [days]	116	130
TTR _{min} [days]	89	93
Variation [days]	27	37

Table 2.3: Optimized transfer from LEO (51.6° inclination) to EML2 Lissajous and Halo orbit via WSB region transfers: Δv values and duration

2.3.4 Conclusions on Optimized Transfer

A method to design optimized transfers for a fixed inclination in LEO departure state has been presented. Systematic scans over a year have been performed and a relation between the relative inclination and the matching Δv_{Match} has been found. The following facts can be revealed by the investigation:

- At every arrival epoch a forced transfer with fixed inclination in LEO is possible.
- A free ω is required at launch.
- The higher the relative inclination towards the inclination from the free transfers gets the higher the Δv_{Match} gets.

3 Lunar Resonance Transfer to EML1

Transfers utilizing lunar resonance have been investigated to design an optimal low cost transfer to the first collinear libration point (EML1) in the Earth-Moon system. Since the WSB transfer make use of the gravitational forces of the Sun the resonance transfer makes use of the gravitational attraction of the Moon. Encountering the Moon in the apogee of an high eccentric orbit around Earth raises the the orbital energy. This effect is triggered by two major parameters:

- apogee altitude at lunar encounter
- phase offset between line of apsides and the Earth-Moon line

The major approach reaching an EML1 orbit will make use of the stable manifold of the orbit. Using the stable manifold has already been used for the WSB transfer to EML2 orbits. The main advantage is the negligible insertion Δv 's to the EML1 orbit.

Guided by these issues the investigation of transfers utilizing lunar resonances will be done in four steps:

- Analyzing the natural behavior of lunar resonances.
- How to approach an EML1 orbit from an orbit around Earth via the stable manifold?
- How to design a LEO to EML1 orbit transfer?
- Optimizing transfers to fixed departure orbit inclinations

3.1 Natural Behavior of Lunar Resonances

As the major working principle of the resonance transfer has been explained in the introducing Chapter 1.4 this section will give some examples to the effects the gravitational drag of the Moon has towards a trajectory at lunar encounter. First the effect of different apogee altitudes at lunar encounter will be investigated, showing the relation between the apogee altitude and the effect of orbital energy raising. In the second part the effect of the phase offset between between the line of apsides and the Earth-Moon line will be investigated.

Figure 3.1 and 3.2 show the effect on different apogee altitudes at lunar encounter with a phase offset of 15° . This means the S/C is chasing the Moon with an angle of 15° between the line of apsides and the Earth-Moon line. As some of the shown orbits have an apogee higher than the Moon's orbit a new classification has to be defined. Moon resonances are encounter with the moon outside its sphere of influence (SOI). Once the distance of closest approach to the moon gets within the SOI (e.g. lower than 60 tkm), we start speaking about moon swing-by's [6]. This is what also happens in the Figures 3.1 and 3.2 at a certain apogee altitude. The raising in apogee explodes and the resulting orbit has no usable effect on the construction of further resonances any more due to a difficult phasing and much to high correctional Δv 's to maintain the resonance sequences.

Besides the apogee altitude also the already mentioned phase offset is an important parameter for the

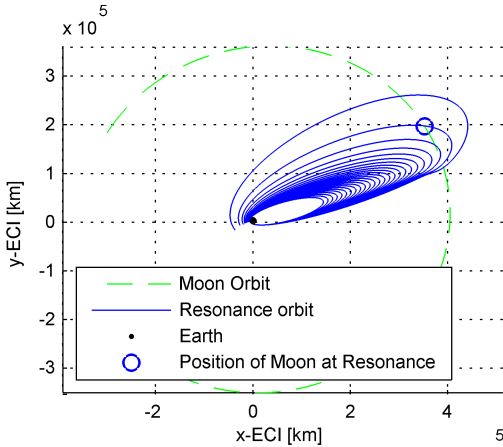


Figure 3.1: lunar resonance: hopping from LEO with 15° phase offset and variable apogee altitudes

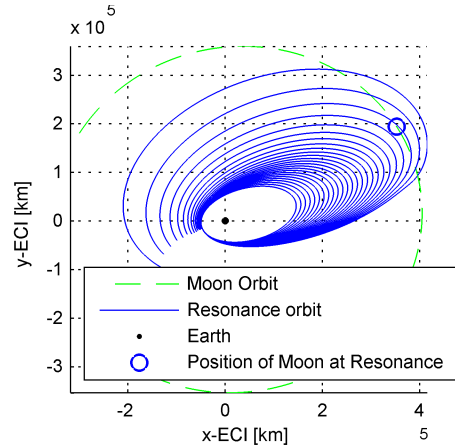


Figure 3.2: lunar resonance: hopping from 50 tkm perigee with 15° phase offset and variable apogee altitudes

resonances. In [6] and [5] an offset of the apogee around 15° behind the moon for the encounter was mentioned as being most effective. Some numerical experiments have been performed to show how the effect of the moon's perturbation on the high elliptic orbits evolves for different apogee altitudes and phase offsets. Integrating from LEO forward in time to apogee's with different phase offsets and different altitudes shall give an idea about the magnitude of drag which results in a higher perigee - Δ Perigee - after the encounter. Figure 3.3 shows the result for different apogee altitudes at the lunar encounter from LEO as perigee. All trajectories do have the same inclination as the orbit of the moon. This means that only in-plane trajectories are investigated. With in-plane the lunar orbital plane w.r.t. to the equator of about 23.5° at the investigated epoch (7400 in MJD200) is meant. For other epochs the in-plane inclination will be different as shown in Figure 1.16 (see Section 1.4). Only the in-plane trajectories have been analyzed to simplify the investigations. An in-plane encounter will have the greatest effect on the S/C as no out-of-plane components are decreasing the magnitude of the lunar drag. Higher or lower inclinations will lead to less efficient resonance hops. Different inclinations at lunar encounter will lead to an out of plane component which will draw the S/C into the orbital plane of the Moon. In Section 3.4 this aspect will be investigated. For now all further investigations will be done in the lunar orbital plane. It can be found from Figure 3.3 that an optimal phase offset of 15° only for lower apogee altitudes is correct. For higher and more efficient apogees a shift towards the moon with phase offsets between 5° and 10° is optimal. As the apogee altitudes are taken from analytical calculation to build the initial guess for the Earth departure state the true apogee is much higher due to the gravitational pull of the Moon. That is also the reason why the diagram stops at $3.4 \cdot 10^5$ km apogee altitude as the apogee then already has reached a lunar orbit altitude in reality.

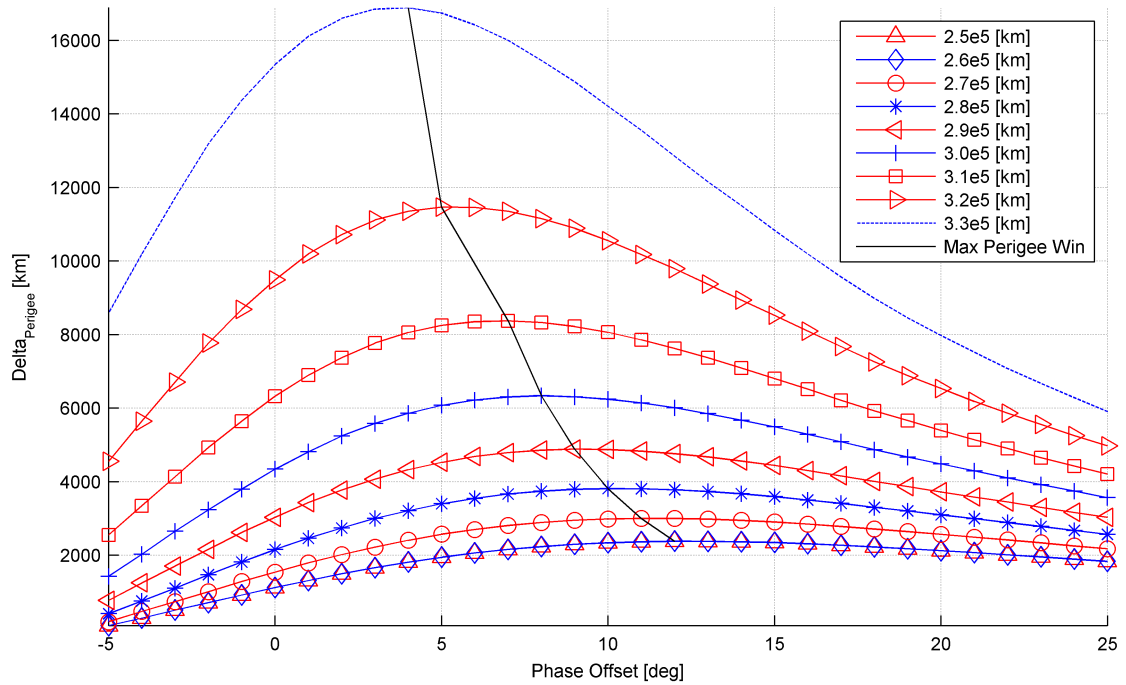


Figure 3.3: variable phase offset for different apogee altitudes from LEO as perigee

3.2 Approaching EML1 Orbits - Traveling along the Invariant Manifold

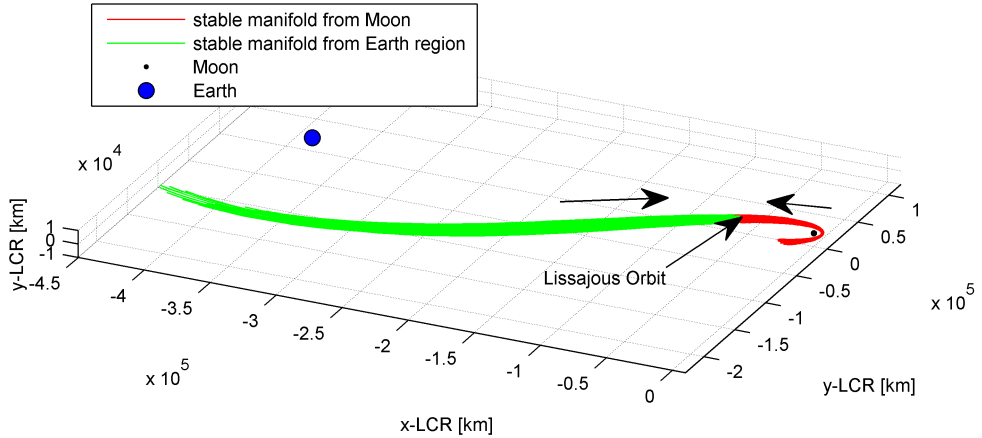


Figure 3.4: Stable manifolds for EML1 Lissajous Orbit

To approach an orbit round EML1 it is necessary reaching the stable manifold - Invariant Manifold

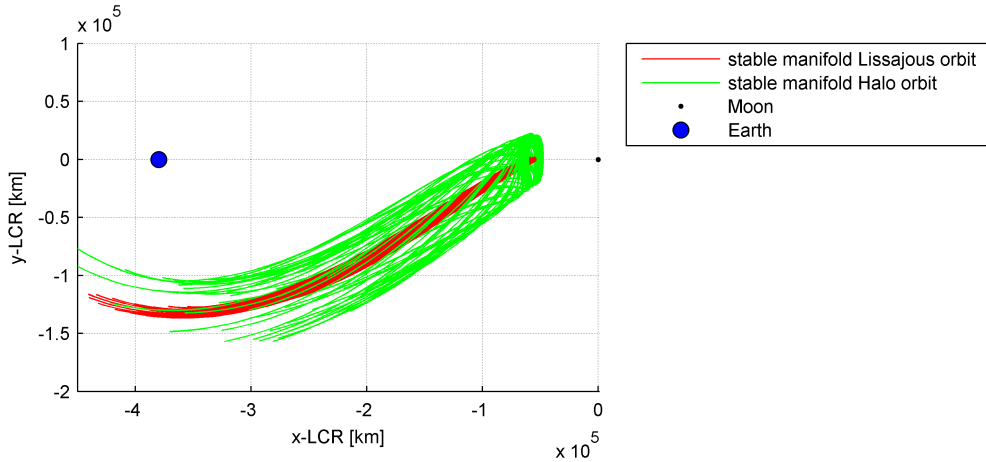


Figure 3.5: Invariant manifolds EML1

- coming from Earth. Figure 3.4 shows the stable manifold for the EML1 Lissajous orbit.

Integrating backwards in time shooting in the negative stable direction will lead on the stable manifold going to a perigee of an orbit around Earth. The stable manifold for every orbit type and size is reaching different perigees as Figure 3.5 shows. A larger orbit can reach a larger spectra of perigees, which means for the 5000 km Halo orbit a much closer possible perigee than for the 2000 km Lissajous orbit. As the amplitude size of the orbit is related to the amplitude size of the possible perigees a more efficient transfer can be designed with a larger libration point orbit because the perigee altitude of the perigee is much lower. As one of the main driver for the efficiency of a resonance transfer the altitude of the first perigee of the stable manifold will be this fact has to be pointed out. Larger EML1 orbit will require less Δv for a resonance transfer.

An numerical experiment was performed starting form different phase angles - which is equal to different times - on the libration point orbit shooting with 1 m/s Δv into the stable direction backwards integrated to the first perigee. Figure 3.6 shows the results of this investigation for a period of 30 days. It can be clearly seen that the amplitude of the perigees of the Halo orbit is much bigger than the one of the Lissajous orbits. This means that with the same Δv a much lower perigee can be reached. At least for the first manoeuvre this means for bigger libration point orbits lower costs to reach a lower perigee. Of course this investigation does not tell anything about the optimality of the results - in fact the perigees are not optimal w.r.t. the Δv - but the perigee altitude is the lowest possible one for this case.

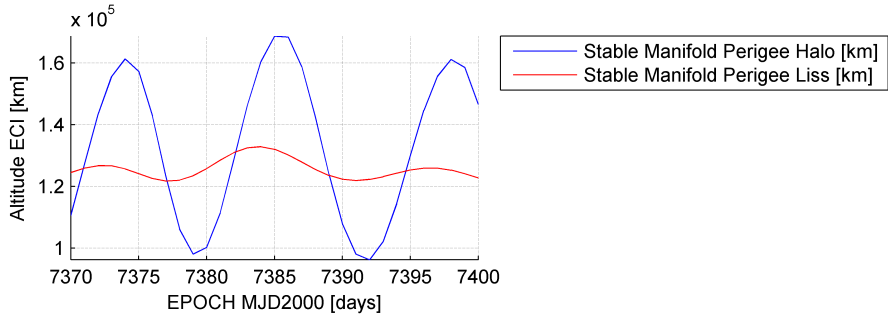


Figure 3.6: EML1 Manifold-Perigee Scans: 30 days

3.3 LEO to EML1 Transfer Trajectory Design - It's all about phasing

To design a transfer from LEO to a libration point orbit via lunar resonances is very similar to a global optimization problem with a nearly undefined space of possible solutions. Finding the best one is a problem of its own. Therefore here only a method to find transfers - but not explicit the most optimal one - will be presented.

The basic idea is a backwards integration in time from the libration point orbit traveling via the stable manifold coming from Earth (shown in Figure 3.4) leaving to an orbit around Earth and utilizing resonance sequences via Δv 's added in the perigees before a resonance. With this method a very sensible tuning of the resonance effect can be carried out towards the phasing.

As this is a straight forward method, which does not imply global optimization techniques, some easy rules for lunar resonance has to be taken into account to find a local optimum case:

1. Apogees should always be as high as possible for a big hop.
2. Resulting from 1. \Rightarrow A 1:3 resonance is more effective than a 1:4 resonance because the semi major axis is larger which means a higher apogee for a constant perigee.
3. A phase offset from apogee to Moon of 5° to 15° (depending on the apogee) leads to the most efficient hop.
4. If phasing with a single lunar revolution is not possible resonance sequences with two lunar revolutions have to be checked (most commonly 2:5, 2:7, etc.)
5. Δv 's should always be performed in the perigee.

As the gravitational attraction of the Moon increases with a decreasing distance to the Moon a high apogee w.r.t. the Earth is more efficient. As already mentioned in the introduction a thin border between a resonance and a swing-by has to be drawn which might interfere the design process. Some lunar encounters might lead to a swing-by increasing both the apogee and the perigee so that a good phasing for the resonance is not possible any more. Rule number two results more or less from rule number 1 as a higher apogee means a higher orbit period which leads to less orbital revolutions within the time of one lunar revolution. Rule number three is a rule of the thumb. For every apogee-perigee configuration an own optimal phase offset can be found. But all of them are located within the range of 5° to 15° . Rule number 4 is the most complex part of the design process because a trade off between time and Δv has to be achieved. For example: If a 1:2 resonance only can be reached by Δv of 100 m/s it might be possible to gain the same perigee raising with a 2:5 resonance as with

only 5 m/s due to the better phasing. Of course the same effect takes twice the time - two instead one lunar revolution - but the Δv saving is significant. This trade has to be done by the designer of the trajectory w.r.t. the mission duration requirements. Last rule is a fact based on the Keplerian laws of motion. Lets do a simple thought experiment: A S/C on a high eccentric orbit around Earth is reaching the apogee with a speed of 5 m/s adding 1 m/s. The kinetic energy defined by:

$$E_{KIN} = \frac{1}{2}m_{S/C} \cdot v^2 \quad (3.1)$$

with a S/C mass of 1 dimensionless making unit - not regarding the loss of mass from manoeuvre - is $6^2 = 36$ units compared to the energy before the manoeuvre of $5^2 = 25$ units. We resolved a energy win of 11 units with the manoeuvre in the apogee. The same S/C in the perigee having a speed of 10 m/s adding 1 m/s gains a energy win of $11^2 - 10^2 = 21$ units. The same manoeuvre in the perigee brought out nearly twice the effect of the manoeuvre in the apogee. This simple experiment without any exact relations to a real orbit, but with the same qualities of a real problem, shows that rule number five is essential for an optimal solution.

As every transfer is a unique sum of resonance sequences these rules have to be applied by the user in the transfer design process. An automatic design of transfers by regarding all different possibilities would excite the scope of this work but can be performed within a global optimization approach. At least these rules represent a best practice guideline for transfer trajectory design which help the user to develop them as efficient as possible. This can be done by hand or by an automatic approach which will be described in Section 3.3.1

3.3.1 Entire Transfer - Strategy and Optimization Issues

Entire Transfer - Optimization Issues

As already mentioned the optimization of entire transfers is a global optimization problem. Here the analysis will only deal with the optimal solution of one resonance but not with the optimal solution regarding all resonances required for an entire transfer from LEO to an EML1 orbit.

Even though transfer design seems to be individual for every arrival epoch the way to design is the same in every epoch. Therefor some tools to make this design process easier have been developed. As optimization can be carried out with different kind of optimization methods the feasibility for the trajectory design process was investigated.

General working principle of the entire resonance transfer form LEO to an EML1 orbit is a backwards integration approach from EML1 orbit divided into two main sections:

1. Going from EML1 orbit into the first resonance by performing a certain Δv from the EML1 orbit.
2. Going from one resonance to another one by performing a certain Δv at the perigee before a lunar encounter occurs.

The second step has to be redone until LEO has been reached. As the entire process is working backwards in time the arrival epoch at EML1 orbit is exactly defined whereas the departure time in LEO is open. Even the orbital elements at the departure are free except of the altitude which is fixed to 400 km.

The cost function always defines the win or loss of perigee altitude w.r.t. to the Earth. For the secondary cost measurement the Δv has to be taken into account. This leads to a multi objective

optimization which can rarely be performed by an easy optimization tool. Therefore techniques have to be developed to find a certain optimum for a transfer.

The basic idea behind the optimization is a backwards integration from the libration point orbit into the first possible resonance. The variational parameter is the Δv used in the libration point orbit. Using a scan over a specified Δv range with a certain step size will give a full view on the possibly reachable perigees. The integration tool is calculating the time to a hop and the altitude of the reached perigee autonomously.

Figure 3.7 shows the result for a scan from a certain epoch from the EML1 Halo orbit. The transfer is going backwards in time traveling the stable manifold leaving the lunar vicinity after about 9 days going into an orbit around Earth. Five orbital and two lunar revolutions later at about 64 days after leaving EML1 the apogee of the orbit is leading to a lunar encounter. The first resonance brings the S/C from an approximated perigee altitude of 100tkm on a perigee altitude of only 60tkm, which is a huge decreasing of the orbital energy by only one lunar encounter.

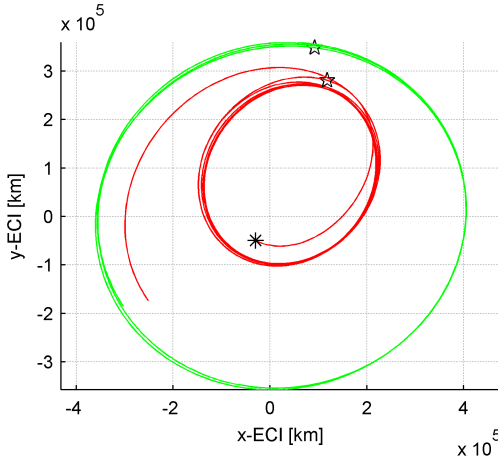


Figure 3.7: Backwards integration from EML1 Halo orbit into the first resonance after leaving the stable manifold.

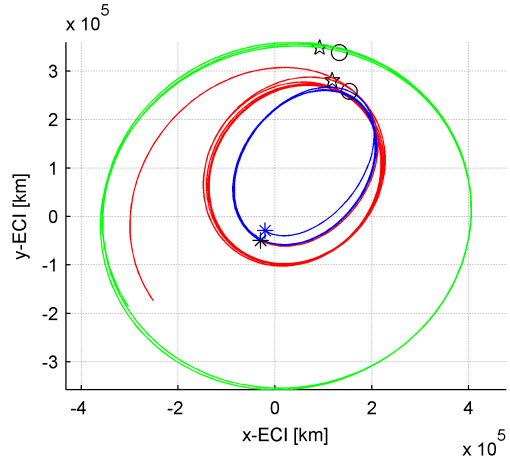


Figure 3.8: Going from one lunar encounter to the next one via backwards integration from last perigee state.

The next step is to scan to the next lunar encounter finding the most optimal resonance. Figure 3.8 shows the result for this step.

Scanning at every stage over a certain Δv range leads in the end to a map of the possible perigee w.r.t. to the Δv - the so called perigee profile - which can be analyzed. The Δv range has been set to -20 up to +20 m/s in normal direction at the perigees and negative stable direction at EML1 orbit. An example analysis has been performed for a scan over a Δv range of zero to 1 m/s with a step size of 0.001 m/s which is small enough to find all possible effects but still has an affordable amount of computational effort. The epoch in EML1 Halo orbit is 7400 days in MJD2000 system and the integration time is 80 days to cover sequences with one (1:2, 1:3 or 1:4) or two (2:5 or 2:7) lunar revolutions. Figure 3.9 shows the results of this analysis for the scan from an Halo orbit into the stable manifold. Figure 3.10 shows the result for a scan of the Δv range from the perigee of one resonance to another. Actually not for every Δv a hop occurs which means that no resonance

is reached because the phasing towards the Moon was not sufficient enough. Therefore some parts of Figure 3.10 does not have any result. Both Figures shows the reached perigee altitude and the

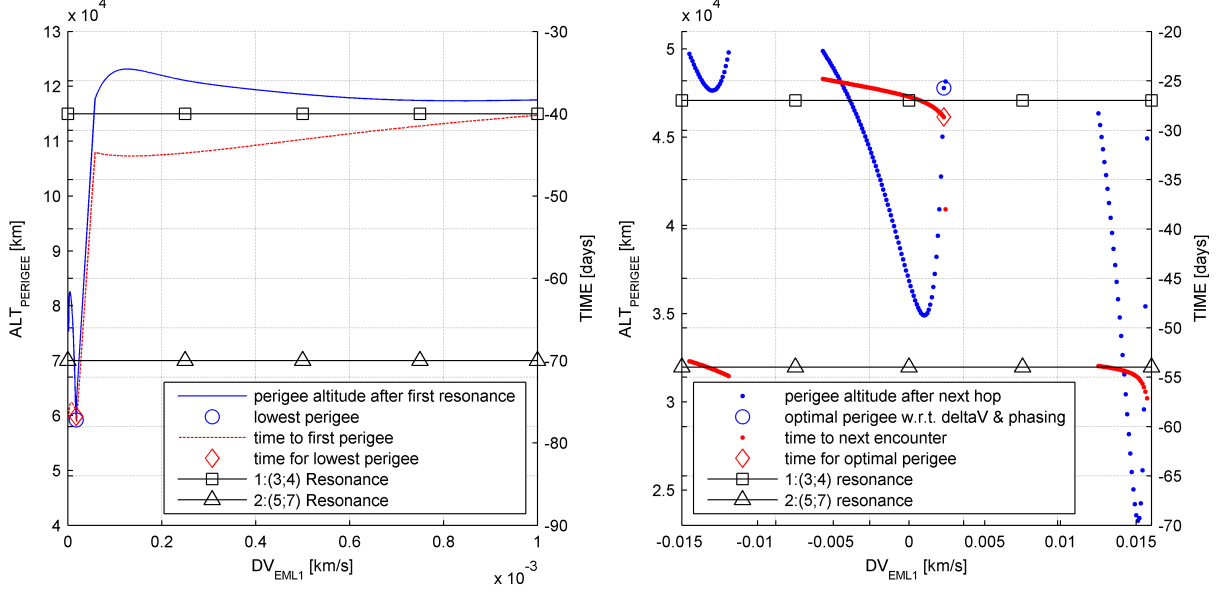


Figure 3.9: EML1 resonance analysis: Backwards scan from EML1 Halo orbit at epoch 7400 MJD2000 finding lowest perigee

Figure 3.10: EML1 resonance analysis between two lunar encounters searching for the optimal phasing

time that was needed to reach them. From the time the number of lunar revolutions directly can be predicted. Taking into account that at least 10 to 12 days coasting time leads to a orbit around Earth resonances occurring around 40 days after the integrations started will result from a 1:X - one lunar revolution - resonance whereas a 70 days event occurs from a 2:X - two lunar revolution - resonance. For Figure 3.10 only the pure lunar period has to be taken into account. In the first case the lowest perigee is reached after a resonance occurring around 70 days after propagation started. This shows an optimal phasing for a 2:X resonance. X can be 5 or 7. In almost all cases the first resonance is reached after 5 revolutions. Theoretically a 1:2 resonance could also appear regarding the semi major axis of the reached orbits. But in all cases a 2:5 resonance appeared both for the Halo and the Lissajous orbit. This can be explained by the phasing. Actually a 2:5 resonance sequence is a mixture between a 1:2 and a 1:3 resonance sequence. After the first lunar revolution already more than 2 orbital revolutions are over and the apogee does not encounter the moon. But after another lunar revolution it fits again and the apogee encounters the moon. Of course one could also force a 1:2 resonance by another manoeuvre or higher Δv 's but in an optimal way it's easier to wait until the phasing matches again. This is something that could be regarded for the orbits later in the procedure when reaching perigees with less than 30 tkm. Due to a good phasing 2:7 resonances can appear. Both phenomena go along with rule number 4 of the best practice rules of the introduction of Chapter 3.3.

Another effect shown in Figure 3.10 is that the space of solutions is not monotone but has more than one local minimum. Therefore a gradient based optimization method is not sufficient for an optimization. At least the entire space of solutions has to be analyzed to find a global minimum for a certain resonance sequence.

Entire Transfer - Strategy

Being able to analyze the resonances due to the Δv which is used in the perigee before a resonance leads to an the possibility to optimize the maneuver towards different issues.

This section deals with different approaches to find the best possible solution for the resonance transfers. In deed, this is no optimization of the entire transfer. It is only a parametric scan over a certain Δv range which can be analyzed later. There is no optimization problem described in this section even though when always "optimization" will be written.

Two major optimization approaches have been successfully implemented and used to analyze the space of solutions:

1. Finding the lowest perigee.
2. Finding best phasing case whether for a 1:X or a 2:X resonance.

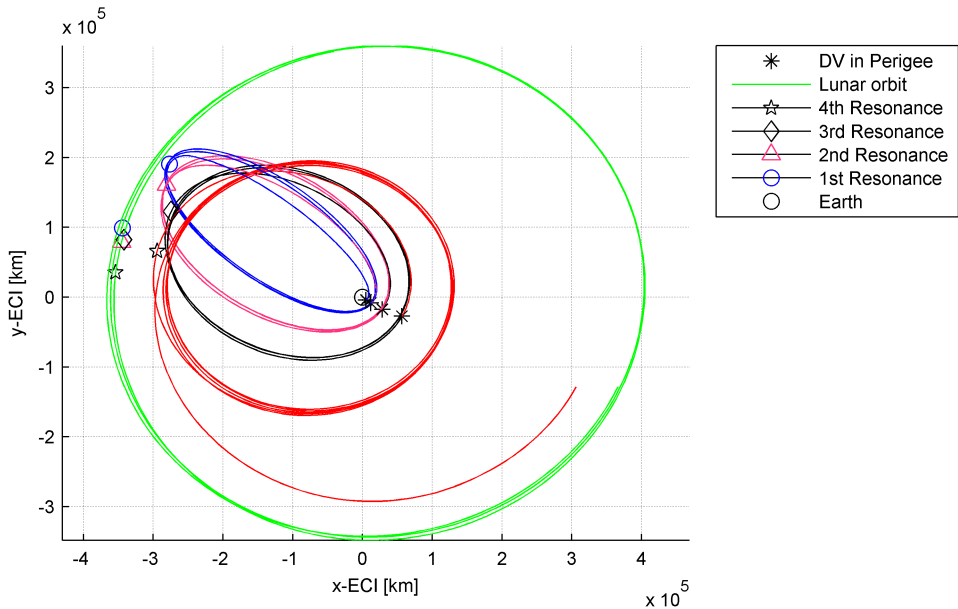


Figure 3.11: transfer from LEO to EML1 Halo orbit arriving at epoch 7468 MJD2000 using resonance sequences

Entire transfers from LEO to both the Lissajous and the Halo orbit could be designed with these optimization approaches. An example of an entire transfers is shown in Figure 3.11 with its altitude profile shown in Figure 3.12. The entire Transfer took 242 days and only needed 64.4 m/s during the resonances while the initial departure burn in LEO needed 3.0625 km/s. A Hohmann transfer - as shown in Figure 3.13 - for the same arrival epoch in EML1 Halo orbit only has a duration of 4 days but needs an departure Δv of 3.0656 km/s and an apogee Δv of 718.29 m/s. The saving for the non-cryogenic Δv 's - $\Delta v_{Resonance}$ and $\Delta v_{ApogeeHohmann}$ - is more than 650 m/s.

Due to the different optimization approaches also different ways to design a transfer exists. The following three ways have been investigated in more detail:

1. Optimizing only by the best perigee.
2. Optimizing only by the best phasing.

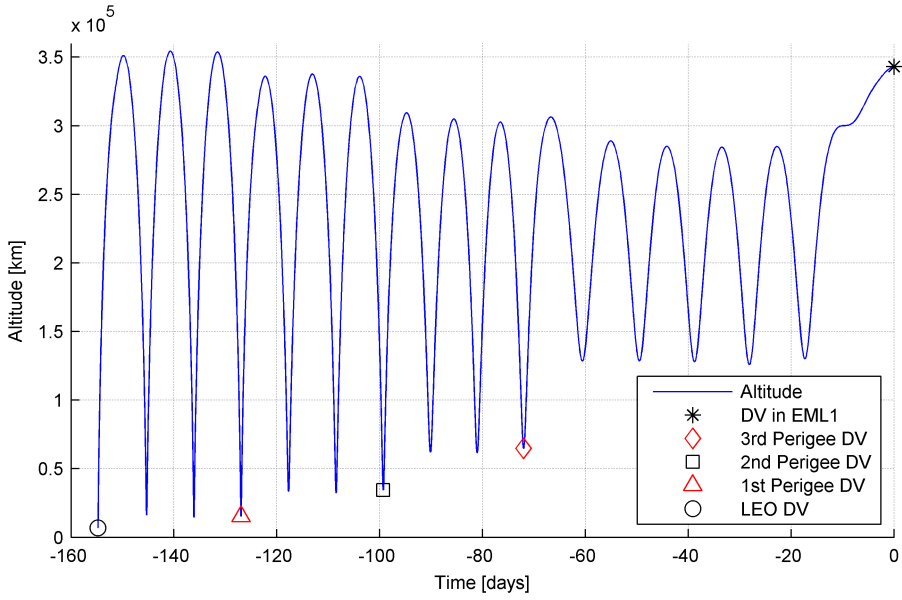


Figure 3.12: transfer from LEO to EML1 Halo orbit arriving at epoch 7468 MJD2000: Altitude profile

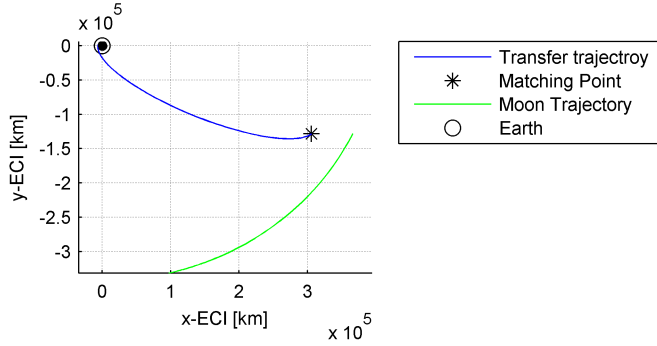


Figure 3.13: Hohmann transfer for epoch 7468 MJD2000

3. Mixed approach by alternately using the optimization issue one and two. After optimizing the resonance due to optimal phasing the next one shall take the maximum perigee win of this optimal phasing.

Scans for entire transfers for a 30 days period from 7400 to 7430 epoch MJD2000 arrival date at EML1 Halo orbit have been performed with all three optimization approaches. The results can be found in Figure 3.14 showing the $\Delta v_{Resonances}$ and the altitude of the initial perigee - the perigee after the first resonance in a backwards integration from the Halo orbit. It can be seen that every approach has some better transfers than the other one for a specific epoch. At least one region between 7417 and 7425 has in all three approaches a significant increasing of the entire $\Delta v_{Resonances}$. As the first part of the trajectory design - going from EML1 orbit to first resonance - used to bring out the same result for every approach without any differences it seemed to be a constant element in each approach which might infect the significant increase of the $\Delta v_{Resonances}$. Further investigation

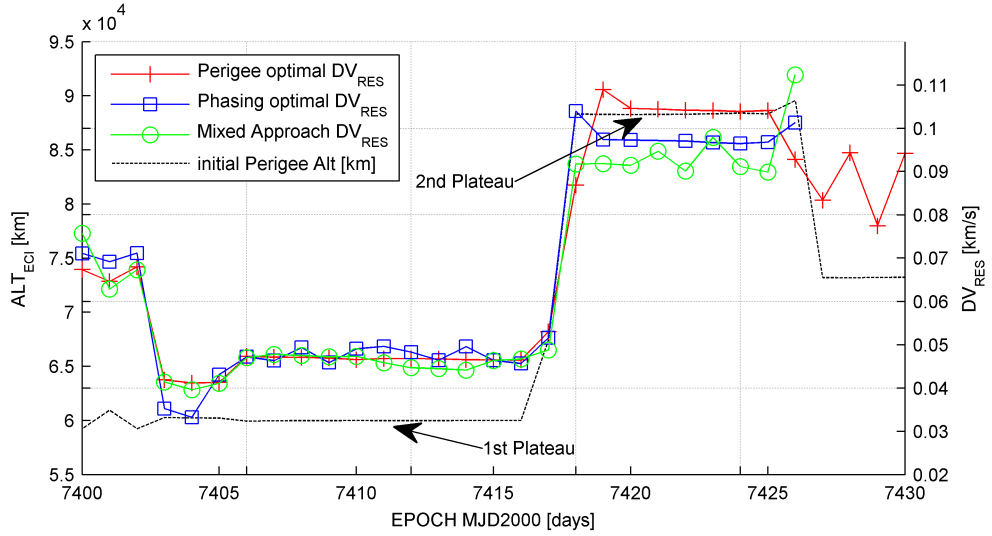


Figure 3.14: $\Delta v_{Resonances}$ for different optimization approaches - Initial Perigee Altitude in ECI frame

brought out that the overall optimization approach for the initial part is the best perigee case in all three approaches.

Plateau-Theory

The investigations showed that a certain perigee altitude will always be reached after the first resonance coming from the EML1 orbit. The perigee is called initial perigee. This phenomenon can be found for clusters of 10 to 14 days of arrival epochs. As a clustering of transfers to a certain launch window - in fact the same initial perigee means the same departure state and therewith a launch window - has a big impact to mission design this issue has to investigated more properly. This section will deal with this phenomenon and the reasons for it.

Figure 3.15 shows how the Δv_{EML1} 's are developing against initial perigee altitudes due to the different arrival epochs. The jump can be moved to the left by increasing the Δv_{EML1} for earlier periods. The same can be done into the other direction. A transition phase between two plateaus of one or two days is giving some space for this. Jumps can be moved within these transitions. With every plateau the Δv_{EML1} is decreasing until transition appears and the Δv_{EML1} is jumping to a maximum again starting to decrease on the next plateau again. Another phenomenon shown on Figure 3.14 are the plateaus for the initial perigee's for a certain period of arrival epoch. It has been identified that the perigees are lying on the same altitudes. In fact all transfers ending up on the same perigee altitude are going to the same point in time and space. This means that over a period of 8 to 10 days all transfers will reach the same initial perigee point. Figure 3.16 shows this phenomenon for both plateaus in Figure 3.14. At least this analysis does not explain why the altitude of the initial perigee's are different. An explanation to this could be found in Figure 3.17 which shows the altitude of the Moon orbit and the Halo orbit w.r.t. the Earth and the altitude profile of the initial sequences for both plateau's of the initial perigee shown in Figure 3.14. It can be found that the transfers are following the Halo orbit for a period of about 10 days and are leaving the Halo orbit at the so called transition point into an Earth orbit. This happens when the distance of the Halo orbit to the Moon has its maximum. The transition can be suppressed by higher Δv_{EML1} , but for the implemented

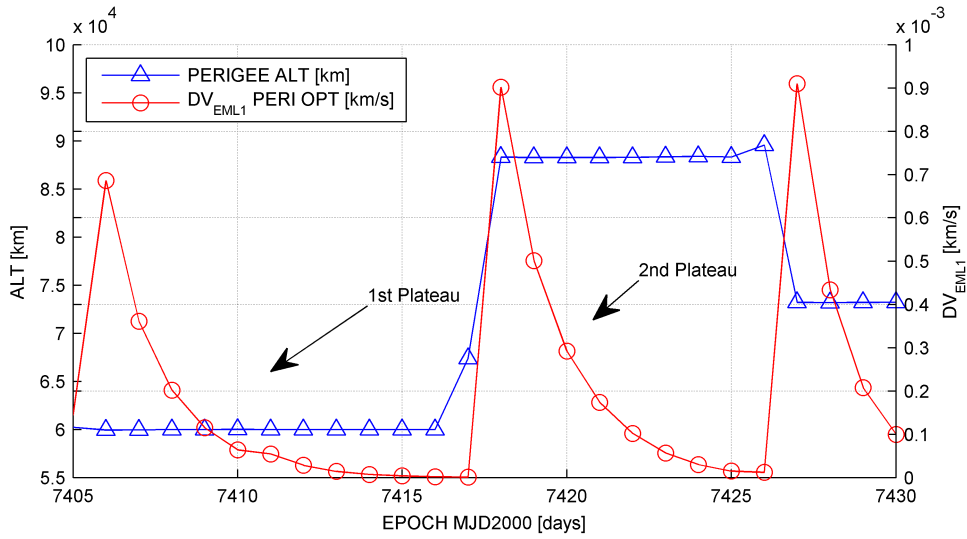


Figure 3.15: Initial Sequence: Δv_{EML1} and the reached perigee altitude

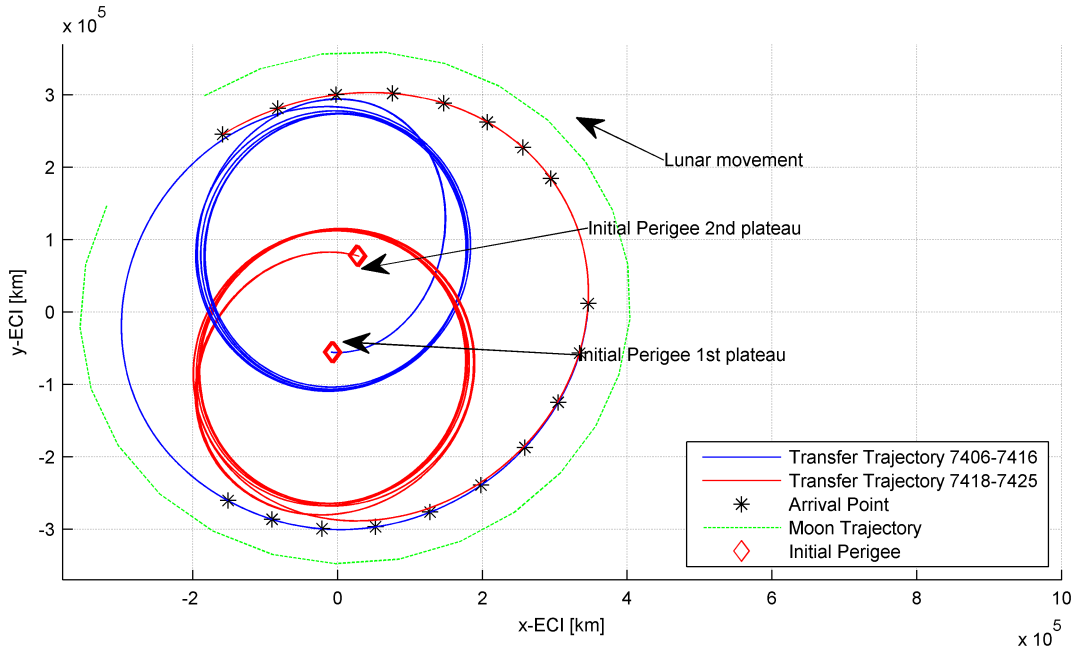


Figure 3.16: perigee optimal trajectories for the initial sequence of 7406-7425 MJD2000

method only Δv_{EML1} 's within a range of 0...1 m/s are considered for the initial maneuver.

Different altitude at the transition leads to different initial perigee altitude and therewith to a different plateau altitude. Depending on the higher initial altitude a higher number of resonances will be required to go to LEO altitude and therewith also a higher Δv . This goes in line with the higher $\Delta v_{Resonances}$ for the second plateau in Figure 3.14. This can explain the higher $\Delta v_{Resonances}$ for

different arrival epochs. Resulting from the analysis of the initial sequence the following theory can

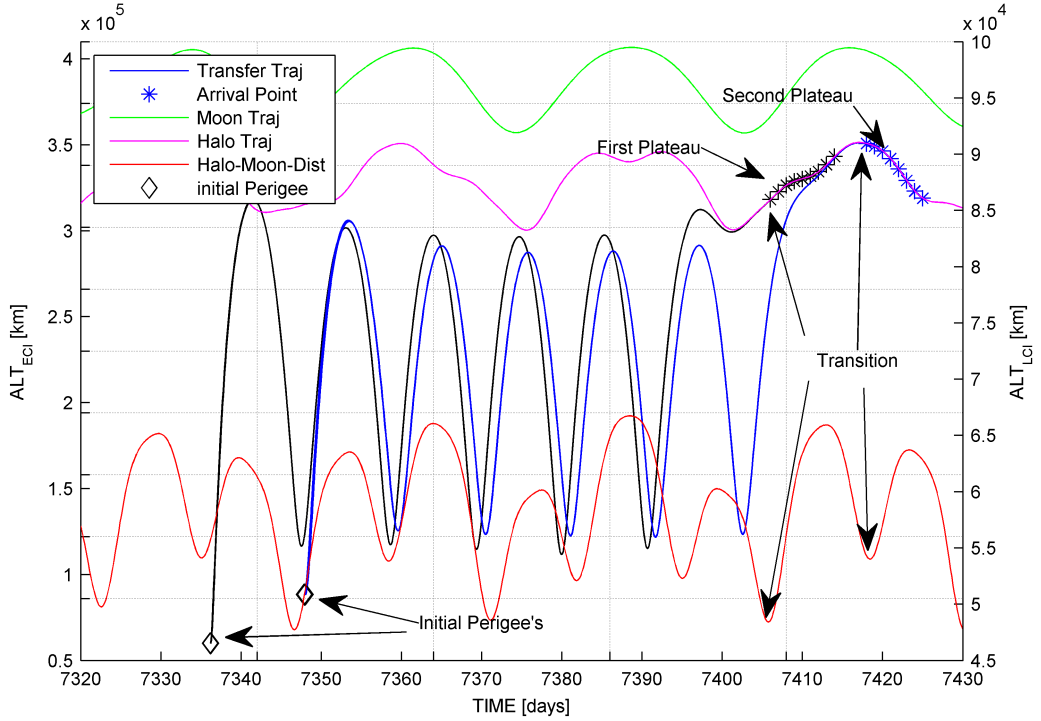


Figure 3.17: Initial Sequence: Altitude profiles vs. lunar distance to Earth and Halo orbit distance to Earth and Halo-LCI-distance

be formulated for transfers using the same initial perigee point:

1. Transfers using the same initial perigee do have the same resonance sequences resulting in the same transfer.
2. The cheapest resonance sequence from each plateau can be used for all arrival epochs of the plateau.
3. W.r.t. the plateau fixed departure times from LEO can be found and a various range of arrival epoch only differing in the Δv_{EML1} .
4. Transition of a plateau appears when the maximum Halo-Moon distance is reached.

Conclusion - Optimization Issues

From this theory it should be possible to find an optimal transfer for every initial perigee and all the transfers going through it. Taking the cheapest transfer solution from the three optimization approaches from one plateau will give the best transfer for all arrival epochs of the plateau. The global optimization problem does not get solved by the given analysis. In the end an optimal sequence of resonances has not been calculated but three strategies how to approach the problem have been presented. At least for every plateau an optimal transfer due to the three cases can be found.

Finally no real optimization has been performed but a parametric scan over a certain Δv range has

been done analyzing the solution space. This is in fact no optimization even if it has been named by that during this section. A true optimization have to implemented in future work.

3.3.2 Computing Transfers - Results

After defining the method used to compute transfers and analyzing them in Section 3.3.1 transfers has to be analyzed over a wider range than 30 days. To achieve a statistically sufficient approach to these transfers they have been computed for an entire year period of 365 days for both EML1 orbits. As some transfers led to wrong LEO orbits due to an problem in the implementation, which was found after computing the transfers, a cleaning to only the relevant LEO altitudes of 400 km (± 10 km) has been performed. Therefore the following figure might not give an value for every arrival epoch. Due to the theory explained in Section 3.3.1 this does not affect the results that much as most of the transfers are located on certain plateaus which leads to the same Δv and departure epoch for the entire transfer. Figures 3.18 and 3.19 shows the results for the $\Delta v_{\text{Resonances}}$ for both investigated EML1 orbits. Due to some uncertainties for the initial perigee calculations the plateaus are not

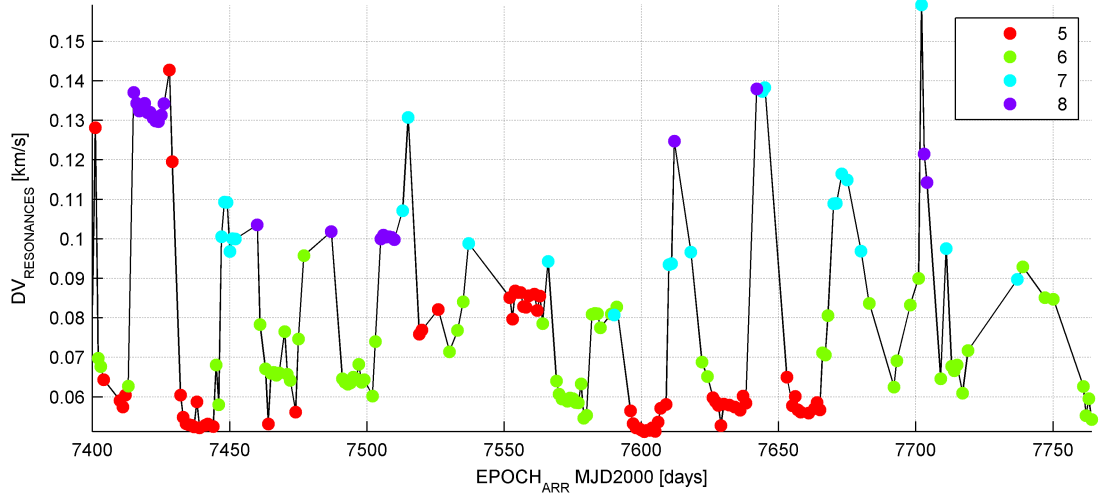


Figure 3.18: LEO to EML1 Lissajous orbit transfer: $\Delta v_{\text{Resonances}}$ w.r.t. the arrival epoch. Scattering due to the number of resonances

sharp for both orbits but at least for the Lissajous orbit they are more precisely visible than for the Halo. Ones knowing the plateau-theory these plateaus can also be found for the Halo orbit. With a sharper scan which would require much higher computational effort this also can be shown. Different colors in both Figures gives the number of resonances that were required to build the transfer. It can be seen that higher $\Delta v_{\text{Resonances}}$ goes along with a higher number of resonances. As the correctional Δv at every resonance requires a certain value ≥ 10 m/s a higher number of resonances will lead to higher $\Delta v_{\text{Resonances}}$.

Figures 3.20 and 3.21 shows the transfer time which also goes along with the number of resonances - shown by the different colors of each value - which is clear due to the fact that one resonance sequence either requires 1 or 2 lunar revolutions. Much clearer than for the $\Delta v_{\text{Resonances}}$ the plateaus can be found for the transfer time. Linear sequences shows that nearly the same transfer time has been used only differing in the later arrival epoch. Finally these sequences will lead to fixed departure epochs.

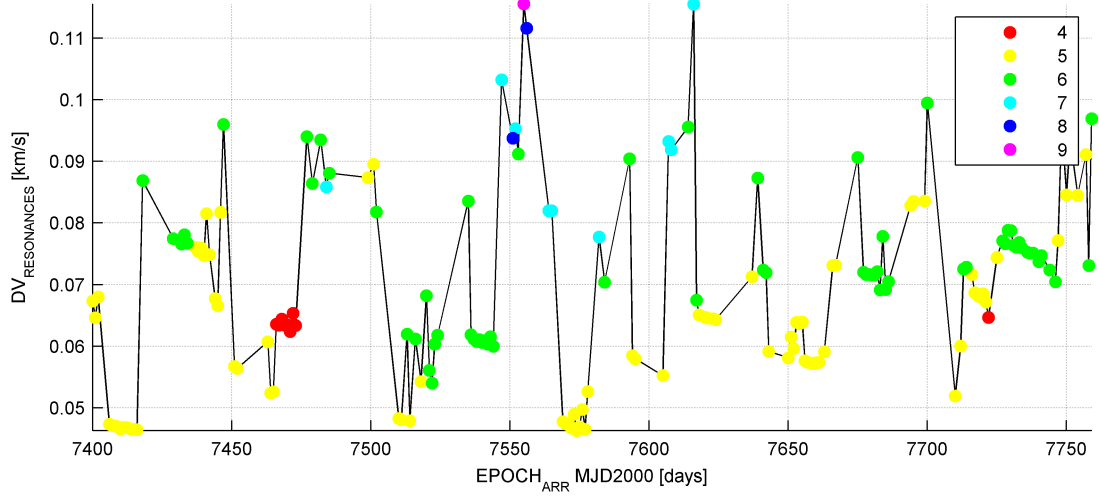


Figure 3.19: LEO to EML1 Halo orbit transfer: $\Delta v_{Resonances}$ w.r.t. the arrival epoch. Scattering due to the number of resonances

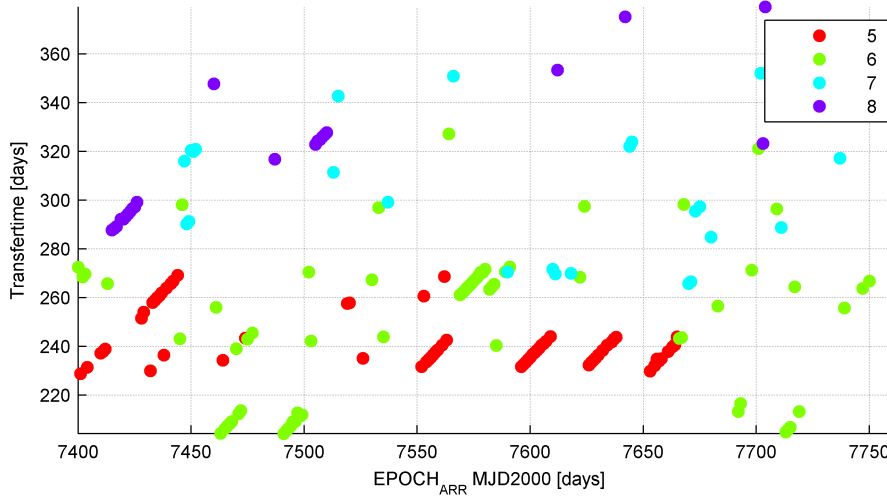


Figure 3.20: LEO to EML1 Lissajous orbit transfer: Transfer time w.r.t. the arrival epoch. Scattering due to the number of resonances

The difference in the transfer time only results from the longer cruising on the invariant manifold. At least only the Δv_{EML1} clarifies when the arrival shall happen. Tuning this final manoeuvre of a transfer makes it possible to hit the correct phase angle of the orbit. This behavior is well known from the WSB transfers described in Chapter 2.

Giving an explanation to the differences of the $\Delta v_{Resonances}$ by the initial perigee altitudes as mentioned in Section 3.3.1, Figure 3.22 shows an significant correlation between both values for the Lissajous orbit. The plateaus can be clearly found for different transfer epochs. Higher plateau altitudes goes along with higher $\Delta v_{Resonances}$.

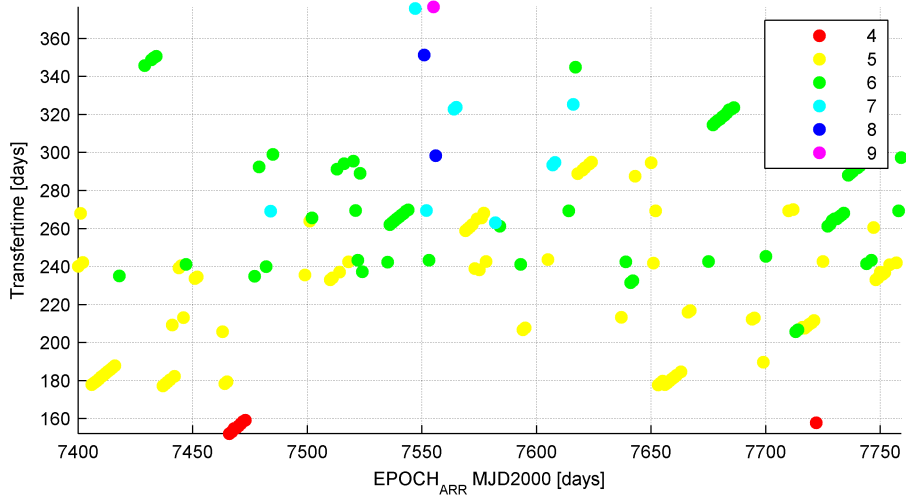


Figure 3.21: LEO to EML1 Halo orbit transfer: Transfer time w.r.t. the arrival epoch. Scattering due to the number of resonances

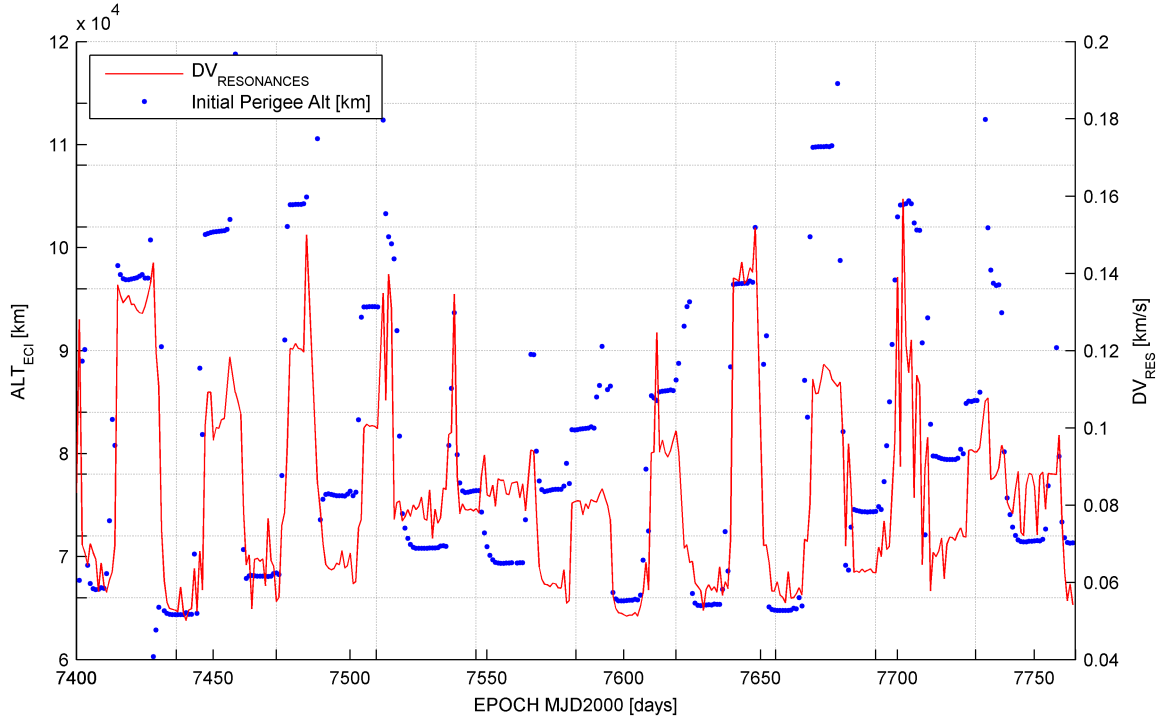


Figure 3.22: Resonance Transfer to EML1 Lissajous orbit: Initial perigee altitude w.r.t. the $\Delta v_{Resonances}$

$\Delta v_{Resonances}$ has been regarded on its own due to the fact that it has to be performed by non-cryogenic fuels with less efficiency. To give a comparable view for other transfer methods now the cryogenic performable Δv_{Earth} for the departure insertion into a high elliptical orbit and the total

amount of $\Delta v_{Resonances}$:

$$\Delta v = \Delta v_{Earth} + \Delta v_{Resonances} \quad (3.2)$$

has to be analyzed.

Figures 3.23 and 3.24 shows the Δv_{Earth} - the Δv required for high elliptical orbit insertion in order to achieve the first lunar encounter.

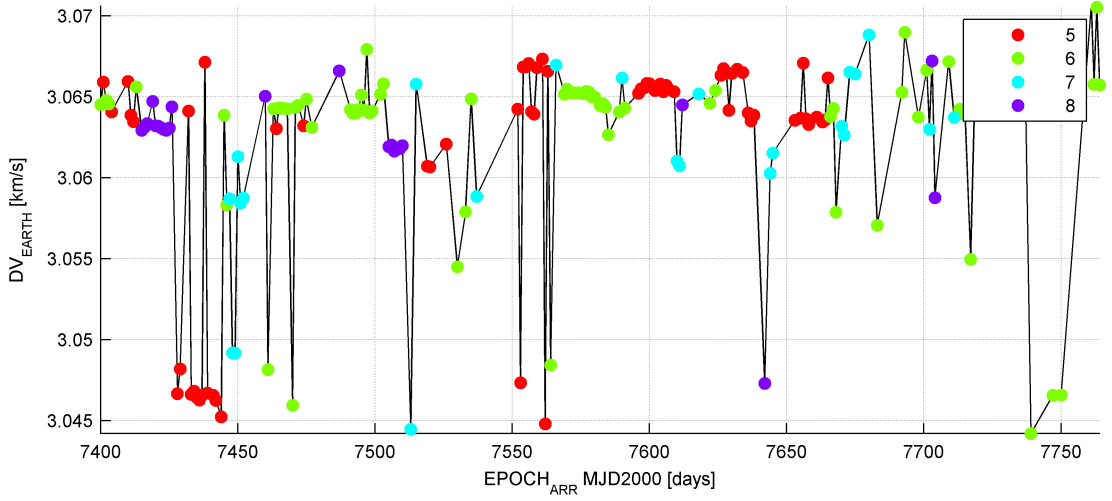


Figure 3.23: LEO to EML1 Lissajous orbit transfer: Δv_{Earth} w.r.t. the arrival epoch. Scattering due to the number of resonances

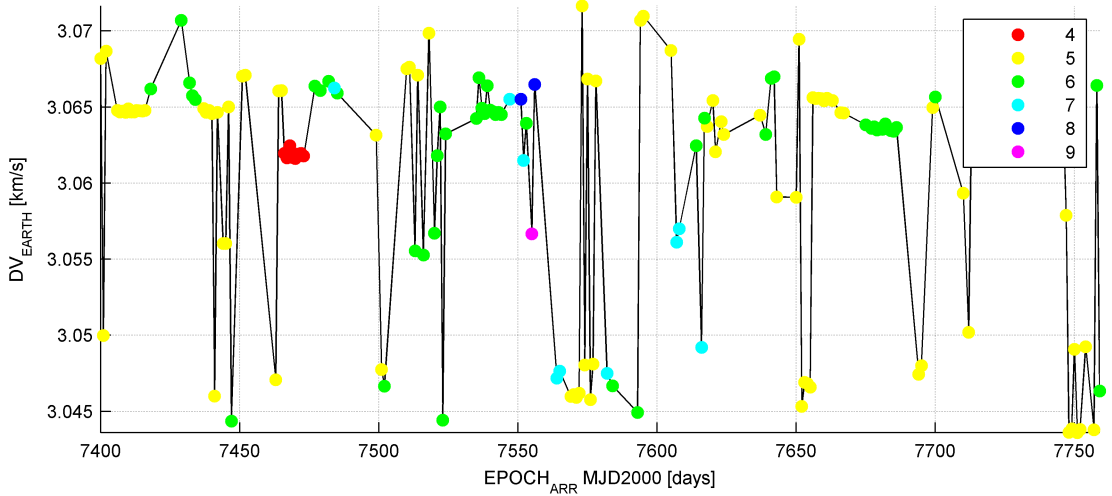


Figure 3.24: LEO to EML1 Halo orbit transfer: Δv_{Earth} w.r.t. the arrival epoch. Scattering due to the number of resonances

Actually there does not seem to be any correlation between the departure Δv_{Earth} and the number of resonances. Figures 3.25 and 3.26 shows the Δv_{Total} for the entire transfer regarding $\Delta v_{Resonance}$ and Δv_{Earth} .

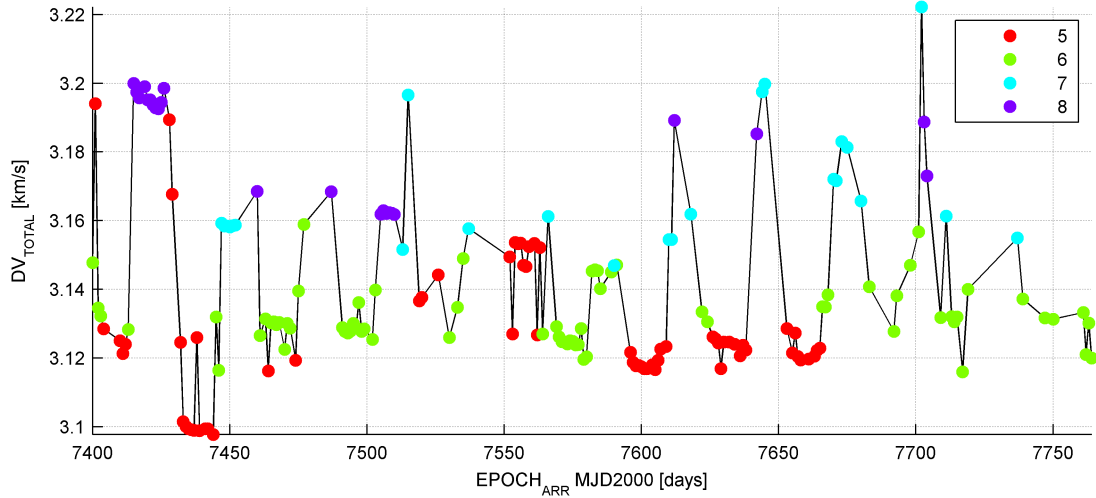


Figure 3.25: LEO to EML1 Lissajous orbit transfer: Δv_{Total} w.r.t. the arrival epoch. Scattering due to the number of resonances

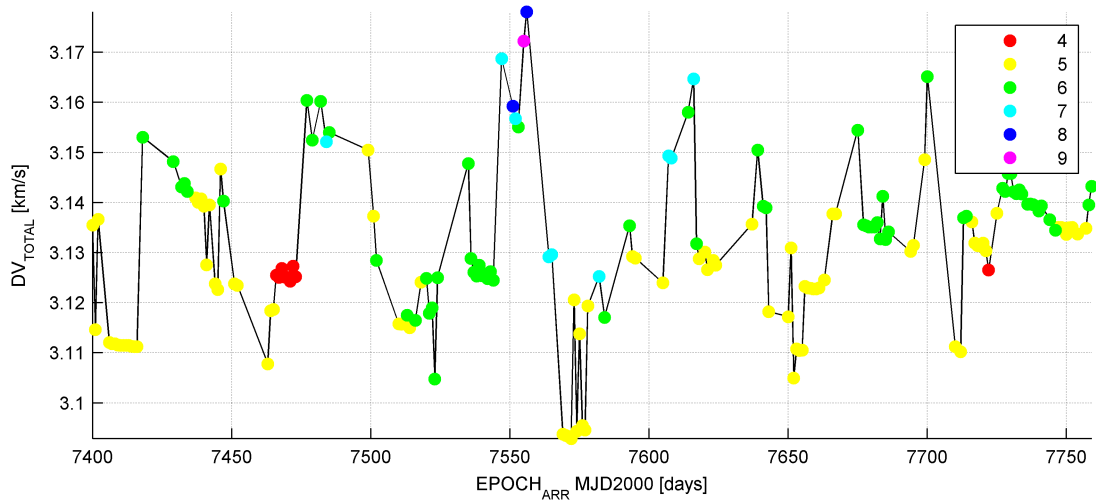


Figure 3.26: LEO to EML1 Halo orbit transfer: Δv_{Total} w.r.t. the arrival epoch. Scattering due to the number of resonances

Table 3.1 shows a summary of the most important values gained from the scans.

	Lissajous Orbit	Halo Orbit
Maximum correction $\Delta v_{Resonances}$ [km/s]	0.159	0.116
Minimum correction $\Delta v_{Resonances}$ [km/s]	0.051	0.046
Variation [km/s]	0.108	0.070
Maximum Earth Departure Δv_{Earth} [km/s]	3.071	3.084
Minimum Earth Departure Δv_{Earth} [km/s]	3.044	3.039
Variation [km/s]	0.027	0.045
Maximum Δv_{Total} [km/s]	3.222	3.178
Minimum Δv_{Total} [km/s]	3.098	3.091
Variation [km/s]	0.124	0.087
TTR _{max} [days]	379	382
TTR _{min} [days]	204	152
Variation [days]	175	230

Table 3.1: LEO to EML1 Lissajous and Halo orbit via resonance transfers: Δv values and duration

3.3.3 Conclusions on the Resonance Transfers without departure orbit consideration

A method to design transfer utilizing lunar resonances has been analyzed and an implementation has been performed. Scans over a 365 days period for both the Lissajous and Halo orbit have been done. Significant Δv_{Total} towards an usual Hohmann transfer could be shown. Longer transfer durations and higher Δv_{Total} compared with the WSB region transfer makes it less efficient to use transfers utilizing lunar resonances. Although the $\Delta v_{Resonances}$ are small, they could not be eliminated completely. Launch window considerations have to be taken into account due to the clustering of the mentioned plateaus.

3.4 Optimized transfers from LEO with fixed inclination

For now only the natural transfers without regarding departure orbit requirements have been investigated. Figure 3.27 shows the inclinations of the departure state of the computed transfers from Section 3.3.

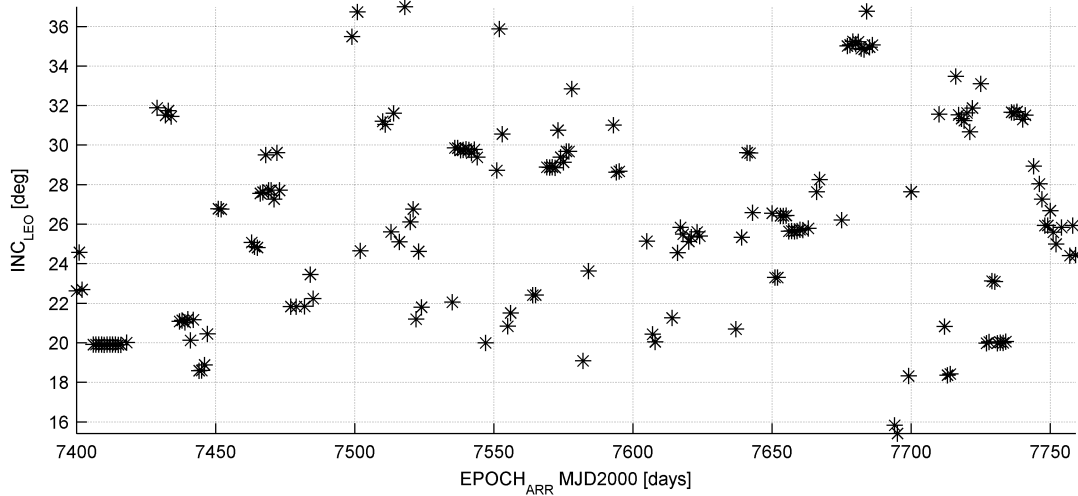


Figure 3.27: Inclination of departure orbit for Transfers from LEO to EML1 Halo orbit

The inclination for these transfers always where depending on the inclination of the Moon orbit w.r.t. the Earth equatorial plane or at least they did not change more than 10° from it. This can be explained by the fact that the Moon always pulls the S/C in its orbital plane. As the departure orbital state should not depend on the inclination of the Moon but should be fixed to launcher performance requirements, the possibilities of using the lunar gravitational drag to change the inclination of the transfers must be investigated. Figure 3.28 shows the possible inclination changes - Δ_{Inc} - at lunar encounter for different apogees and inclinations relative to the lunar orbit inclination computed by a forward methode from LEO with different departure inclinations.

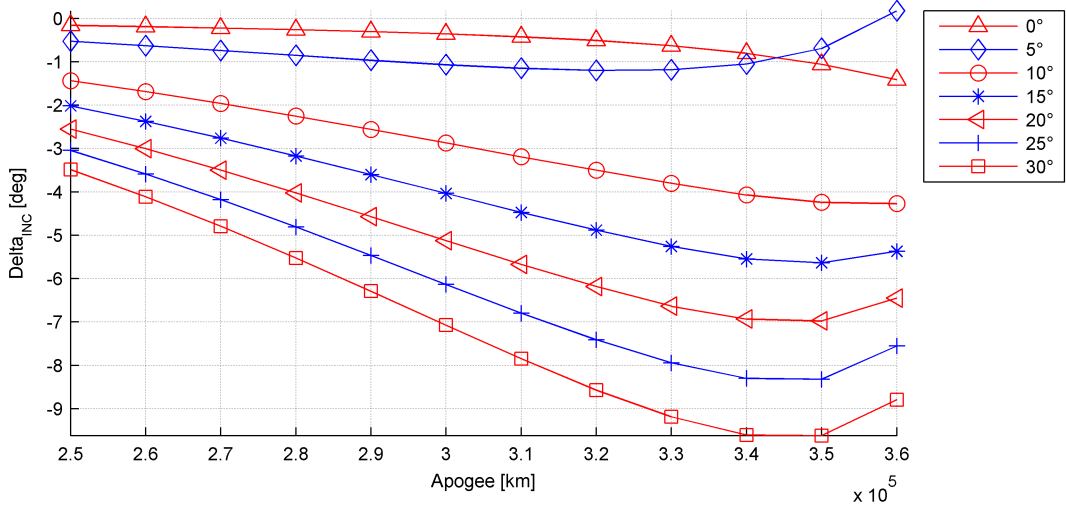


Figure 3.28: Ability to change the inclination at lunar encounter for different apogee altitudes and different relative inclinations of the encountering orbit w.r.t. the lunar orbit inclination

The allover optimization approach for reaching certain inclinations must consider both the perigee changing ability of a lunar encounter and the inclination change. This leads to a multi objective optimization again. Following optimization methods could be used:

1. Shooting from perigee into the next resonance sequence as described in Section 3.3.
2. Finding the hop with the highest change in inclination.

This makes it possible to use the same implementation as already described in Section 3.3, only changing the optimization to the best inclination change. To resolve additionally variational parameters a gradient based optimization in all three spatial velocity components could be used. This method has not been considered in this work any longer.

4 Summary and Conclusions

4.1 Summary

Two transfers have been investigated towards their efficiency and characteristics, such as:

- Δv
- Travel time
- Launcher requirements (Inclination, ω and Ω)
- Usage of cryogenic or non-cryogenic fuel

A method to find WSB transfers to EML2 with $\Delta v_{EML2} \sim 0$ has been presented via backwards propagation methods combined with a bisection for high precision departure orbit localization.

Based on this method a implicit time matching and explicit space matching optimization method - based on the gradient optimization Tool SNOPT [25] - for WSB transfers for fixed inclination has been implemented.

Furthermore, a method to compute autonomously transfers from LEO to EML1 orbits utilizing lunar resonances has been implemented and proven.

All three methods have been used to compute transfers for a 365 days period for both Lissajous and Halo orbits at EML1 and EML2 and the following tools have been created:

- LEO to EML2 "Free Transfers" Bisection: Backwards integration - in ECI-Coordinate-System - from certain EML2 orbit epoch for free transfers without any mid course manoeuvres.
- LEO to EML2 "Optimized Transfers": Backwards integration - in ECI-Coordinate-System - from certain EML2 orbit epoch with correctional manoeuvre to optimize the Transfer for fixed departure states in LEO
- Initial Guess Generator for LEO to hit a certain point of interest.
- LEO to EML1 Lunar Resonance Transfer Generator (LRTG): Backwards integration - in ECI-Coordinate-System - from certain EML1 orbit epoch to LEO designing an entire transfer utilizing lunar resonance.

All described tools are available on the DVD attached to this work. Implementation has been done with MATLAB (version 2007b) using MATLAB-executable-functions (mex-function) written in FORTRAN for the integration due to the speed-up for FORTRAN implemented software. Integration has been performed by a 7th order Runge-Kutta-Fehlberg-Scheme Formula 7(8) [14] - also known as RKF78 - which is a standard integration routine for astrodynamical computations. This version is based on ESOC's mission analysis software.

4.2 Conclusions

Table 4.1 sums up all advantages and disadvantages that have been found for both transfer methods.

	WSB Transfer	Resonance Transfer
Pros	<ul style="list-style-type: none"> - $\Delta v_{EML2} \sim 0$ - Minimal propulsion required beyond LEO <ul style="list-style-type: none"> - usage of cryogenic fuel - ≤ 3 months travel time 	<ul style="list-style-type: none"> -Using Lunar attraction to save Δv
Cons	<ul style="list-style-type: none"> -free ω required at launch -Δv_{Match} for fixed launch inclinations -inclination variable for free transfer 	<ul style="list-style-type: none"> -$\Delta v_{Resonances}$ not negligible -Medium propulsion required beyond LEO ≥ -3 months travel time (up to 1 year!)

Table 4.1: pros and cons for WSB and resonance transfer

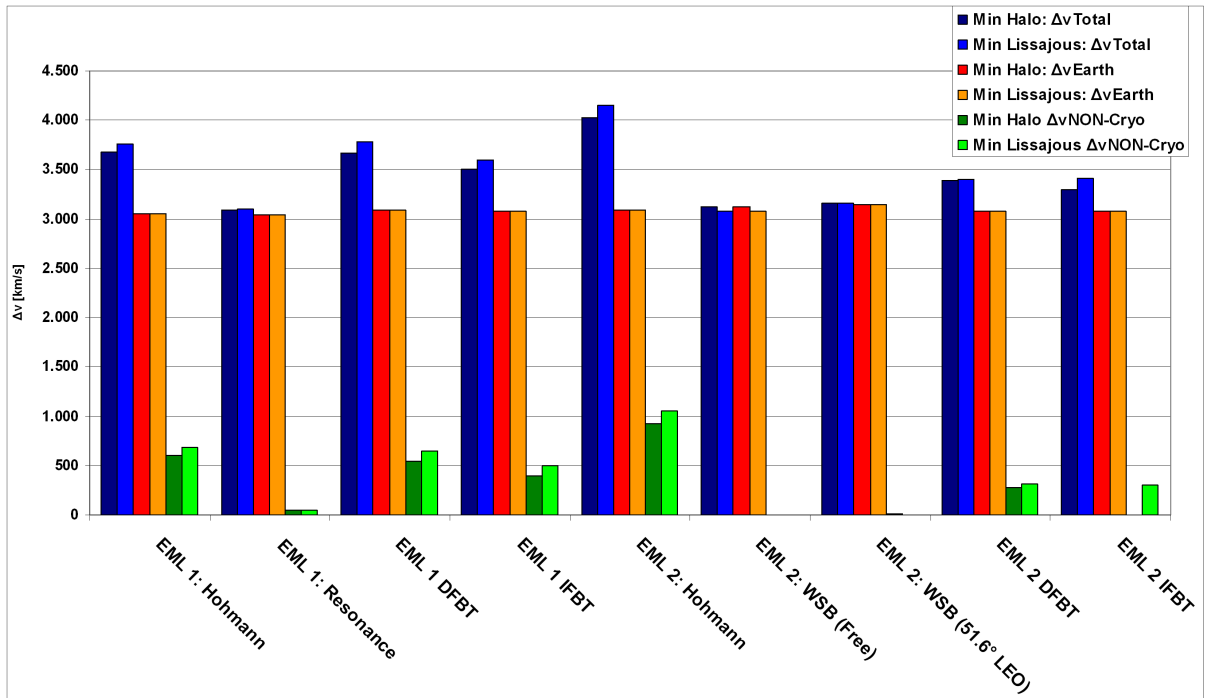


Figure 4.1: Comparison between transfers computed by F. Renk [4] and transfers of this study

Due to the relatively long transfer time and the not negligible $\Delta v_{Resonances}$ transfers, utilizing lunar resonances seems to make a trade off between EML1 and EML2 easy to prefer EML2 as potential staging location for future manned space exploration. As mentioned by F. Renk [4] EML2 seems to be from this point of view the favorable location to base exploration plans on.

At least this study could show that utilization of natural effects is an efficient way to reduce the Δv requirements for future cargo and supply missions in the scope of manned and unmanned space exploration.

Using the WSB region transfer could make it possible for smaller satellites - student satellites like

cubesat or even nano satellites - to perform science at the Moon without any powerful main engine requirements. Lowering the complexity of future mission design and giving the unique chance to open a window to cheap transfer to the next possible outpost of mankind in space.

A comparison between the transfers from this study with other transfer types investigated by F. Renk in [4] brings out the following Figure 4.1 Even though the mentioned transfers are not comparable due to the transfer time as both the WSB and the resonance transfer last much longer, a comparison due to the Δv_{Total} gives a clear advantage for these two transfers. Only the difference in the non-cryogenic Δv gives the crucial bonus to the WSB transfer.

Finally EML2 seems to be the more favorable libration point due to operational issues. The fast fly-by transfers described by Renk in [4] together with longterm WSB transfer could give a proper mission concept due to operational needs of a permanent outpost at EML2.

Via usage of heteroclinic connection [26] EML1 could even be reached via EML2 in a lower transfer time than with the transfer utilizing resonances.

The following possibilities using the WSB transfer are considerable:

- cargo & supply missions
- infrastructure missions (Relay-Satellites, Modules, etc.)
- scientific observation missions
- utilizing EML1 via heteroclinic connections
- student satellites

In this scope the presented transfer methods could be the backbone of future exploration activities beyond LEO.

4.3 Outlook

The following questions have been raised during this work to be worth analyzed in more detail in future work:

- Launcher requirements identification for the gained departure state data \Rightarrow optimizing the found transfers towards different launchers.
- Resonance transfers form higher inclined departure orbits \Rightarrow The ability to change inclination with resonances.
- Optimization of transfers utilizing lunar resonances.

Bibliography

- [1] Robert W. Farquhar, David W. Dunham, Yanping Guo, and James V. McAdams. Utilization of libration points for human exploration in the sun earth moon system and beyond. *Acta Astronautica*, 55:687–700, 2004.
- [2] W. Huntress, D. Stetson, R. Farquhar, J. Zimmerman, B. Clark, W. O’Neil, R. Bourke, and B. Foing. The next steps in exploring deep space - A cosmic study by the IAA. *Acta Astronautica*, 58:304–377, March 2006.
- [3] E.W. Messerschmid, F. Renk, J. Noll, B. Ganzer, and J. Schlutz. Space station final report 2008. Technical report, Department of Astronautics at Universität Stuttgart, 2008. <http://www.irs.uni-stuttgart.de/SSDW>.
- [4] F. Renk, M. Hechler, and E. Messerschmid, editors. *Exploration Missions in the Sun Earth Moon System: A Detailed view on Selected Transfer Problems*, number IAC-08-A5.3.5, 2008.
- [5] J. Schoenmaekers. Cross-scale mission analysis, transfer using moon resonances. Technical Report MAS Working Paper No. 511, Issue 1, European Space Agency, Directorate of Technical and Operational Support, Ground System Engineering Department, Flight Dynamics Division, Mission Analysis, June 2007.
- [6] J. Schoenmaekers, J. Pulido (TOS/GFI), and J. L. Cano (TOS/OFA). Smart-1, moon mission: Trajectory design using the moon gravity. Technical Report S1-ESC-RP-5501, Issue 1, European Space Agency, Directorate of Technical and Operational Support, Ground System Engineering Department, May 1999.
- [7] E. Belbruno and J. P. Carrico, editors. *Calculation of Weak Stability Boundary Ballistic Lunar Transfer Trajectories*, number 2000-4142, Denver, Colorado, 2000. AIAA/AAS Astrodynamics Specialist Conference.
- [8] NASA. Wilkinson microwave anisotropy probe: Homepage. <http://map.gsfc.nasa.gov/mission/>, 2008.
- [9] E. Canalias and J. J. Masdemont. Computing natural transfers between Sun-Earth and Earth-Moon Lissajous libration point orbits. *Acta Astronautica*, 63:238–248, July 2008.
- [10] Team Red. Esa cdf study report: Red team architecture for moon. Technical Report CDF67(A),ESA, ESA, December 2007.
- [11] Vladimir A. Chobotov. *Orbital Mechanics*. AIAA EDUCATION SERIES. American Institute of Aeronautics and Astronautics, Inc., 1801 Alexander Bell Drive, Reston, Virginia 20191-4344, 2002.
- [12] Wikipedia. Orbital elements. www.wikipedia.org/orbitalelements, 2008.
- [13] D.A. Vallado and W. D. McClain. *Fundamentals of Astrodynamics and Applications*. Springer, 2001.
- [14] E. Fehlberg. Nasa: Technical report no. 287: Classical fifth-, sixth-, seventh-, and eighth- order

runge- kutta formulas with stepsize control. Technical report, NASA, George C. Marshall Space Flight Center, 1968.

- [15] A. McInnes. An introduction to libration point orbits. unpublished paper, 2006.
- [16] V.G. Szebehely. *Theory of Orbits: The restricted Problem of three Bodies*. Academic Press, New York, May 1967.
- [17] G. Gómez, R. Martine, and J. Llibre. *Dynamics and Mission Design Near Libration Points Volume 1*. World Scientific Publishing Co Pte Ltd, May 2001.
- [18] M. Hechler. Herschel planck paper. Technical report, ESA internal Report, ESOC, Darmstadt, 2000.
- [19] G. Gómez, W. S. Koon, M. W. Lo, J. E. Marsden, J. Masdemont, and S. D. Ross. Connecting orbits and invariant manifolds in the spatial restricted three-body problem. *Nonlinearity*, 17:1571–1606, September 2004.
- [20] W. S. Koon, M. W. Lo, J. E. Marsden, and S. D. Ross. Low Energy Transfer to the Moon. In *Bulletin of the American Astronomical Society*, volume 33 of *Bulletin of the American Astronomical Society*, pages 1195–+, November 2001.
- [21] E. A. Belbruno. *Capture Dynamics and Chaotic Motions in Celestial Mechanics: With Applications to the Construction*. Princeton University Press, 2004.
- [22] E. Belbruno. Ballistic lunar capture transfers using the fuzzy boundary and solar perturbations: a survey. *Journal of the British Interplanetary Society*, 47:73–80, February 1994.
- [23] E. A. Belbruno and M. Martinez-Sanchez, editors. *Lunar capture orbits, a method of constructing earth moon trajectories and the lunar GAS mission*. AIAA, May 1987.
- [24] B. Bello, F. Garziani, and P. Teofilatto. Study on software tool for construction of weak stability boundary transfers. Technical Report GMV-WESBOT-FR, GMV, S.A., ESA internal Report, 2000.
- [25] E. Philip Gill. *Users Guide for SNOPT Version 7: Software for Large-Scale Nonlinear Programming*. Departement of Mathematics, University of California, San Diago, February 2006.
- [26] M. Gidea and J.M. Masdemont. Geometry of homoclinic connections in a planar circular restricted three-body problem. *Int. J. Bif. Chaos*, 2006.

5 Appendix

5.1 Appendix: Introduction

5.1.1 Libration Point Orbits

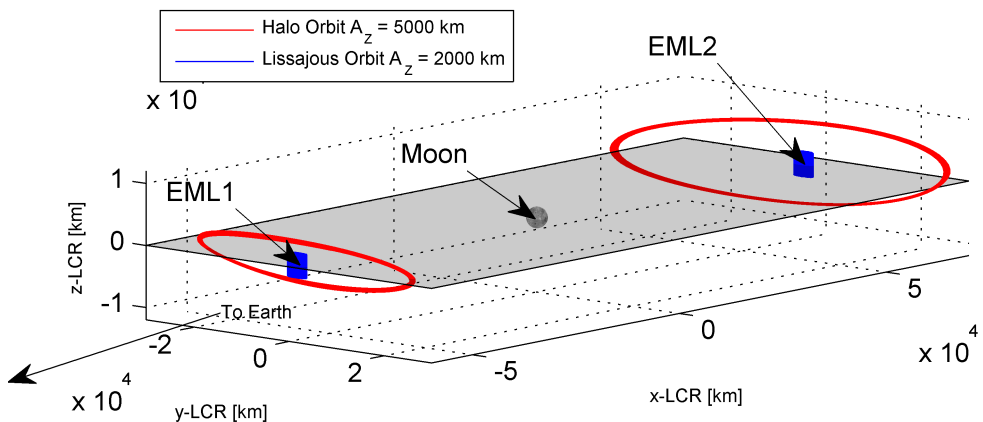


Figure 5.1: used libration point orbit in this work

The initial conditions for libration point orbits will always be taken from the same orbits around EML1 and EML2. For both libration points the same type of orbits:

- a Halo orbit with a 5000 km z-amplitude
- a Lissajous orbit with a 2000 km z-amplitude

Figure 5.1 gives a brief view to the described orbits with the Moon as the primary body. To make the results comparable to the transfers described and investigated in [4] these orbits have been chosen. The used orbits were generated with the ORBGEN tool described by F. Renk [4]. The integration has been performed in an lunar-centered-rotating (LCR) frame - setting the Moon into the center of the coordinate frame and considering all forces resulting from the lunar rotation around the Earth - and is based upon the JPL ephemeris data for the Moon, the Sun and the Earth from 2020 to 2040. The next sections will show the orbits and explain how to generate them by using the ORBGEN Tool

EML2: 2000 km Lissajous Orbit

MATLAB command:

```
mue = 0.01215058162343;
x_L = 0.16783273173707;
c_2 = 2.91260415241092;
[TEPOCH,XADIM,XLISS,IERR] = orbgeneml2([1-mue+x_L + 2000/424400/c_2/1.03
0 2000/404400 0 0 0],40,40,5*365,0.01,5);
```

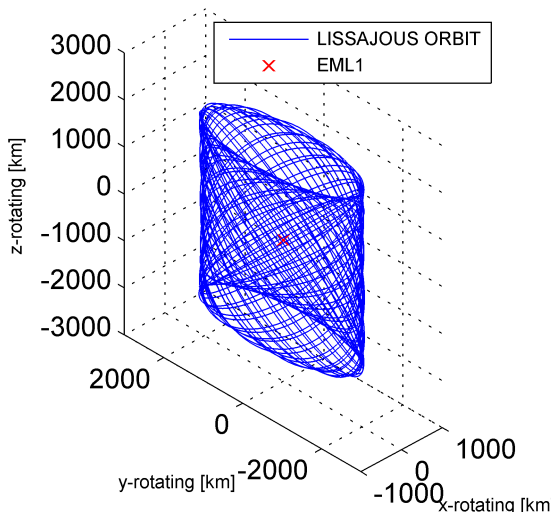


Figure 5.2: EML2 Lissajous orbit: ISO view

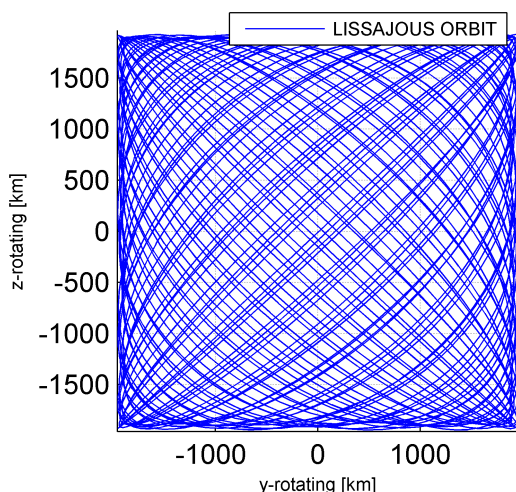


Figure 5.3: EML2 Lissajous orbit: YZ view

EML2: 5000 km Halo Orbit

MATLAB command:

```
[TEPOCH,XADIM,XLISS,IERR] = orbgeneml2([1.17904    0.00
0.01300728407908/1.08    0.00   -0.15683527663229  0.00],40,50,2*365,0.015,5);
```

EML1: 2000 km Lissajous Orbit

MATLAB command:

```
[TEPOCH,XADIM,XLISS,IERR] = orbgeneml1([0.83564093521029  0
0.00495221685949  0  0  0]',30,40,2*365,0.02,5);
```

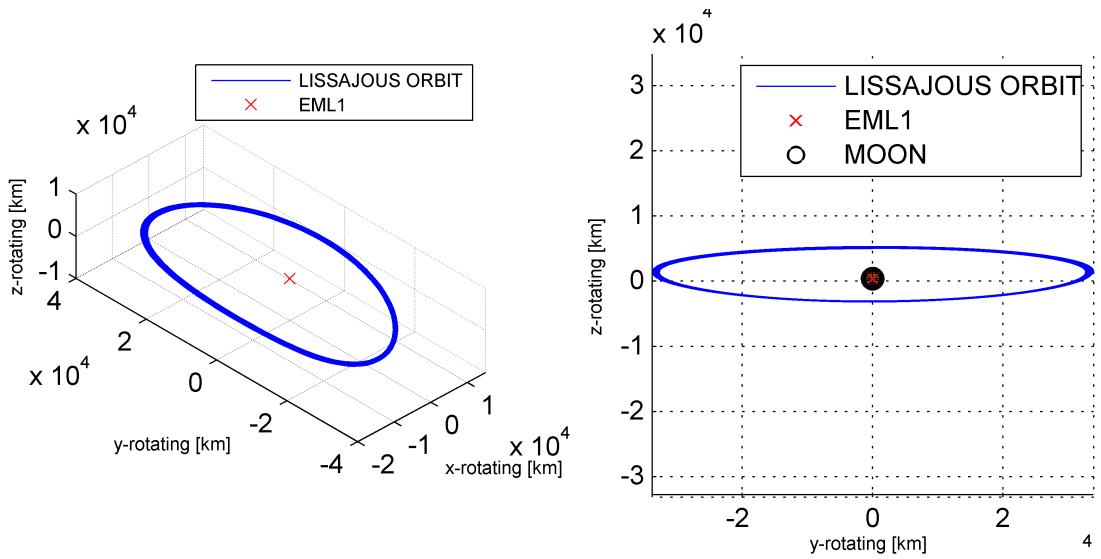


Figure 5.4: EML2 Halo orbit: ISO view

Figure 5.5: EML2 Halo orbit: YZ view

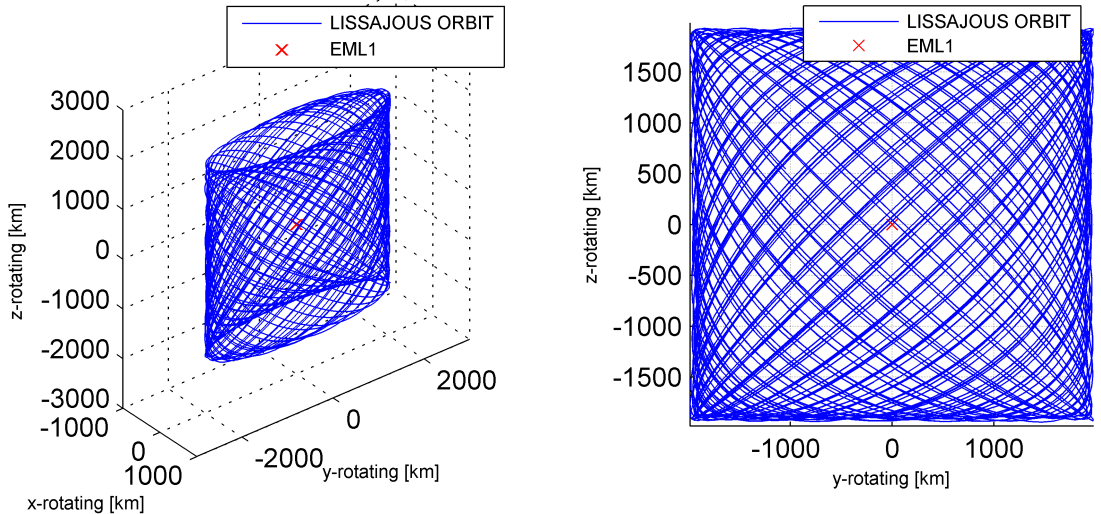


Figure 5.6: EML1 Lissajous orbit: ISO view

Figure 5.7: EML1 Lissajous orbit: YZ view

EML1: 5000 km Halo Orbit

MATLAB command:

```
[TEPOCH,XADIM,XLISS,IERR] = orbgeneml1([0.83564093521029 0
0.00495221685949 0 0 0]',30,40,2*365,0.02,5);
```

To give an idea about distances Figure 5.10 shows the distance from each of the mentioned orbits to the Moon center. They are taken from the LCI coordinates.

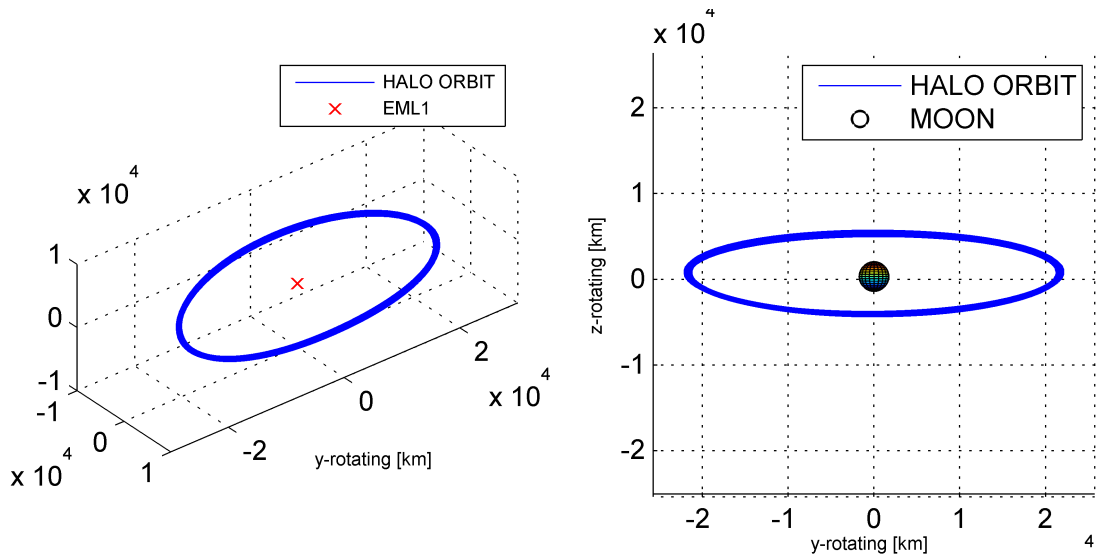


Figure 5.8: EML1 Halo orbit: ISO view

Figure 5.9: EML1 Halo orbit: YZ view

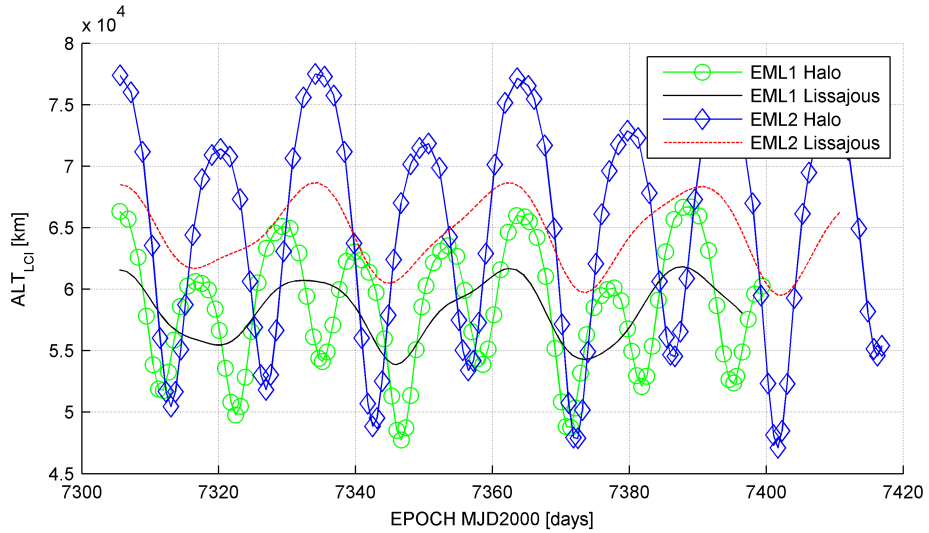


Figure 5.10: Distance of the Libration Point orbit to the Moon in Lunar center inertia System

5.2 Tools

The following tools have been developed to compute the described transfers to EML1 and EML2:

- LEO to EML2 "Free Transfers": Backwards integration - in ECI-Coordinate-System - from certain EML2 orbit epoch for free transfers without any mid course manoeuvres.
- LEO to EML2 "Optimized Transfers": Backwards integration - in ECI-Coordinate-System - from certain EML2 orbit epoch with correctional manoeuvre to optimize the Transfer for fixed departure states in LEO

- Initial Guess Generator for LEO to hit a certain point of interest
- LEO to EML1 Lunar Resonance Transfer Generator (LRTG): Backwards integration - in ECI-Coordinate-System - from certain EML1 orbit epoch to LEO designing an entire transfer utilizing lunar resonance.

All described tools are available on the DVD attached to this work. Implementation has been done with MATLAB (version 2007b) using MATLAB-executable-functions (mex-function) written in FORTRAN for the integration due to the speed-up for FORTRAN implemented software. Integration has been performed by a 7th order Runge-Kutta-Fehlberg-Scheme Formula 7(8) [14] - also known as RKF78 - which is a standard integration routine for astrodynamical computations. This version is based on ESOC's mission analysis software. Optimization is based on the nonlinear gradient optimization tool SNOPT [25].

Most of the used tools have been explained in the main part of the study but some have been referenced to the appendix for further explanations. These tools will be described in more detail in the following sections.

5.2.1 Optimized transfers from LEO with fixed inclination

Initialization of Optimization - The Initial Guess Generator

The initial guess will be generated from Keplerian elements calculation taken from [11]. As the entire state vector of the apogee is known from the backwards integration these coordinates can be used for the calculation. From the high ecliptic transfer orbit the following parts are known:

- Inclination in LEO
- Perigee altitude: 400 km above Earth surface (6778 km)
- Apogee state in Cartesian coordinates: from last point of backwards integration from EML2

The calculation is based on a semi hybrid analytical/numerical calculation of the Ω and ω of the transfer orbit. Semimajor axis and eccentricity can be calculated from the perigee and apogee by:

$$a = \frac{(r_{Peri} + r_{Apo})}{2} \quad (5.1)$$

$$e = a(1 - e^2) \quad (5.2)$$

The true anomaly (Θ) is set to zero degrees for the perigee and 180 degrees for the apogee. As known a , e , i and Θ only Ω and ω are missing. Transformation between Cartesian and Keplerian elements gives the following relation:

$$z = r \cdot (-\sin(\omega) \cdot \sin(i)) \quad (5.3)$$

which can be transform to:

$$\omega = \arcsin\left(\frac{-z}{r \cdot \sin(i)}\right). \quad (5.4)$$

The coordinate z is taken from the apogee state. After knowing the argument ω the numerical part of the guess generation is starting. From the fact that Θ is 180° in the apogee and all other Keplerian elements except the right ascension (Ω) are known makes it easy to scan over the entire Ω range of 0° to 360° . Exactly this is what the algorithm makes. With a stepsize of 0.1° Ω gets shifted and every step the Keplerian state vector gets transformed into the Cartesian one. Then the x and y values gets

compared with the ones from the apogee. If they match Ω has been found if not Ω gets increased by 0.01° and the scan goes on until a matching has been found. This procedure is very robust against changes in the quadrants of the Cartesian coordinate system. As the analytical solution for Ω does not tell anything about the quadrant and it has to be calculated separately. The presented hybrid analytical/numerical approach is a very fast and robust method to get precise results. A later method should also calculate Ω analytically and check every quadrant for a matching. This seems more efficient and also robust.

Another feature of the initial guess generator is the separation between north- and southbound solution. Both solution differs by:

$$\omega_{South} = \pi - \omega_{North}. \quad (5.5)$$

Figures 5.11 and 5.12 shows the results of the initialization for arrival epoch 7400.

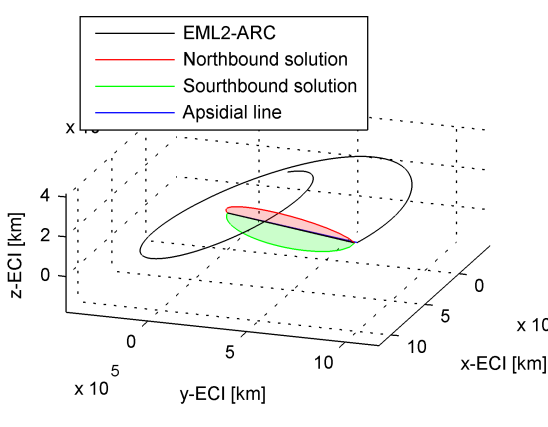


Figure 5.11: Optimization initialization: ISO I

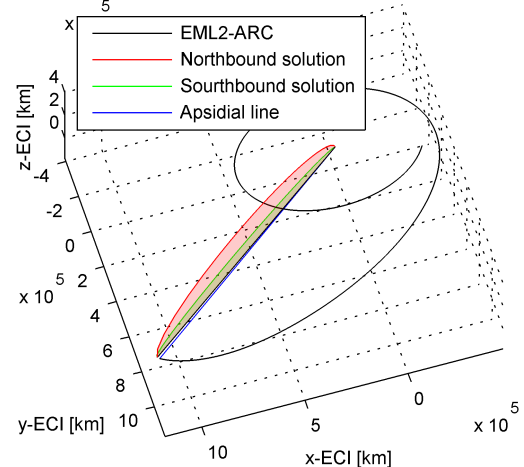


Figure 5.12: Optimization initialization: ISO II

5.3 Results

In this part of the Appendix all results of the computations that could not be shown in the main part of the study will be presented.

5.3.1 Optimized transfers from LEO with fixed inclination

Optimized transfers: North- and Southbound solutions

The initial state for the optimization could be created either for the north- or the southbound solution as explained in appendix section 5.2.1. The following subsection will give an overview to the result gained from the optimization for both north- and southbound solution. In the main results only the best solution w.r.t. Δv_{Total} has been chosen.

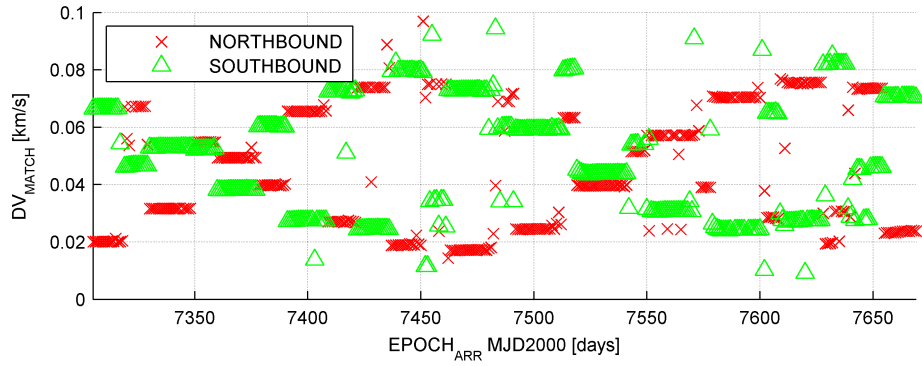


Figure 5.13: Halo north/south comp.: Δv_{Match}

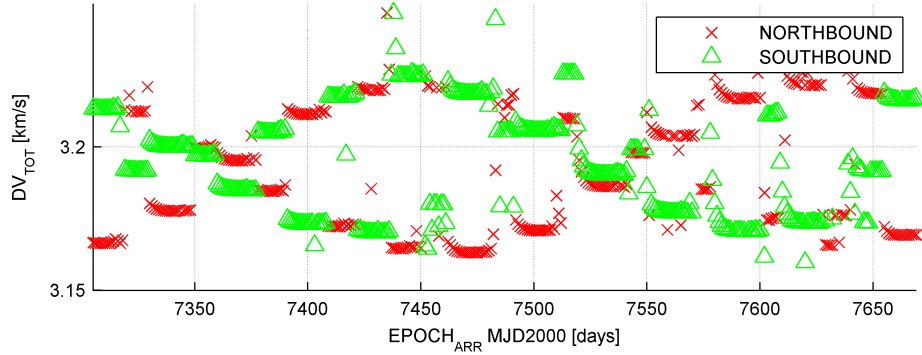


Figure 5.14: Halo north/south comp.: Δv_{Total}

Lissajous Orbit

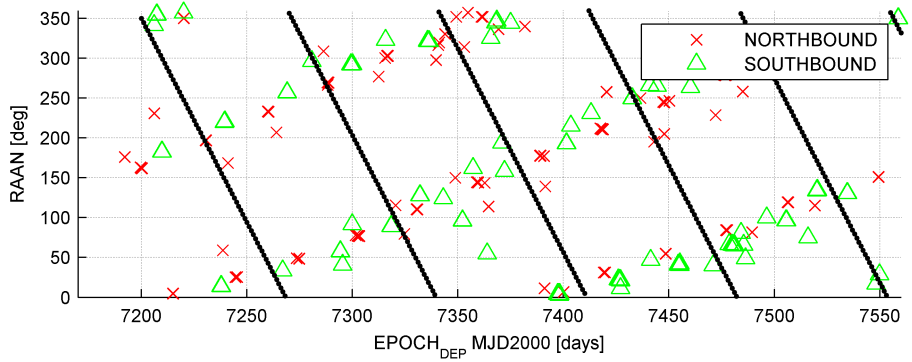


Figure 5.15: Halo north/south comp.: Ω

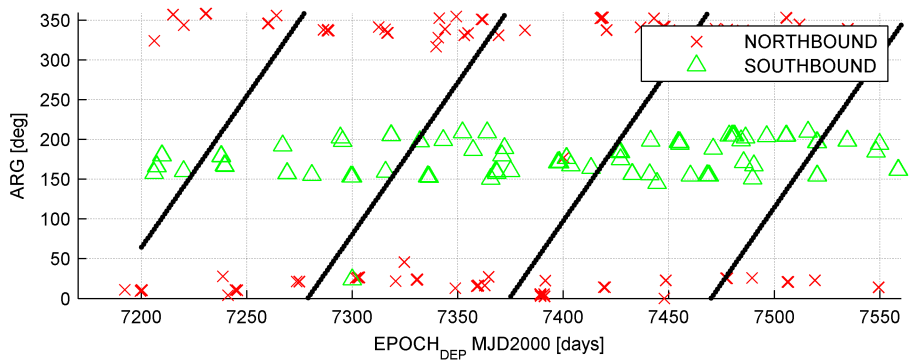


Figure 5.16: Halo north/south comp.: ω

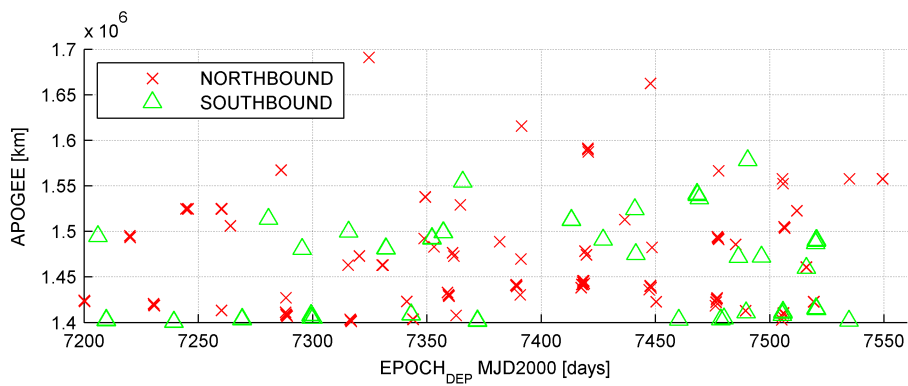


Figure 5.17: Halo north/south comp.: WSB Apogee

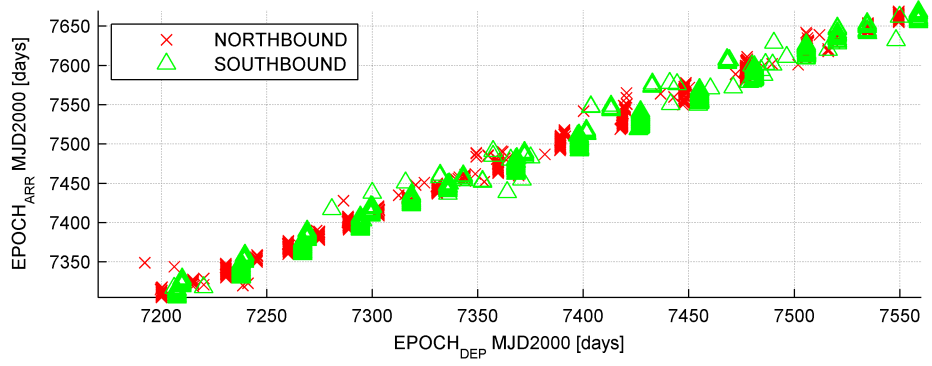


Figure 5.18: Halo north/south comp.: Launch Windows

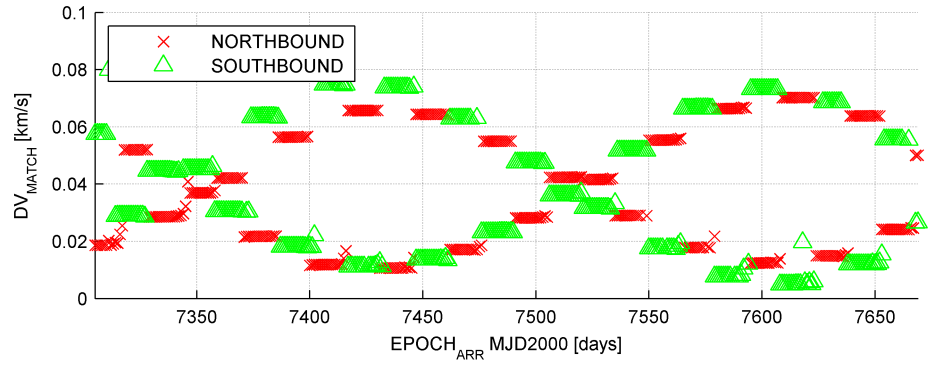


Figure 5.19: Lissajous north/south comp.: Δv_{Match}

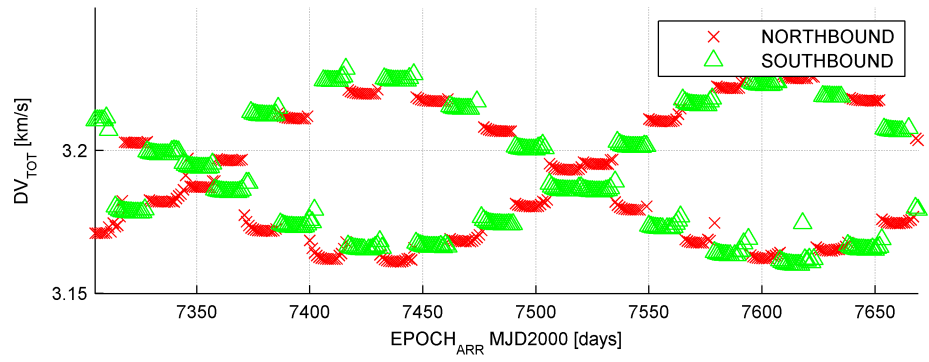


Figure 5.20: Lissajous north/south comp.: Δv_{Total}

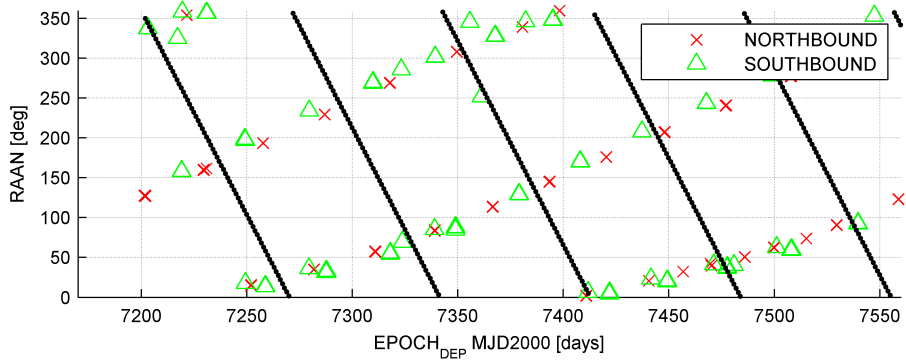


Figure 5.21: Lissajous north/south comp.: Ω

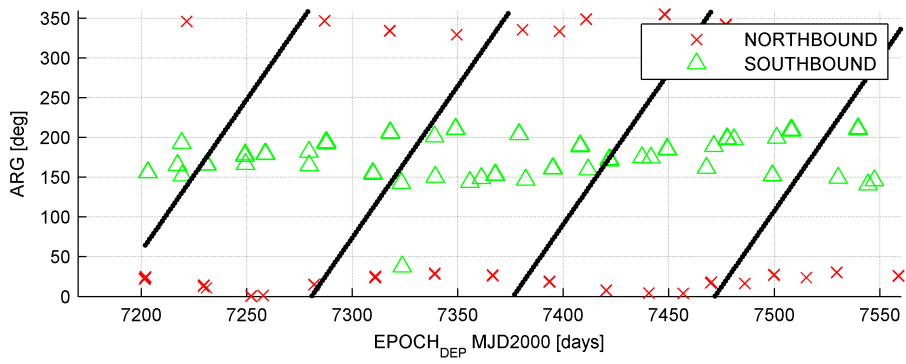


Figure 5.22: Lissajous north/south comp.: ω

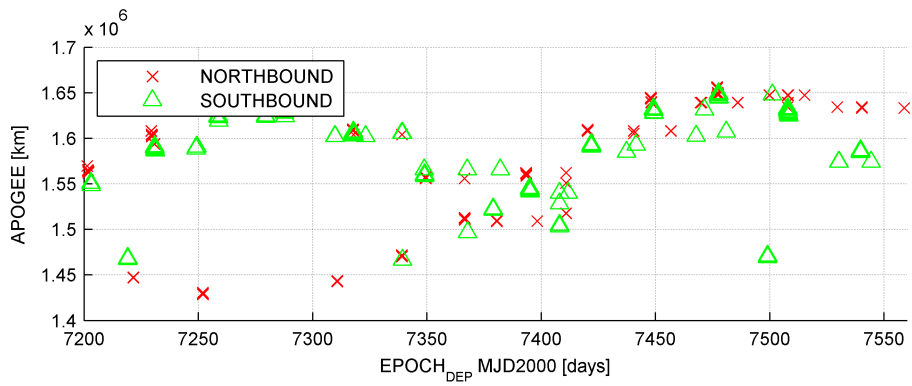


Figure 5.23: Lissajous north/south comp.: WSB Apogee

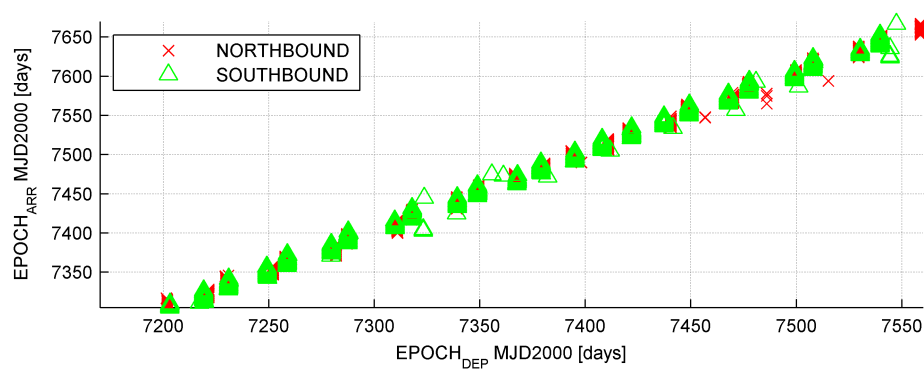


Figure 5.24: Lissajous north/south comp.: Launch Windows